

KH
NASA CR-7275



FINAL REPORT
STUDY OF STORAGE AND HANDLING
OF THE 260-IN.-DIA SOLID ROCKET MOTOR

Volume 2

Prepared by:

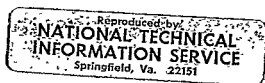
Aerojet Solid Propulsion Company
Advanced Technology
Sacramento, California

Author: H. K. Whitfield



National Aeronautics and Space Administ
Lewis Research Center
Cleveland, Ohio

Technical Management
J. J. Pelouch, Project Manager



aerojet solid propulsion company

A DIVISION OF AEROJET-GENERAL

Facility Form 602

ACCESSION NUMBER	THRU
N70-41471	1
(CODE)	(CATEGORY)
183	28
(PAGES)	
CR-7275-2	
(NASA CR OR TMX OR AD NUMBER)	

NOTICE

This report was prepared as an account of Government-sponsored work. Neither the United States, nor the National Aeronautics and Space Administration (NASA), nor any person acting on behalf of NASA:

- A.) Makes any warranty or representation, expressed or implied, with respect to the accuracy, completeness, or usefulness of the information contained in this report, or that the use of any information, apparatus, method, or process disclosed in this report may not infringe privately-owned rights; or
- B.) Assumes any liabilities with respect to the use of, or for damages resulting from the use of, any information, apparatus, method, or process disclosed in this report.

As used above, "person acting on behalf of NASA" includes any employee or contractor of NASA, or employee of such contractor, to the extent that such employee or contractor of NASA or employee of such contractor prepares, disseminates, or provides access to any information pursuant to his employment or contract with NASA, or his employment with such contractor

2-1
mik

NASA CR-72757

FINAL REPORT

STUDY OF STORAGE AND HANDLING
OF THE 260-IN. -DIA SOLID ROCKET MOTOR

VOLUME 2

Prepared by:

Aerojet Solid Propulsion Company
Advanced Technology
Sacramento, California

Author: H. K. Whitfield

September 1970

Contract NAS3-12052

Prepared for:

National Aeronautics and Space Administration
Lewis Research Center
Cleveland, Ohio

Technical Management
J. J. Pelouch, Project Manager



aerojet solid propulsion company

A DIVISION OF AEROJET GENERAL

TASK I - SEQUENCE OF OPERATIONS FOR THREE HANDLING METHODS

I. HANDLING METHOD NO. 1

A. DADE COUNTY PLANT TO KSC LC-37B

1. Removal of the Stage from the C&C Facility
and Placement on the Barge

a. Push modified ARD barge into position in graving/loading dock at the C&C facility.

b. Tie barge to dock mooring.

c. Ballast the barge to the bottom of the dock.

d. Connect portable winch to transporter and pull transporter to designated station at stern end of barge.

e. Install transporter rotation load bracing structure.

f. Connect trunnion lift adapters to aft trunnions.

g. Engage trunnion lift adapters and stiff-leg derrick load cables.

h. Raise stage vertically to clear forward lightweight environmental closure assembly platform.

i. Boom over assembly platform and install stage forward environmental closure to forward skirt.

j. Boom stage into position over transporter forward trunnion cradles.

k. Lower stage vertically until forward trunnions engage transporter cradles.

I.A. Dade County Plant to KSC LC-37B (cont)

1. Rotate stage until aft trunnions engage the transporter aft trunnion cradles.

m. Disengage and remove aft trunnion lift adapters; return lift adapters to storage.

2. Preparation for Shipment

a. Tie-down stage to transporter.

b. Inspect stage/transporter tie-down.

c. Remove transporter rotation load bracing structure and return to storage.

d. Connect barge mounted winch to transporter.

e. Place 3-in.- (7.62-cm) dia steel rollers in path of transporter.

f. Pull stage/transporter to shipping position on barge and disconnect winch.

g. Tie down transporter to barge.

h. Inspect transporter/barge tie-down.

i. Connect dry N_2 source to pressure regulator on aft nozzle plug.

j. Pressurize stage interior with dry N_2 , as required.

k. Connect vibration accelerometers, temperature sensors and pressure transducers to data recording system.

I.A. Dade County Plant to KSC LC-37B (cont)

k. Disconnect, remove, and store barge/transporter tie-down rigging.

l. Connect tow-bar between transporter forward end (barge stern) and tow-tractor.

5. Offloading at KSC

a. Place steel rollers in transporter path and pull stage/transporter onto dock using barge winch as a braking system.

b. Disconnect barge-mounted winch from transporter.

c. Connect tow-tractor by cable to transporter aft end for braking.

d. Pull stage transporter under sun-shade at inspection area.

e. Inspect stage.

f. Pull stage/transporter into position at rotating pit.

g. Install transporter rotation load bracing structure.

h. Install transporter aft end side-load structure between transporter and rotating pit foundation structure.

i. Disconnect and remove transporter aft-end transverse shear-load structure to provide clearance for stage rotation.

j. Disconnect stage/transporter tie-down rigging and place in storage.

k. Return steel rollers to storage after move operations are completed.

I.A. Dade County Plant to KSC LC-37B (cont)

6. Rotation, Transport to the Pad and Placement on the Pad

- a. Bring Roll-Ramp gantry into position over stage.
- b. Connect trunnion lift adapters to forward trunnions.
- c. Engage trunnion lift adapters to gantry lift bar.
- d. Rotate stage to vertical by raising the Roll-Ramp lift bar and moving the gantry on the gantry rails in coordinated movements.
- e. Raise stage vertically to proper elevation for placement on the launch pad.
- f. Install bracing structure between the stage aft section and the gantry to eliminate swinging movement of the stage.
- g. Move the stage/gantry into position over the launch pad using the gantry powered truck and braking trucks.
- h. Remove the aft stage bracing structure and return to storage.
- i. Lower the stage onto the pad support points by actuation of the Roll-Ramp mechanism.
- j. Disconnect trunnion lift adapters and raise adapters with gantry.
- k. Move gantry to storage area and lower trunnion lift adapters.
- l. Remove and store trunnion lift adapters.

I. Handling Method No. 1 (cont)

B. DCP TO KSC STORAGE

1. DCP Operations through Preparation for Shipment

Same as I.A.1 and I.A.2.

2. Barge Route

a. Same as I.A.3.a through I.A.3.g.

b. Continue on the Banana River barge channel and the channel access to the storage area dock.

c. Move barge stern first into position at the storage area graving/loading dock.

3. Preparation for Offloading at KSC

Same as I.A.4.

4. Offloading at KSC

a. Place steel rollers in transporter path and pull stage/ transporter onto dock using barge winch as a braking system.

b. Disconnect barge-mounted winch from transporter.

c. Connect tow-tractor by cable to transporter aft end for braking.

d. Pull stage transporter into storage building.

e. Return steel rollers to storage after move operations are completed.

I.B. DCP to KSC Storage (cont)

- f. Inspect stage.

5. Preparation for Storage

- a. Tie-down transporter to storage facility structure.
- b. Connect dry N₂ source to pressure regulator in nozzle plug.
- c. Pressurize stage as required to 1.5 to 2.0 psig (1.03 to 1.37 N/cm² gage).
- d. Connect temperature sensors to recording instruments.

II. HANDLING METHOD NO. 2

A. DCP to KSC LC-37B

1. Removal of the Stage from the C&C Facility and Placement on the Transporter

- a. Bring Roll-Ramp gantry into position over stage.
- b. Connect trunnion lift adapters to forward trunnions.
- c. Engage trunnion lift adapters to gantry lift-bar load cable.
- d. Raise stage vertically, using Roll-Ramp mechanism, a sufficient distance to clear forward light weight environmental closure assembly platform.
- e. Install bracing structure between the stage forward section and the gantry to eliminate swinging movement of the stage.

II.A. DCP to KSC LC-37B (cont)

f. Move stage/gantry into position over assembly platform and install environmental closure to forward skirt.

g. Move stage/gantry into position over truck-rail transporter forward trunnion cradles.

h. Install transporter rotation load bracing structure.

i. Pressurize transporter pneumatic bladder cradle to required pressure.

j. Remove stage/gantry bracing structure and return to storage.

k. Lower stage vertically until forward trunnions engage transporter cradles.

l. Move gantry over transporter and rotate stage until aft trunnions engage transporter cradles.

m. Disengage and remove aft trunnion lift adapters; return lift adapters to storage.

n. Tie-down stage to transporter.

o. Inspect stage/transporter tie-down.

p. Remove transporter rotation load bracing structure and return to storage.

2. Preparation for Shipment

a. Install barge-to-dock rail bridge structure.

II.A. DCP to KSC LC-37B (cont)

b. Move stage/transporter to shipping position on barge using transporter powered wheels and braking wheels.

c. Tie-down transporter to barge.

d. Inspect transporter/barge tie-down.

e. Connect dry N_2 source to pressure regulator on nozzle plug.

f. Pressurize stage interior with dry N_2 , as required, to 1.5 to 2.0 psig (1.03 to 1.37 N/cm^2 gage).

g. Connect dry N_2 (or dry air) source to pneumatic bladder pressure regulator and pressurize.

h. Connect vibration accelerometers, temperature sensors, and pressure transducers to data recording system.

i. Connect stage environmental shelter lift slings to 300-ton (272-Mg) derrick.

j. Lift stage environmental shelter from storage pad and install on barge; disconnect lift slings and return to storage.

k. Secure stage environmental shelter to barge attach fittings.

l. Inspect preparation for shipment operations.

m. Float barge by pumping out ballast.

n. Connect tug to barge and remove barge tie-down to dock mooring.

II.A. DCP to KSC LC-37B (cont)

3. Barge Route

Same as I.A.3.

4. Preparation for Offloading at KSC

- a. Tie barge to dock mooring.
- b. Ballast the barge to the bottom of the dock.
- c. Pressurize stage interior, as required, to 1.5 to 2.0 psig (1.03 to 37 N/cm² gage), disconnect dry N₂ source.
- d. Pressurize pneumatic bladder, as required, and disconnect dry N₂ (or dry air) source.
- e. Disconnect accelerometer and thermocouple instrumentation.
- f. Inspect stage/handling system.
- g. Install barge-to-dock rail bridge structure.
- h. Disconnect stage environmental shelter from barge.
- i. Connect environmental shelter lift slings to mobile crane.
- j. Remove environmental shelter from barge and place on dock storage pad; return lift slings to storage.
- k. Disconnect, remove and store barge/transporter tie-down rigging.

II.A. DCP to KSC LC-37B (cont)

5. Offloading at KSC

- a. Move stage/transporter off barge to inspection area under a sun shade using truck-rail transporter powered wheels and braking wheels.
- b. Inspect stage.
- c. Move stage/transporter into position at rotating pit using truck-rail transporter powered wheels and braking wheels.
- d. Install transporter rotation load bracing structure.
- e. Install transporter aft-end side-load structure between transporter and rotating pit foundation structure.
- f. Disconnect and remove transporter aft end transverse shear load structure to provide clearance for stage rotation.
- g. Disconnect stage/transporter tie-down rigging and place in storage.

6. Rotation, Transport to the Pad and Placement on the Pad

Same as I.A.6.

B. DCP TO KSC STORAGE

1. DCP Operations through Preparation for Shipment

Same as II.A.1 and II.A.2.

II.B. DCP to KSC Storage (cont)

2. Barge Route

Same as I.B.2.

3. Preparation for Offloading at KSC

Same as II.A.4.

4. Offloading at KSC

a. Move stage/transporter off barge into position at the storage area using truck-rail transporter powered wheels and braking wheels.

b. Inspect stage.

5. Preparation for Storage

Same as I.B.5.

III. HANDLING METHOD NO. 3

A. DCP TO KSC LC-37B

1. Removal of the Stage from the C&C Facility and Placement on the Transporter

a. Connect trunnion lift adapters to aft trunnions.

b. Engage trunnion lift adapters to aft trunnions.

c. Raise the stage vertically sufficient distance for aft trunnions to clear transporter.

III.A. DCP to KSC LC-37B (cont)

- d. Install trunnion lift adapters to forward trunnions.
- e. Lower forward system winch cable and engage forward trunnion lift adapters and forward winch system load cables.
- f. Rotate stage to horizontal using forward winch system.
- g. Adjust transporter center support sling to proper position.
- h. Bring truck-rail transporter into position under stage using the transporter powered wheels and braking wheels; tie down transporter.
- i. Lower stage horizontally to engage forward and aft trunnions in transporter forward and aft cradles.
- j. Disengage and remove forward and aft trunnion lift adapters; return lift adapters to storage.
- k. Tie down stage to transporter.
- l. Inspect stage/transporter tie-down.
- m. Remove transporter tie-down structure and return to storage.
- n. Move stage/transporter to forward environmental closure assembly area.
- o. Attach environmental closure lift slings to 300-ton derrick; attach slings to environmental closure handling fixture.
- p. Install environmental closure to forward skirt; remove handling fixture and return lift slings and handling fixture to storage.

III.A. DCP to KSC LC-37B (cont)

2. Preparation for Shipment

- a. Install barge-to-dock rail bridge structure.
- b. Move stage/transporter into shipping position on the barge using the transporter powered wheels and braking wheels.
- c. Tie down transporter to barge.
- d. Inspect transporter/barge tie-down.
- e. Connect dry N_2 source to pressure regulator on nozzle plug.
- f. Pressurize stage interior, as required, with dry N_2 to 1.5 to 2.0 psig (1.03 to 1.37 N/cm^2 gage).
- g. Adjust tension load in transporter center sling, as required.
- h. Connect vibration accelerometers and temperature sensors to data recording system.
- i. Connect stage environmental shelter lift slings to mobile crane.
- j. Lift stage environmental shelter from storage pad and install on barge; disconnect lift slings and return to storage.
- k. Secure stage environmental shelter to barge attach fittings.
- l. Inspect preparation for shipment operations.
- m. Float barge by pumping out ballast.
- n. Connect tug to barge and remove barge tie-down to dock mooring.

III.A. DCP to KSC LC-37B (cont)

3. Barge Route

Same as I.A.3.

4. Preparation for Offloading at KSC

- a. Tie barge to dock mooring.
- b. Ballast the barge to the bottom of the dock.
- c. Pressurize stage interior, as required, to 1.5 to 2.0 psig (1.03 to 1.37 N/cm² gage); disconnect dry N₂ source.
- d. Adjust load in transporter support sling, as required.
- e. Disconnect accelerometer and thermocouple instrumentation.
- f. Inspect stage/handling system.
- g. Install barge-to-dock rail bridge structure.
- h. Disconnect stage environmental shelter from barge.
- i. Connect environmental shelter lift slings to mobile crane.
- j. Remove environmental shelter from barge and place on dock storage pad; return lift slings to storage.
- k. Disconnect, remove and store barge/transporter tie-down rigging.

5. Offloading at KSC

- a. Move stage transporter off barge to inspection area under sun shade using truck-rail transporter powered wheels and braking wheels.

III.A. DCP to KSC LC-37B (cont)

b. Inspect stage.

c. Move stage/transporter into position at rotating pit adjacent to launch pad using truck-rail transporter powered wheels and braking wheels.

d. Install transporter rotation load bracing structure.

e. Install transporter aft end side-load bracing structure between transporter and rotating pit foundation structure.

f. Disconnect and remove transporter aft end transverse shear load structure to provide clearance for stage rotation.

g. Disconnect stage/transporter tie-down rigging and place in storage.

6. Rotation and Placement on the Pad

a. Connect trunnion lift adapters to forward trunnions.

b. Engage trunnion lift adapters and stiff-leg derrick load cable.

c. Rotate stage to vertical position.

d. Elevate stage vertically sufficient distance to clear launch pad structure and boom into position over pad.

e. Lower the stage onto the pad support points.

f. Disconnect trunnion lift adapters and return to storage.

g. Dismantle, install launch environment protection as required and store derrick.

III. Handling Method No. 3 (cont)

B. DCP TO KSC STORAGE

1. DCP Operations through Preparation for Shipment

Same as III.A.1 and III.A.2.

2. Barge Route

Same as I.B.2.

3. Preparation for Offloading at KSC

Same as III.A.4.

4. Offloading at KSC

Same as II.B.4.

STRUCTURAL ANALYSIS OF 260-IN.-DIA SOLID ROCKET MOTOR

I. INTRODUCTION

Stress analyses were conducted to evaluate the three proposed handling and storage methods for the 260-in.-dia stage. The propellant grain structure and the motor case shell structure were both considered in the evaluation. The critical load conditions related to the proposed handling methods were established and used as a basis for the analyses. The results of this study are intended to provide a definition of the magnitude of the motor stresses and strains developed during these handling and storage operations. In turn, these data are to be used to define the allowable handling loads associated with each handling procedure.

II. ANALYSIS

A. PROPELLANT GRAIN

1. Method

a. Theoretical Basis

To evaluate in detail the propellant grain structure, the finite element technique was used as the method of analysis (1)*. The finite element approach replaces the continuous structure with a system of elastic quadrilateral rings (elements) interconnected at a finite number of nodal points (joints). The equilibrium equations, in terms of unknown nodal point displacements, are developed at each nodal point with the solution of these equations being the solution to the system. In the procedure, the displacements, loads, or stresses subjected to the structure are replaced by equivalent values acting at the nodal points of the finite element system. Since each element may have separate mechanical properties and loading, the propellant grain, insulation, and motor case structure of arbitrary geometry can be evaluated. The effects

* A list of references for this structural analysis is given in Section V of this appendix.

II.A. Propellant Grain (cont)

of finite length, curved boundaries and variable boundary conditions are completely accounted for in the solution. Since the propellant grain will behave as a nearly incompressible material ($\nu = 0.5$), variational principles are used to account for this condition.

b. Nonaxisymmetric Load Condition

The analysis of the propellant grain subjected to transverse acceleration loads during horizontal storage or transportation is conducted on the basis of a modification of the finite element method (2, 3). This modification was developed for analysis of solids of revolution subjected to nonaxisymmetrical body forces and boundary conditions. The technique expresses the nonsymmetrical loads and boundary conditions in terms of Fourier Series expansions. A separate problem is solved for each term in the series expansion, and these results are combined to give an overall solution to the body at specified hoop stations.

2. Criteria

a. Design Analysis Conditions

The following load and environmental conditions were determined to be associated with the three proposed handling procedures. These data provide the basis for establishing the propellant grain structural analyses required for comparing the critical motor stress and strain conditions.

(1) Handling Method 1

(a) Vertical Storage

1 Postcast Motor Assembly and Prelaunch Pedestal

a Long term (1 g axial)

II.A. Propellant Grain (cont)

(b) Vertical Hoist

1 Postcast and Prelaunch Pedestal

a Short term (axial g load)

(c) Motor Rotation

1 Postcast and Prelaunch Pedestal

a Short term (axial g load, transverse g load, and combined transverse and axial g load)

b Above with internal pressure

(d) Horizontal Transportation

1 Ground Transportation (Steel Rollers)

a Short term (lateral g load)

b Above combined with internal pressure

2 Barge Transportation

a Short term (lateral g load at various response rates)

b Above with internal pressure

II.A. Propellant Grain (cont)

(e) Horizontal Storage

1 Long Term and Short Term Storage

a Long term (lateral g load)

b Above with internal pressure

(2) Handling Method 2

The analysis conditions will be the same as Handling Method 1 except as follows.

(a) There would be no internal motor pressure condition for long term horizontal storage.

(b) An external pneumatic bladder pressure (constant pressure distribution) with varying angular contact and length would be combined with horizontal transportation and storage.

(c) Horizontal ground transportation would involve a rail system instead of steel rollers.

(3) Handling Method 3

The analysis conditions will be the same as Method 1 except as follows.

(a) Internal motor pressure would not be required for horizontal handling, but would be required for horizontal long term storage.

II.A. Propellant Grain (cont)

(b) A transporter for horizontal ground transportation handling would incorporate a hammock (sling) arrangement with varying angular contact and length. This system would apply a constant external pressure distribution to the motor case similar to a pneumatic bladder pressure if no appreciable shear exists between the sling and the motor case.

(c) Horizontal ground transportation would involve a transporter instead of steel rollers.

b. Geometry and Material Properties

(1) Motor Case

The motor case configuration and material properties used in the propellant grain analysis are summarized in Table B-1. These data were obtained from the Douglas Report SM-51896 (4).

(2) Propellant Grain

The propellant grain geometry used as a basis for the evaluation of the storage and handling operations is depicted in Figure B-1. The mechanical properties of ANB-3105 propellant were used in the analyses and are summarized in Tables B-2 and -3. The time-dependent characteristics of the insulation system were assumed to be similar to that of the propellant.

(a) Relaxation Modulus

A significant parameter in the structural analysis of propellant grains is the relaxation modulus of the propellant. Solid propellants exhibit inelastic properties such as creep and stress relaxation at normal operating temperatures. As a result, structural grain analyses for

II.A. Propellant Grain (cont)

long-time storage conditions or the short-time dynamic conditions encountered during transportation must involve consideration of these time-dependent response characteristics for various stress-strain-temperature environments. Several different tests are used to obtain the propellant response properties. Tests include the measurement of creep, stress relaxation, constant-rate tensile behavior, and dynamic response under uniaxial and multiaxial conditions and at various temperatures. The test data are reduced to form a "master relaxation curve" that describes the propellant modulus as a function of time over the full operational range at a given reference temperature. "Shift factors" are developed from the data to define a modulus-vs-time curve for analyses at temperatures that differ from the reference value. Figure B-2 shows the "master relaxation curve" for ANB-3105 propellant with the upper and lower bounds of the relaxation modulus as indicated. Figure B-3 provided the time-temperature shift factors associated with the master relaxation curve. In the stress calculations for hoisting, transportation and storage, the various moduli values used are indicated in Table B-2. The modulus indicated for the firing pressure condition was obtained from the strain rate data given in Figure B-4.

(b) Allowable Bond Strength

Allowable bond stresses for motor storage are derived from the results of tests-to-failure of poker-chip specimens subjected to constant load conditions. The poker-chip specimen consists of a thin, round sandwich (diameter/thickness ratio >10) of propellant and liner bonded between heavy metal plates. The heavy metal plates and large diameter-to-thickness ratio simulate the bilateral restraint effects of the motor case on the propellant grain. It has been determined that plots of the data in the form of log time-to-failure are linear, with high statistical correlation coefficients. Therefore, these data can be extrapolated to storage times that correspond to the expected useful life of a particular motor design. Allowable tensile and

II.A. Propellant Grain (cont)

shear strength data are presented in Figure B-5. The change in bond strength with different temperatures was determined on the basis of the time-temperature shift factors indicated in Figure B-3.

(c) Allowable Strain

Uniaxial test specimens are employed to evaluate the ultimate properties of the propellant. These data are adjusted for biaxial conditions by correlation factors determined in the laboratory for a wide range of temperatures and strain rates. Figure B-6 gives the allowable strain for long-time storage, while Figures B-7 and -8 show the strain allowables related with rapid loading due to acceleration forces and firing pressure transients.

(d) Insulation Configuration

The proposed insulation system given in Figure 33 of Reference (6) incorporates booted forward and aft heads. However, to facilitate the comparison of the insulation bond stresses developed under the three different handling procedures, a completely bonded system was assumed in the analyses made for evaluating the storage and handling operations.

Subsequent analyses were conducted for the actual proposed insulation configuration with booted heads (6) and skirt supports.

3. Analysis Configurations

a. Axisymmetrical Model

The propellant grain configuration as shown in Figure B-1 is an axisymmetrical body with 12 nonaxisymmetrical fins in the vicinity of the forward head. The nonaxisymmetrical aspects of the configuration are not directly

II.A. Propellant Grain (cont)

amenable to an analytical evaluation. Presently available analytical techniques of three-dimensional propellant grain bodies are limited to axisymmetrical shapes. Therefore, the usual procedure for conducting a stress evaluation of this type of configuration is to assume a three-dimensional analytical model with inner-diameter dimensions that include the base of the fin slot and outer-diameter dimensions equivalent to the fin tips. Accordingly, the density and hoop stiffness of the material representing the fin region are adjusted to properly simulate the actual physical conditions. Figure B-9 shows this axisymmetrical propellant grain model used to determine the bond stresses and bore strains developed by the proposed handling methods for axial and transverse body forces, thermal contraction, and internal pressure. Figure B-9 depicts the finite element grid system, the propellant insulation bond element, and the inner bore nodal points used in the analysis locations. Figure B-10 shows the similar model, which includes the proposed insulation systems with booted forward and aft heads. The analyses of the propellant-insulation bond system in the booted regions is accomplished by assuming the insulation material has a 0.1 modulus for thermal, acceleration, and pressure loads. In the case of pressure loading, the elements representing the boots were assigned a negative pressure (pressure acting outwards against case and propellant) to simulate "booting effects."

b. Plane Strain Model

One analytical procedure for obtaining a stress evaluation of the propellant grain structure supported horizontally by external transverse loads is the "plane strain" solution of a typical cross section. The method provides a detailed definition of the circumferential distribution of propellant-insulation bond stresses and bore strains under this load condition. This technique was used to determine bond stresses and bore strains for both a continuous lateral support system and a local control support. An analysis for the local central support was accomplished by applying appropriate shear stresses to a

II.A. Propellant Grain (cont)

simulated motor case shell to achieve an equilibrium in forces for a given lateral support pressure. Figure B-11 shows the finite element grid system and the propellant-insulation bond element locations used for the analyses.

c. Nonaxisymmetrical Load Model

A three-dimensional solution of the propellant grain supported horizontally by both the skirts and a finite central support may be obtained from a finite element solution utilizing Fourier Series expansions. The method accounts for the edge effects of the lateral load and defines an axial stress and strain distribution. However, practical limitations on computer capacity preclude obtaining a comprehensive solution for the entire motor structure. This is indicated by the necessarily simplified finite element grid used in this analyses (Figure B-12). The results of solutions obtained by this procedure were used to confirm maximum values obtained from the plane strain analyses.

4. Analyses

A review of the possible load conditions related to the three handling methods, as given above, defines the following analyses as regards comparing the handling methods. The hammock-type support is assumed to apply a constant external pressure distribution to the motor case similar to a pneumatic bladder pressure, i.e., lateral support by Handling Methods 2 and 3 are similar.

a. Axisymmetrical Solutions (Handling Methods 1, 2 and 3)

(1) Vertical Storage and Hoist Load

(a) Geometry (Figures B-9 and -10)

Entire motor structure supported at aft skirt.

II.A. Propellant Grain (cont)

(b) Load

1 g forward axial acceleration

(2) Thermal Conditions

(a) Geometry (Figures B-9 and -10)

Entire motor structure supported at aft skirt.

(b) Load

Assume 10°F thermal difference.

(3) Internal Pressure

(a) Geometry (Figures B-9 and -10)

Entire motor structure supported at aft skirt.

(b) Load

Assume 10 psi internal pressure.

b. Nonaxisymmetrical Solutions

(1) Horizontal Storage or Transportation with Skirt Supports (Handling Method 1)

(a) Geometry (Figures B-9 and -10)

Entire motor structure supported at forward

and aft skirts

II.A. Propellant Grain (cont)

(b) Load

1 g transverse acceleration

(2) Motor Rotation (Handling Methods 1, 2, and 3)

(a) Geometry (Figures B-9 and -10)

Entire motor structure supported at forward and aft skirts.

(b) Loads

Combination of transverse and axial accelerations for combined 1 g loading at various angles of rotation as follows:

$$\phi = 30^\circ$$

$$\phi = 45^\circ$$

$$\phi = 60^\circ$$

c. Nonaxisymmetrical Plane Strain Solutions

(1) Horizontal Storage or Transportation with Central Support (Handling Methods 2 and 3)

(a) Geometry (Figure B-11)

Motor structure supported at the forward and aft skirts on a finite-length support at the center of the motor. The central support is assumed to react approximately 1/3 the weight of the motor by an applied external air bag or sling with constant lateral contact pressure.

II.A. Propellant Grain (cont)

(b) Loads

1 g transverse acceleration with central support combinations as follows:

<u>Contact Lateral Pressure, psi</u>	<u>Contact Angle, degree</u>	<u>Contact Length, in.</u>	<u>Average Lateral Shell Shear, psi</u>
49	120	100	15.9
24.5	120	200	4.8

The lateral shear is applied to the shell cross section to simulate the effects of the finite length support.

(2) Horizontal Storage or Transportation with Continuous Lateral Support (Handling Methods 2 and 3)

(a) Geometry (Figure B-11)

A typical cross section of the motor at the central section is shown in Figure B-11. Central support would represent that applied by an external air bag or sling with contact pressure for full support of the motor along the entire length.

(b) Loads

1 g transverse acceleration with central support conditions as follows:

<u>Contact Lateral Pressure, psi</u>	<u>Contact Angle (θ), degrees</u>	<u>Contact Length, in.</u>
12.4	152	1160
13.9	120	1160
17.3	88	1160

II.A. Propellant Grain (cont)

d. Nonaxisymmetrical Three-Dimensional Solution

(1) Horizontal Storage or Transportation with Central Support (Handling Methods 2 and 3)

(a) Geometry (Figure B-12)

The motor structure is supported at forward and aft skirts and on a finite-length support at the center of the motor. The central support is assumed to react approximately 1/3 the weight of the motor by an applied external air bag or sling with constant lateral contact pressure.

(b) Loads

1 g transverse acceleration with central support external pressure applied over 120-degree contact angle for 100 and 200 in. lengths. A Fourier Series definition for the external pressure is determined as:

$$p = \frac{W}{(\pi)(L)(130)(\sin \theta_1)} \left[1 + \theta_1 - \pi + (\sin \theta_1 - \sin \theta_2) \cos \theta \right. \\ \left. + \frac{1}{2} (\sin 2 \theta_1 - \sin 2 \theta_2) \cos 2\theta \right. \\ \left. + \frac{1}{3} (\sin 3 \theta_1 - \sin 3 \theta_2) \cos 3\theta \right. \\ \left. + \frac{1}{4} (\sin 4 \theta_1 - \sin 4 \theta_2) \cos 4\theta \right. \\ \left. + \dots \right]$$

Where

p = external pressure (psi)

L = contact length (in.)

W = support load (lb).

θ_1 = 1/2 contact angle

θ_2 = 360 - θ_1 contact angle

θ = angular location

II. Analysis (cont)

B. MOTOR CASE

1. Method

The three proposed handling methods for the motor in the horizontal attitude are evaluated on the basis of motor-case shell stresses and elastic stability. Elastic stability is evaluated by a method (7) that is based on statistical considerations of available classical stability theories modeled for 90 and 99% probability buckling allowables. A 90% probability value was assumed in the calculations. The additional buckling capacity developed by use of internal pressurization is considered. Also, the case stiffening effect of the propellant core is determined by the theory of Reference (8). The shell stresses developed in the motor case by a local lateral support pressure are determined by the "band loaded cylinder program" (9). This program is intended for use in the analysis of simply supported cylindrical shells subjected to band surface loads of arbitrary distributions in the three principal directions of the cylinder. The shape of the surface load in any direction is defined and approximated by the use of finite double Fourier Series.

2. Criteria

The motor case configuration and material properties used in the analysis are given in Table B-1

3. Handling Method 1

a. Elastic Stability

The maximum compressive stress is due to bending. The motor structure is assumed to be on "simple supports" and supported at the skirts.

II.B. Motor Case (cont)

(1) Geometric Parameters

$$L = 1060 \text{ in. (Tangency Plane - Tangency Plane)}$$

$$= 1143 \text{ (Center to Center of Handling Rings)}$$

$$t = 0.603 \text{ in.}$$

$$E = 27.5 (10^6) \text{ psi}$$

$$\rho_{\text{propellant}} = 0.063 \text{ lb/in.}^3$$

$$\rho_{\text{case}} = 0.289 \text{ lb/in.}^3$$

$$R_{\text{case}} = 130 \text{ in.}$$

(2) Critical Buckling Stress

From Reference (7):

With no internal pressure:

$$R/t = 130/0.603 = 215$$

$$L/R = 1142/130 = 8.78$$

$$\frac{\sigma_{cr}}{E} (10^3) = 1.28$$

$$\sigma_{cr} = 35,200 \text{ psi (90% probability)}$$

For internal pressure:

$$\bar{P} = \frac{p}{E} \left(\frac{R}{t} \right)^2 = \frac{p}{27.5(10^6)} (215)^2 = 0.00168 p$$

(Reference (7)
90% probability)

$$p = 20 \text{ psi}$$

$$\bar{P} = 0.0336$$

II.B. Motor Case (cont)

$$\begin{aligned}(\Delta \sigma_{cr}) &= \frac{(\Delta \bar{\sigma}_{cr})}{R/t} (E) \\&= (0.13) \cdot \frac{(27.5)}{215} (10^6) = 16,600 \text{ psi}\end{aligned}$$

Similarly,

$$p = 50 \text{ psi}$$

$$(\Delta \sigma_{cr}) = 22,400 \text{ psi}$$

$$p = 100 \text{ psi}$$

$$(\Delta \sigma_{cr}) = 29,500 \text{ psi}$$

b. Bending Stresses

In computing a design bending moment for the motor case the propellant and chamber weights were assumed to be uniformly distributed between the handling ring centerlines which were taken as 1142 in. apart. The nozzle and TVC weights of 78,160 lb were assumed to be concentrated at a point 150 in. aft of the aft ring centerline. Based on these assumptions the maximum moment can be approximated by the following expression:

$$\begin{aligned}M_{\max} &= \frac{(W_p + W_c) \ell}{8} - W_N \left(\frac{150}{\ell} \times \frac{\ell}{2} \right) \\&= \frac{(W_p + W_c) \ell}{8} - 75 W_N\end{aligned}$$

Where: W_p = propellant weight

$$= 3,400,000 \text{ lb}$$

W_c = chamber weight

$$= 227,140 \text{ lb}$$

W_N = nozzle weight

$$= 78,160 \text{ lb}$$

$$\ell = 1142 \text{ in.}$$

II.B. Motor Case (cont)

$$M_{\max} = \frac{(3,400,000 + 227,140) 1142}{8} - 75 (78,160)$$

$$= 51,840,000 \text{ in.-lb}$$

$$\sigma_c (\max) = \frac{M_{\max}}{\pi R^2 t}$$

$$= \frac{511,84 \times 10^6}{\pi (130)^2 (0.603)}$$

$$= 15,990 \text{ psi}$$

c. Shell pressure stress with

$$p = 100 \text{ psi}$$

$$\sigma_{\text{hoop}} = \frac{PR}{t} = \frac{100 (130)}{(0.603)} = 21,500 \text{ psi}$$

$$\sigma_{\text{merid}} = \frac{PR}{2t} = 10,750 \text{ psi}$$

d. Allowable acceleration load without pressure.

$$"g" = \frac{35,200}{15,990} = 2.20 \text{ (90\% probability)}$$

e. Allowable acceleration load with internal pressure.

$$\sigma_{\text{bending}} = 15,990(g) - \sigma_{\text{meridional}}$$

$$\sigma_{\text{cr total}} = \sigma_{\text{cr}} + (\Delta \sigma_{\text{cr}})$$

$$= 35,200 + (\Delta \sigma_{\text{cr}})$$

$$g_{\text{allow}} = \frac{\sigma_{\text{cr tot}} + \frac{pr}{2t}}{15,990}$$

II.B. Motor Case (cont)

$\frac{p}{\text{internal,}}$ $\frac{\text{psi}}{\text{psi}}$	$\frac{\sigma_{cr}^{\text{total,}}}{\text{psi}}$	$\frac{\sigma_{\text{meridional,}}}{\text{psi}}$	$\frac{\text{allowable}}{\text{(90\% prob)}}$
20	51,800	2,150	3.37
50	57,600	5,400	3.94
100	64,700	10,750	4.72

These data are depicted in Figure B-13 as "g" load capacity with increase in internal pressure.

f. Stiffening Effect of Propellant Core from Reference (8)

$$\phi_1 = \sqrt[4]{\frac{12(1 - \nu_c^2)}{4(1 - \nu_c)}} \frac{E_{\text{propellant}}}{E_{\text{case}}} \left(\frac{R}{t}\right)^{3/2}$$

$$= \frac{1.81}{2} \frac{E_{\text{propellant}}}{2.75 (10^6)} (215)^{3/2} = \frac{104 E_{\text{propellant}}}{10^6}$$

for $E_{\text{propellant}} = 200 \text{ psi}$

$$\phi_1 = 2.08 (10^{-2})$$

$$\frac{\sigma_{cr}^I}{\sigma_{cr}} - 1 = 2 \times 10^{-2}$$

$$\sigma_{cr}^I = 1.02 \sigma_{cr}$$

for $E_{\text{propellant}} = 400 \text{ psi}$

$$\phi_1 = 4.16 (10^{-2})$$

$$\frac{\sigma_{cr}^I}{\sigma_{cr}} - 1 = 4 \times 10^{-2}$$

$$\sigma_{cr}^I = 1.04 \sigma_{cr}$$

where σ_{cr}^I = critical buckling stress including the stiffening effect of propellant. Therefore the stiffening effect of the propellant core provides approximately 1%/100 psi propellant modulus. This effect will be conservatively neglected.

II.B. Motor Case (cont)

4. Handling Methods 2 and 3

For Handling Methods 2 and 3 it was assumed that a central support would be designed to react 1/3 of the total motor weight. For conservatism and simplicity the total weight was taken as 3,985,300 lb, which includes the handling rings, and this total weight was assumed to be uniformly distributed over an effective length of 1160 in. This produces a distributed load of 3436 lb/in. An analysis of this condition indicates maximum bending moments of 2.57×10^8 in.-lb in the "spans" and 1.93×10^8 in.-lb at the center support. A detail stress analysis of this condition is presented below:

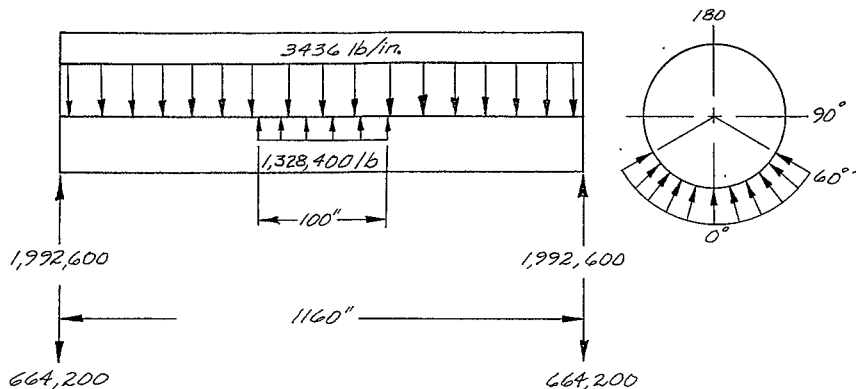
a. "Beam" Bending Stresses

$$\begin{aligned} c_b (\text{span}) &= \frac{2.57 \times 10^8}{\pi (130)^2 (0.603)} \\ &= 8030 \text{ psi} \end{aligned}$$

b. Local Stresses at Central Support

The local stresses due to the central support were evaluated by means of a computer program to handle band loads on thin-walled cylinders (9). For this solution, the 1,328,000 lb central reaction was assumed to be supplied by uniform pressure over a 120° arc 100 in. long, with this load reacted at the ends of the cylinder. The combined loading diagrams for this and the "beam" loading are indicated below:

II.B. Motor Case (cont)



From the band load program the following maximum stresses were obtained:

Type Stress	Value	Location (see above sketch)
Axial Compression	24,400 psi	$\theta = 45^\circ$, $X = 580$ in.
Bending (hoop)	$\pm 44,890$ psi	$\theta = 45^\circ$, $X = 580$ in.
Bending (longitudinal)	$\pm 15,830$ psi	$\theta = 45^\circ$, $X = 540$ in.

c. Buckling Capability

For the purpose of this analysis it was assumed that the critical buckling stress would be the same for the centrally supported conditions as for the unsupported condition, i.e., $\sigma_{cr} = 35,200$ psi. In addition, the critical applied stress was considered to be the combination of axial compression from the band load solution and the axial compression from the beam bending solution:

$$\begin{aligned}
 \sigma_c \text{ (TOT.)} &= 24,400 + 8030 \\
 &= 32,430 \text{ psi/"g"} \\
 \text{"g"s"} &= \frac{35,200}{32,430} \\
 &= 1.09 \text{ (for unpressurized chamber)}
 \end{aligned}$$

II.B. Motor Case (cont)

d. Effect of Internal Pressure

As indicated in the analysis of Condition 1 (End Rings Only), internal pressure could be utilized to increase the allowable "g" loads on the motor. A table indicating this increase for various pressure levels is indicated below:

P internal, psi	σ_{cr} total, psi	σ_{merid} , psi	g Allowable (90% prob.)
20	51,800	2,150	1.66
50	57,600	5,400	1.94
100	64,700	0,750	2.33

These data are presented in Figure B-14 as "g" load capacity with increase in internal pressure.

III. RESULTS

A. PROPELLANT GRAIN

1. Storage and Handling Method Comparison

The maximum propellant-liner bond stresses and bore strains determined separately for each various load condition considered for the comparison of handling procedures are summarized in Table B-4. All of these data were computed using the upper or lower bound modulus at 77°F; whichever gave the greatest magnitude of stress or strain. Handling Methods 2 and 3 were assumed to apply similar lateral pressure loading to the motor case. Also, as previously indicated, these bond stresses and bore strains were obtained from a completely bonded insulation configuration to facilitate data comparison by eliminating local stress concentrations. The bore strains are basic values which do not include the strain concentration effects in the fin region.

III.A. Propellant Grain (cont)

Tables B-8 through -25 define the bore strain or deflection and bond stress distributions in the motor for hoisting, vertical storage, horizontal storage, and transportation by the proposed handling procedures. All these stress values are separated inertia, thermal, or pressure stresses that have not been superimposed for the total stress condition.

a. Vertical Hoisting and Inverting

The maximum calculated bond stresses and basic bore strains are shown in Table B-4. Tables B-8 and -18 give the stress and strain distributions for the vertical storage inertia loads. The magnitude of the stress and strains determined for the inverting condition were within the range of those obtained for the vertical or horizontal solutions. Therefore these data were not tabulated. Table B-4 shows that vertical hoisting and inverting of the motor by the skirt structure produces no adverse conditions in the propellant grain.

b. Horizontal Transportation and Storage

Tables B-9 through -15 give the bond stress distributions obtained for the horizontal support analyses. The corresponding basic bore strain or deflection distributions are shown in Tables B-18 through -25.

Table B-5 gives the temperature and internal-pressure stresses and strains combined with the 1 g horizontal transportation load values. Table B-6 gives the similar data for horizontal storage. A comparison is made of the stresses and strains developed by Handling Methods 1, 2 and 3 at ambient temperature both with and without internal pressurization. The allowable transportation "g" load values in Table B-5 were based on the bond stress or bore strain allowables at 77°F given in Table B-3.

III.A. Propellant Grain (cont)

The above data show that the use of internal pressure in the motor further increases the ability of the propellant grain insulation system to withstand the bond tensions developed by the acceleration loads. The allowable transverse accelerations for the skirt support system (Handling Method 1) is limited by the bond tensile stresses. The use of a lateral support system on the motor case for transportation or storage conditions (Handling Methods 2 and 3) was found to produce much higher or excessive local bore strain in the propellant grain than was produced by a skirt support system.

These higher strains were determined to be the limiting strength for an allowable motor acceleration load. The use of internal pressurization under this condition does not affect this allowable. It was noted that increasing the contact angle of the lateral support reduces the basic bore strain.

The results of the plane strain solution for local (100 or 200 in.) lateral pressure support are included for comparison and because the three-dimensional solution does not conveniently provide bond shear values. The three-dimensional solution provides a solution which accounts for the length and edge effect of the local lateral pressure load. These results show that increasing the length of the lateral support from 100 to 200 in. does not appreciably change the local maximum stress or strain values. However, the optimum values of support length, external lateral pressure, and contact area combined with skirt supports were not determined.

Tables B-5 and -6 show that horizontal transportation and storage of the motor by the skirt structure is an acceptable method.

2. Skirt Supported Motor with Booted Insulation

The maximum bond stresses and bore strains calculated for handling, storage, and firing pressure conditions of the motor with the proposed insulation system are summarized in Table B-7. These data are for an

III.A. Propellant Grain (cont)

operating temperature of 60°F and include the strain concentration effects of the fins in the forward head. The strain concentration factors were obtained from (10) and are based on geometrical factors. Figures B-15 through -18 show the stress and strain distributions associated with vertical storage, horizontal storage, temperature change, and internal pressure. These results indicate that the minimum margins of safety occur for the long-term, 3-year horizontal-storage condition for both the bore strain and bond stresses. The maximum bond stresses occur at the end of the aft boot near the tangency plane, whereas the highest bore strain occurs at the edge of the fin slots. The high storage bond tensile stress condition may be alleviated by using internal pressure for any long term storage.

B. MOTOR CASE

1. Handling Method 1 assumes a simple support system at the skirts. Allowable acceleration loads were determined by buckling allowables based on a 90% probability as follows:

<u>Internal Pressure, psi</u>	<u>g Allowable Transverse Acceleration Load</u>
0	2.2
20	3.4
50	3.9
100	4.7

2. Handling Method 2 or 3 assume one finite length middle support and two skirt supports equally loaded. Allowable acceleration loads were determined by buckling allowables based on a 90% probability as follows:

III.B. Motor Case (cont)

<u>Internal Pressure, psi</u>	<u>Allowable Transverse Acceleration Load</u>
0	1.1
20	1.7
50	1.9
100	2.3

3. The above data demonstrate that the use of a finite length midsupport system instead of a skirt-support system will result in lower allowable transverse "g" loads. This condition is caused by the additional local bending stresses developed in the shell structure at the support load reaction.

IV. SUMMARY AND CONCLUSIONS

A. The load and environmental conditions associated with the three proposed handling procedures were determined. These data provided a basis for establishing the structural analyses required for comparing the critical motor stress and strain conditions. The analytical procedures used in these structural analyses were defined in detail.

B. The motor case and propellant grain configuration used in the analyses were obtained from Douglas Report SM-51896 (4). The mechanical properties of ANB-3105 propellant were used in the grain analyses.

C. The hammock-type lateral support proposed for Handling Method 3 was assumed to apply a constant external pressure distribution to the motor case similar to the pneumatic bladder-pressure lateral support proposed for Handling Method 2. Also, to facilitate the comparison of the insulation bond stresses developed under the different handling procedures, a completely bonded system was assumed in the analyses. Separate analyses were conducted for the actual proposed insulation with booted heads and supported by the skirts.

IV. Summary and Conclusions (cont)

D. The propellant bond stresses and basic bore strains were determined for vertical hoisting, motor inverting, horizontal transportation, vertical storage, and horizontal storage by the proposed handling procedures. The results of these data show:

1. Vertical hoisting and inverting the motor produces no adverse conditions in the propellant grain.

2. The allowable transverse acceleration for the skirt support system (Handling Method 1) is limited by bond tensile stresses. Horizontal transportation and storage of the motor by the skirt structure (Handling Method 1) is acceptable.

3. The use of internal pressure further increases the ability of the propellant grain insulation system to withstand the bond tensions developed by acceleration loads.

4. The use of a lateral support system on the motor case for transportation or storage conditions (Handling Method 2 or 3) was found to produce much higher or excessive local bore strain in the propellant grain than a skirt support system. These higher strains were determined to be the limiting factor for an allowable motor acceleration load. The use of internal pressurization under this condition does not affect this allowable. Increasing the length of the lateral support from 100 to 200 in. did not appreciably change maximum bond stresses or bore strain values. Increasing the contact angle of the support did reduce the basic bore strain. However, the optimum value of support length, external lateral pressure, and contact area combined with skirt supports was not determined.

E. The maximum bond stresses and bore strains for a motor with booted insulation were calculated for handling, storage, and firing pressure conditions. These results indicate:

IV. Summary and Conclusions (cont)

1. Minimum margins of safety occur for the long-term, 3-yr horizontal-storage condition for both the bore strain and bond stresses.

2. The maximum bond stresses occur at the end of the aft boot near the tangency plane, whereas the highest bore strain occurs at the edge of the fin slots.

3. The high storage bond tensile stress condition may be alleviated by using internal pressure for any long-term storage.

F. The analyses of the motor case structure determined that the use of a finite-length midsupport system instead of a skirt support system will result in lower allowable transverse "g" loads. However, the allowable 2.2 g transverse acceleration load determined for the skirt-only support system is adequate for any 260-in.-dia stage handling and transportation loads expected to be encountered. Motor internal pressurization could be used to increase the allowable transverse acceleration load in the event design criteria are subsequently established that exceed the 2.2 g level.

V. REFERENCES

1. Becker, E. B., Brisbane, J. J., "Application of the Finite Element Method to Stress Analysis of Solid Propellant Rocket Grains," Rohm and Haas Company, Report No. S-76, Vol. I (Second Edition), January 1966
2. Becker, E. B., Brisbane, J. J., "Stress Analysis of Solid Propellant Grains under Transverse Acceleration Loads," Rohm and Haas Company, Report No. S-116, March 1967
3. Herrmann, L. R., "Three-Dimensional Elasticity Analyses of Non-Axisymmetrically Loaded Solids of Revolution," University of California, Davis, User's Manual for NAAS, December 1968.
4. "Saturn 1B Improvement Study (Solid First Stage) Phase II, Final Detailed Report," Douglas Missile and Space Systems Division, Report SM-51896, March 1966
5. "Propellant Mechanical Properties Data Manual," AGC Report, (Rev. 1), January 1966
6. "Development of Cost-Optimized Insulation System for Use in Large Solid Rocket Motors," Vol. IV: Task IV-260-in.-Dia. Motor Insulation System Design and Process Plan, Report NASA CR-72584, August 1969
7. Schumacher, J. G., Lincoln, B., "Development of Design Curves for the Stability of Thin Pressurized and Unpressurized Circular Cylinders," Convair Astronautics Division, Report AZS-27-275, May 1969
8. "The Stability Under Axial Compression and Lateral Pressure of Circular-Cylindrical Shells With a Soft Elastic Core - Paul Seide Journal of the Aerospace Sciences, Vol. 29, July 1962, No. 7, Page 851
9. AGC Structures Manual Computer Program No. 788
10. AGC Structures Manual

TABLE B-1. ~ MOTOR CASE CONFIGURATION AND MATERIAL PROPERTIES
FOR PROPELLANT GRAIN ANALYSIS

Weight:

Weight propellant = 3,400,000 lbs

Weight motor inert = 305,300 lbs

Weight handling rings = 280,000 lbs

Weight total motor = 3,985,300 lbs

Pressure:

Chamber MEOP = 764 psi

Geometry: (Figure 3-6 of Report SM-51896)

Type - Monolithic, cylindrical w/hemispherical closures

I.D. = 260 inch

Length:

1 Skirt-Skirt = 1160 in.

2 Tangency plane-tangency plane = 1060 in.

Material Properties:

$\alpha_{\text{case}} = 5.6 \times 10^{-6} \text{ in/in/}^{\circ}\text{F}$

$t_{\text{case}} = 0.603 \text{ in.}$

$\sigma_{\text{case}} = 0.289 \text{ lb/in.}^3$

$E_{\text{case}} = 27.5 \times 10^6 \text{ psi}$

$\nu_{\text{case}} = 0.31$

TABLE B-2. - 260-IN.-DIA MOTOR PROPELLANT MECHANICAL PROPERTIES

LOAD CONDITION	ATTITUDE	TIME	TEMP.* (°F)	MODULUS E (psi)		POISSON'S RATIO ν	LINEAR COEF. EXPANSION α (in/in/°F)	DENSITY ρ (Lb/In ³)
				Max.	Min.			
HOISTING	VERTICAL	0.2 Sec.	77	700	200	0.5	5.4×10^{-5}	.0635
			60	1140	260			
TRANSPORT	HORIZONTAL	0.2 Sec.	77	700	200			
			60	1140	260			
STORAGE	VERTICAL	30 Day	60	83	55			
			77	78	54			
	HORIZONTAL	30 Day	60	83	55			
			77	78	54			
	HORIZONTAL	30 Yr.	60	74	50			
			77	70	50			
STORAGE PRESSURE	AXISYMMETRICAL	30 Day	60	83	55			
			77	78	54			
FIRING PRESSURE	AXISYMMETRICAL	0.2 Sec.	60	900				
THERMAL	AXISYMMETRICAL	3 Yr.	60	74	50			
			77	70	50			

*Cure temperature = 140°F

TABLE B-3. - ANB-3105 PROPELLANT ALLOWABLE STRESS AND STRAIN*

CONDITION	TIME	BORE STRAIN		BOND NORMAL STRESS			
		$\epsilon_{\text{Allow.}}$ (%)		$\sigma_{\text{Allow.}}$ (psi)		$\tau_{\text{Allow.}}$ (psi)	
		77°F	60°F	77°F	60°F	77°F	60°F
HOISTING OR TRANSPORT	0.2 Sec.	22	22	70	> 70	> 50	> 50
STORAGE	30 Day	12	12	28	30	22	23
	3 Yr.	12	12	20	24	15	17
FIRING	0.2 Sec.	35	34	-	-	> 50	> 50

*Reference Figures B-3 to -8

TABLE B-4. - PROPELLANT GRAIN ANALYSIS FOR FULLY BONDED INSULATION SYSTEM, SUMMARY OF STORAGE AND HANDLING ANALYSES, MAXIMUM BORE STRAINS AND BOND STRESSES

LOAD * CONDITION	t Time	Location*** Maximum Strain		ϵ_0 max. Basic Bore Strain (%)	Location*** Maximum Stress		σ_N max. Bond Normal Stress (psi)	Location*** Maximum Stress		τ_{0N} max. Bond Shear Stress (psi)
		Fig. B-	Nodal Point		Fig. B-	Elem.		Fig. B-	Elem.	
VERTICAL HOISTING	.2 Sec.	9	1-48	1.1	9	14-49	6.1	9	14-31	3.4
MOTOR INVERTING	.2 Sec.									
SKIRT SUP- PORT	$\phi = 30^\circ$	9	1-43	0.74	9	14-19	7.5	9	14-49	1.38
	$\phi = 45^\circ$	9	1-43	0.50	9	14-19	7.0	9	14-49	1.47
	$\phi = 60^\circ$	9	1-43	0.46	9	14-19	5.9	9	14-49	1.38
HORIZONTAL TRANSPORT	.2 Sec.									
SKIRT SUPPORT		9	1-44	0.84	9	14-20	6.7	9	14-12	1.1
LATERAL SUPPORT										
ENTIRE WT. OF MOTOR	L = 1160" $\theta = 88^\circ$	11	1-1	6.6	11	14-33	6.3	11	14-12	5.9
	$\theta = 120^\circ$	11	1-45	3.4	11	14-34	6.0	11	14-15	4.0
	$\theta = 152^\circ$	11	1-46	2.2	11	14-35	5.4	11	14-19	2.5
	L = 100" $\theta = 120^\circ$	11	1-1	11.9	11	14-30	9.6	11	14-14	5.6
1/3 WT. OF MOTOR	L = 200" $\theta = 120^\circ$.2 Sec. 11	1-1	7.0	11	14-33	6.3	11	14-14	2.9
VERTICAL STORAGE	30 Days	9	1-48	4.1	9	14-49	6.1	9	14-31	3.4
HORIZONTAL STORAGE	30 Days									
SKIRT SUPPORT	3 Yrs.	9	1-42	3.3	9	14-19	6.9	9	14-12	1.1
LATERAL SUPPORT										
ENTIRE WT. OF MOTOR	L = 1160" $\theta = 88^\circ$	11	1-30	7.5	11	14-45	7.2	11	14-12	1.7
	$\theta = 120^\circ$	11	1-35	3.7	11	14-45	6.9	11	14-16	.97
	$\theta = 152^\circ$	11	1-46	2.4	11	14-45	6.2	11	14-19	.71
	L = 100" $\theta = 120^\circ$	11	1-46	13.6	11	14-42	5.8	11	14-16	1.1
1/3 WT. OF MOTOR	L = 200" $\theta = 120^\circ$	11	1-46	8.2	11	14-45	6.2	11	14-15	.75
LATERAL SUPPORT (3-D)										
1/3 WT. OF MOTOR	L = 100" $\theta = 120^\circ$	3 Yrs. 12	100	12.1	12	23	7.2	12	-	Not Calc.
	L = 200" $\theta = 120^\circ$	3 Yrs. 12	100	11.9	12	23	7.2	12	-	Not Calc.
TEMP. STORAGE AT = 10°F	3 Yrs.	9	1-30	.57	9	14-32	.26	9	14-49	.10
INTERNAL PRESSURIZATION AP = 10 psig	30 Days	9	1-24	.07	9	14-22	-9.947 (min. compr.)	9	14-49	.014

* θ = External Radial Load Overall Contact Angle

ϕ = Inverting Angle From Horizontal Position

All acceleration loads are 1.0 "g".

** Fin strain concentration factor not included.

*** Reference Figures B-9, -11, and -12.

TABLE B-5. - PROPELLANT GRAIN ANALYSIS, COMPARISON OF HANDLING METHODS, HORIZONTAL TRANSPORTATION, MAXIMUM BORE STRAIN AND BOND STRESSES

HANDLING * METHOD		CENTRAL SUPPORT		Internal Motor Pressure (psi)	Location Maximum Strain		ϵ_0 max. Basic Bore Strain (Z)/g	Location Maximum Stress		σ_N max. Bond Normal Stress (psi)/g	Location Maximum Stress		τ_{0N} max. Bond Shear Stress (psi)/g	g's ** Allowable Accel. Load
		Length (in.)	Contact (Deg.)		Fig B-1	N.P.		Fig B-1	Elem.		Fig B-1	Elem.		
(1)	SKIRT SUPPORT	None	None	0	9	1-30	4.32	9	14-20	8.1	9	14-12	1.2	10.2
		None	None	10	9	1-30	4.39	9	14-20	-1.9	9	14-12	1.2	11.7
(2&3) LATERAL SUPPORT														
PLANE STRAIN ANALYSIS	TOTAL MOTOR WEIGHT SUPPORTED BY LATERAL PRESSURE	1160	88	0	11	1-1	10.2	11	14-33	7.9	11	14-12	6.3	2.8
		1160	120	0	11	1-46	7.0	11	14-34	7.6	11	14-15	4.4	5.4
		1160	152	0	11	1-46	5.8	11	14-35	7.0	11	14-19	2.9	8.4
		1160	88	10	11	1-1	10.3	11	14-33	-2.1	11	14-12	6.3	2.8
		1160	120	10	11	1-46	7.1	11	14-34	-2.3	11	14-15	4.5	5.4
		1160	152	10	11	1-46	5.9	11	14-35	-2.9	11	14-19	3.0	8.4
PLANE STRAIN ANALYSIS	1/3 MOTOR WEIGHT SUPPORTED BY LATERAL PRESSURE	100	120	0	11	1-1	15.5	11	14-30	11.2	11	14-14	6.0	1.5
		200	120	0	11	1-1	10.6	11	14-33	7.9	11	14-14	3.3	2.6
		100	120	10	11	1-1	15.6	11	14-30	1.3	11	14-14	6.1	1.5
		200	120	10	11	1-1	10.7	11	14-33	-2.0	11	14-14	3.4	2.6
3-D ANALYSIS	1/3 MOTOR WEIGHT SUPPORTED BY LATERAL PRESSURE	100	120	0	12	100	10.4	12	23	12.1	12	-	-	2.7
		200	120	0	12	100	10.3	12	23	12.1	12	-	-	2.7
		100	120	10	12	100	10.5	12	23	2.1	12	-	-	2.7
		200	120	10	12	100	10.4	12	23	2.1	12	-	-	2.7

* T_{cure} = 140°F; @ 77°F ΔT = 63°F T = 77°F

** Fin strain concentration factor not included.


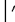


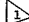
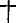


TABLE B-6. - PROPELLANT GRAIN ANALYSIS, COMPARISON OF HANDLING METHODS, HORIZONTAL LONG TERM STORAGE, MAXIMUM BORE STRAIN AND BOND STRESSES

HANDLING * METHOD		CENTRAL SUPPORT		Internal Motor Pressure (psi)	Location Maximum Strain		ϵ_{θ} max. Basic Bore Strain (%)	Location Maximum Stress		σ_N max. Bond Normal Stress (psi)	Location Maximum Stress		$\tau_{\theta N}$ max. Bond Shear Stress (psi)
		Length (in.)	Contact (Deg.)		Fig B-1	N.P.		Fig B-1	Elem.		Fig B-1	Elem.	
(1) SKIRT SUPPORT		None	None	0	9	1-30	6.6	9	14-19	8.2	9	14-12	1.1
		None	None	10	9	1-30	6.7	9	14-19	-1.8	9	14-12	1.1
(2 & 3) LATERAL SUPPORT													
PLANE STRAIN ANALYSIS	TOTAL MOTOR WEIGHT SUPPORTED BY LATERAL PRESSURE	1160	88	0	11	1-30	11.1	11	14-45	8.8	11	14-12	2.1
		1160	120	0	11	1-35	7.3	11	14-45	8.5	11	14-16	1.4
		1160	152	0	11	1-46	6.0	11	14-45	7.8	11	14-19	1.2
		1160	88	10	11	1-30	11.2	11	14-45	-1.1	11	14-12	2.2
		1160	120	10	11	1-35	7.4	11	14-45	-1.4	11	14-16	1.4
		1160	152	10	11	1-46	6.1	11	14-45	-2.1	11	14-19	1.2
PLANE STRAIN ANALYSIS	1/3 MOTOR WEIGHT SUPPORTED BY LATERAL PRESSURE	100	120	0	11	1-46	17.2	11	14-30	7.4	11	14-14	1.5
		200	120	0	11	1-46	11.8	11	14-33	7.8	11	14-14	1.2
		100	120	10	11	1-46	17.3	11	14-30	-2.5	11	14-14	1.6
		200	120	10	11	1-46	11.9	11	14-33	-2.1	11	14-14	1.2
3-D ANALYSIS	1/3 MOTOR WEIGHT SUPPORTED BY LATERAL PRESSURE	100	120	0	12	100	15.7	12	23	8.8	12	-	Not Calc.
		200	120	0	12	100	15.5	12	23	8.8	12	-	Not Calc.
		100	120	10	12	100	15.8	12	23	-1.1	12	-	Not Calc.
		200	120	10	12	100	15.6	12	23	-1.1	12	-	Not Calc.

* $T_{cure} = 140^{\circ}F$; @ $77^{\circ}F$ $\Delta T = -63^{\circ}F$

** Fin strain concentration factor not included.

TABLE B-7. - INSULATION SYSTEM WITH RELEASED HEADS - STORAGE, TRANSPORTATION,
AND FIRING - PROPELLANT GRAIN ANALYSIS RESULTS - MAXIMUM BORE
STRAIN AND BOND STRESSES

Motor Attitude	Load Condition	t Time	E Modulus (psi) Max./ Min.	Location Maximum Strain		ϵ_0 Max. Basic Bore Strain (%)	ϵ_{allow} Allow. Bore Strain (%)		Location Maximum Stress		σ_N Max. Bond Normal Stress (psi)	σ_{allow} Allow. Bond Tensile (psi)		Location Maximum Stress		τ_{0N} Max. Bond Shear Stress (psi)	τ_{allow} Allow. Bond Shear Stress (psi)		
				Fig B-	N.P.			M.S.	Fig B-	Elem.				M.S.	Fig B-	Elem.		M.S.	
VERTICAL	HOISTING 1-g 	.2 Sec.	1140/260	10	2-24	1.8	22	High	10	14-42	2.5	> 70	High	10	14-43	19.7	> 50	High	
	STORAGE 1-g	30 Days	83/55		2-24	2.2	12	High		14-42	2.2	30	High		14-43	10.8	23	+1.13	
HORIZ.	TRANS. 1-g 	.2 Sec.	1140/260		2-23	7.0	22	2.14		14-42	46.8	> 70	\$0.50		14-14	19.9	> 50	High	
	STORAGE 1-g	30 Days	83/55		2-23	6.5	12	0.85		14-42	25.1	30	+0.20		14-14	11.0	23	+1.09	
	STORAGE 1-g	3 Yrs.	74/50		2-23	6.8	12	0.77		14-42	24	24	0		14-14	10.8	17	+0.57	
VERTICAL	FIRING @ IGNITION p = 764	.2 Sec.	900		2-24	4.2	34	High	10	-	(COMPRESSION)				10	14-17	3.4	> 50	High

T_{cure} = 140°F; ΔT = -80°F T = 60°F

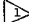
 This condition considers an additional 1 g acceleration load applied in 0.2 sec. to a motor conditioned to 60°F. This results in a total of 2 g's combined with the thermal condition. The allowables for this condition are based on high rate test data.

TABLE B-8. - PROPELLANT-INSULATION BOND STRESSES, 1-G AXIAL LOAD

Location* (Element Number)	σ Bond Bond Normal Stress (psi)	τ Bond Bond Shear Stress (psi)	Location Element Number	σ Bond Bond Normal Stress (psi)	τ Bond Bond Shear Stress (psi)
1	-4.958	2.028	26	-.126	3.341
2	-4.093	2.224	27	-.180	3.367
3	-4.439	1.636	28	.013	3.388
4	-4.897	1.309	29	-.073	3.40
5	-4.622	1.158	30	-.110	3.411
6	-4.421	1.149	31	.034	3.415
7	-3.760	1.219	32	.212	3.415
8	-3.294	1.313	33	.115	3.408
9	-2.377	1.451	34	.308	3.397
10	-1.683	1.636	35	.200	3.377
11	-1.088	1.901	36	.424	3.350
12	-.592	2.124	37	.327	3.311
13	-.658	2.43	38	.609	3.274
14	-.507	2.721	39	.463	3.228
15	-.716	2.915	40	.772	3.172
16	-.652	3.039	41	.618	3.091
17	-.958	3.081	42	.960	2.992
18	-.719	3.101	43	.7951	2.841
19	-.901	3.114	44	1.028	2.569
20	-.479	3.125	45	.8637	2.316
21	-.833	3.132	46	2.32	2.124
22	-.346	3.142	47	2.53	1.998
23	-.591	3.181	48	3.89	2.502
24	-.331	3.249	49	6.07	3.215
25	-.331	3.302			

* Refer to Figure B-9

T = 77°F

E = 700 psi

TABLE B-9. - PROPELLANT-INSULATION BOND STRESSES, HORIZONTAL SKIRT SUPPORT

Location* Element Number	σ Bond Bond Normal Stress Sta. 180° (psi)	τ Bond Bond Shear Stress Sta. 90° (psi)	Location Element Number	σ Bond Bond Normal Stress Sta. 180° (psi)	τ Bond Bond Shear Stress Sta. 90° (psi)
1	.078	.164	26	6.516	.470
2	.519	.341	27	6.508	.466
3	1.468	.435	28	6.527	.466
4	2.43	.521	29	6.514	.470
5	3.206	.613	30	6.501	.470
6	3.741	.691	31	6.488	.473
7	4.219	.785	32	6.486	.478
8	4.430	.858	33	6.457	.483
9	4.660	.924	34	6.449	.490
10	4.706	.983	35	6.414	.499
11	5.131	1.068	36	6.399	.510
12	5.117	1.101	37	6.331	.527
13	4.852	1.035	38	6.296	.548
14	5.034	.970	39	6.158	.576
15	5.553	.882	40	6.073	.608
16	6.008	.795	41	5.879	.647
17	6.26	.735	42	5.827	.691
18	6.439	.672	43	5.484	.740
19	6.620	.627	44	5.630	.812
20	6.692	.591	45	5.331	.830
21	6.557	.568	46	5.054	.770
22	6.573	.548	47	4.408	.732
23	6.592	.524	48	3.558	.708
24	6.522	.493	49	2.704	.802
25	6.513	.478			

* Refer to Figure B-9

T = 77°F
E = 700 psi

PRECEDING PAGE BLANK NOT FILMED.

TABLE B-11. - PROPELLANT-INSULATION BOND STRESSES, LATERAL SUPPORT
ENTIRE LENGTH OF MOTOR, RADIAL CONTACT ANGLE = 120°

Location * (Element Number)	σ Bond Bond Normal Stress (psi)	τ Bond Bond Shear Stress (psi)	Location Element Number	σ Bond Bond Normal Stress (psi)	τ Bond Bond Shear Stress (psi)
1	-9.84	1.910	26	4.407	.929
2	-8.236	1.992	27	4.662	1.183
3	-5.675	2.379	28	4.94	1.423
4	-5.74	1.711	29	5.138	1.634
5	-5.328	1.627	30	5.338	1.803
6	-5.174	1.642	31	5.517	1.933
7	-5.119	1.734	32	5.654	2.039
8	-5.111	1.859	33	5.779	2.116
9	-5.143	1.987	34	5.991	1.684
10	-5.152	2.125	35	5.80	2.114
11	-5.057	2.309	36	5.752	2.04
12	-4.605	2.619	37	5.687	1.924
13	-3.611	3.071	38	5.624	1.773
14	-1.837	3.590	39	5.531	1.596
15	.591	3.954	40	5.447	1.397
16	2.967	3.839	41	5.326	1.179
17	4.505	3.259	42	5.187	.949
18	5.122	2.534	43	5.015	.712
19	5.088	1.881	44	4.82	.475
20	4.796	1.352	45	4.647	.281
21	4.416	.934			
22	4.09	.611			
23	3.868	.422			
24	3.917	.464			
25	4.122	.673			

* Refer to Figure B-11

T = 77°F
E = 700 psi

TABLE B-12. - PROPELLANT-INSULATION BOND STRESSES, LATERAL SUPPORT
ENTIRE LENGTH OF MOTOR, RADIAL CONTACT ANGLE = 152°.

Location * Element Number	σ Bond Bond Normal Stress (psi)	τ Bond Bond Shear Stress (psi)	Location Element Number	σ Bond Bond Normal Stress (psi)	τ Bond Bond Shear Stress (psi)
1	-7.049	.605	26	4.702	.489
2	-6.341	.724	27	4.723	.522
3	-5.66	.730	28	4.816	.616
4	-5.303	.690	29	4.912	.727
5	-5.15	.651	30	5.025	.834
6	-5.109	.643	31	5.138	.929
7	-5.102	.669	32	5.235	1.014
8	-5.107	.715	33	5.324	1.083
9	-5.125	.767	34	5.365	1.125
10	-5.153	.815	35	5.389	1.133
11	-5.198	.855	36	5.388	1.115
12	-5.237	.897	37	5.375	1.072
13	-5.268	.953	38	5.354	1.006
14	-5.251	1.035	39	5.313	.920
15	-5.097	1.188	40	5.270	.819
16	-4.644	1.448	41	5.203	.703
17	-3.703	1.818	42	5.124	.579
18	-2.059	2.236	43	5.029	.500
19	.195	2.524	44	4.928	.327
20	2.445	2.448	45	4.849	.238
21	4.014	2.032			
22	4.767	1.524			
23	4.948	1.086			
24	4.883	.762			
25	4.757	.562			

* Refer to Figure B-11

T = 77°F

E = 700 psi

TABLE B-13. ~ PROPELLANT-INSULATION BOND STRESSES, LATERAL SUPPORT 1/3 WEIGHT
MOTOR, CONTACT ANGLE = 120°, CONTACT LENGTH = 100 IN.

Location * (Element Number)	σ Bond Bond Normal Stress (psi)	τ Bond Bond Shear Stress (psi)	Location Element Number	σ Bond Bond Normal Stress (psi)	τ Bond Bond Shear Stress (psi)
1	-7.08	.055	26	2.412	.140
2	-6.947	.169	27	2.756	.132
3	-6.784	.287	28	3.147	.192
4	-6.590	.406	29	3.533	.270
5	-6.358	.522	30	3.894	.345
6	-6.093	.634	31	4.226	.413
7	-5.787	.739	32	4.526	.468
8	-5.447	.835	33	4.793	.511
9	-5.065	.920	34	5.027	.540
10	-4.652	.991	35	5.228	.552
11	-4.119	1.050	36	5.402	.552
12	-3.713	1.094	37	5.547	.542
13	-3.197	1.126	38	5.658	.521
14	-2.668	1.137	39	5.736	.487
15	-2.127	1.126	40	5.787	.442
16	-1.591	1.093	41	5.813	.388
17	-1.066	1.040	42	5.819	.330
18	-.566	.967	43	5.808	.271
19	-.091	.880	44	5.789	.219
20	.352	.782	45	5.771	.186
21	.764	.673			
22	1.142	.559			
23	1.491	.442			
24	1.812	.327			
25	2.113	.220			

* Refer to Figure B-11

T = 77°F
E = 50 psi

TABLE B-14. - PROPELLANT-INSULATION BOND STRESSES, LATERAL SUPPORT 1/3 WEIGHT MOTOR, CONTACT ANGLE = 120°, CONTACT LENGTH = 200 IN.

Location * (Element Number)	σ Bond Bond Normal Stress (psi)	τ Bond Bond Shear Stress (psi)	Location Element Number	σ Bond Bond Normal Stress (psi)	τ Bond Bond Shear Stress (psi)
1	-6.831	.040	26	2.035	.218
2	-6.730	.113	27	2.368	.157
3	-6.595	.189	28	2.689	.100
4	-6.428	.265	29	2.998	.048
5	-6.226	.339	30	3.307	.013
6	-5.993	.410	31	3.670	.048
7	-5.725	.477	32	4.017	.086
8	-5.427	.539	33	4.339	.118
9	-5.096	.594	34	4.635	.144
10	-4.737	.641	35	4.904	.159
11	-4.349	.680	36	5.150	.169
12	-3.933	.710	37	5.369	.176
13	-3.494	.735	38	5.560	.178
14	-3.039	.749	39	5.721	.175
15	-2.572	.750	40	5.856	.167
16	-2.101	.738	41	5.964	.156
17	-1.631	.715	42	6.048	.143
18	-1.167	.681	43	6.108	.130
19	-.715	.639	44	6.146	.119
20	-.275	.589	45	6.165	.113
21	.150	.533			
22	.559	.473			
23	.952	.410			
24	1.329	.346			
25	1.690	.281			

* Refer to Figure B-11

T = 77°F
E = 50 psi

TABLE B-15. - PROPELLANT-INSULATION BOND NORMAL STRESSES, THREE DIMENSIONAL ANALYSIS LATERAL SUPPORT 1/3 WEIGHT MOTOR; CONTACT ANGLE = .120°

Location* (Element Number)	σ Bond Max. Bond Normal Stress (psi)	
	Length = 100"	Length = 200"
7	6.89	6.89
15	6.85	6.85
23	7.19	7.19
31	7.04	7.04
39	6.95	6.95
47	6.91	6.91
55	6.85	6.85
63	6.77	6.78
71	6.71	6.75
79	6.74	6.75
87	6.79	6.73
95	6.72	6.66
103	6.53	6.55
111	6.39	6.42
119	6.32	6.33
127	6.26	6.26
135	6.20	6.20
143	6.06	6.06
151	5.79	5.79
159	5.80	5.80

* Refer to Figure B-12

T = 77°F

E = 50 psi

TABLE B-16. - PROPELLANT-INSULATION BOND STRESSES, TEMPERATURE CHANGE $\Delta T = -10^{\circ}\text{F}$

Location* (Element Number)	σ Bond Bond Normal Stress (psi)	τ Bond Bond Shear Stress (psi)	Location Element Number	σ Bond Bond Normal= Stress (psi)	τ Bond Bond Shear Stress (psi)
1	.139	.072	26	.249	.013
2	.089	.068	27	.251	.009
3	.091	.043	28	.259	.006
4	.112	.028	29	.257	.004
5	.113	.017	30	.262	.001
6	.118	.013	31	.258	.001
7	.114	.010	32	.260	.004
8	.117	.011	33	.252	.006
9	.112	.009	34	.252	.008
10	.113	.011	35	.240	.010
11	.099	.012	36	.238	.013
12	.101	.018	37	.222	.016
13	.097	.031	38	.217	.019
14	.114	.046	39	.196	.021
15	.135	.055	40	.190	.023
16	.170	.058	41	.167	.024
17	.180	.056	42	.163	.025
18	.202	.051	43	.135	.026
19	.209	.044	44	.130	.026
20	.226	.038	45	.098	.028
21	.216	.034	46	.131	.033
22	.230	.030	47	.110	.040
23	.223	.026	48	.121	.069
24	.230	.021	49	.190	.106
25	.237	.017			

* Refer to Figure B-9

$T = 77^{\circ}\text{F}$
 $E = 70 \text{ psi}$

TABLE B-17. - PROPELLANT-INSULATION BOND STRESSES, PRESSURE = 10 PSI

Location* (Element Number)	σ Bond Bond Normal Stress (psi)	τ Bond Bond Shear Stress (psi)	Location Element Number	σ Bond Bond Normal Stress (psi)	τ Bond Bond Shear Stress (psi)
1	-9.991	.007	26	-9.966	.001
2	-9.989	.004	27	-9.966	.001
3	-9.986	.006	28	-9.966	.001
4	-9.991	.004	29	-9.967	.000
5	-9.987	.000	30	-9.963	.000
6	-9.987	.005	31	-9.966	.000
7	-9.990	.001	32	-9.965	.001
8	-9.987	.004	33	-9.967	.001
9	-9.993	.000	34	-9.966	.001
10	-9.999	.005	35	-9.969	.001
11	-9.990	.005	36	-9.968	.002
12	-9.976	.004	37	-9.970	.002
13	-9.980	.006	38	-9.971	.002
14	-9.982	.007	39	-9.976	.003
15	-9.981	.009	40	-9.973	.003
16	-9.977	.008	41	-9.980	.003
17	-9.974	.008	42	-9.977	.003
18	-9.971	.009	43	-9.984	.003
19	-9.978	.007	44	-9.972	.005
20	-9.974	.003	45	-9.988	.000
21	-9.957	.001	46	-9.984	.001
22	-9.947	.012	47	-9.998	.005
23	-9.966	.005	48	-9.995	.007
24	-9.969	.002	49	-9.964	.017
25	-9.969	.002			

* Refer to Figure B-9

T = 77°F
E = 90 psi-

TABLE B-18. - PROPELLANT BASIC BORE STRAINS, AXISYMMETRICAL SOLUTION
BONDED INSULATION SYSTEM

Location * (Nodal Point)	ϵ Basic 1-G Axial $E = 200$ (%)	ϵ Basic $\Delta T = 10^\circ F$ $E = 70$ (%)	ϵ Basic $p = 10$ psi $E = 90$ (%)
23	-.103	.457	.063
24	-.080	.504	.067
25	-.059	.524	.065
26	-.041	.536	.064
27	-.027	.547	.064
28	-.015	.555	.064
29	-.006	.561	.065
30	-.003	.565	.066
31	.012	.563	.064
32	.020	.559	.066
33	.027	.553	.064
34	.035	.545	.063
35	.042	.531	.062
36	.052	.519	.061
37	.062	.501	.060
38	.075	.488	.058
39	.084	.450	.053
40	.093	.416	.049
41	.103	.383	.046
42	.115	.351	.044
43	.132	.320	.042
44	.167	.289	.041
45	.232	.263	.035
46	.260	.256	.033
47	.313	.242	.028
48	.318	.210	.025
49	.209	.131	.020
50	.035	.046	.015

* Refer to Figure B-9

$T = 77^\circ F$

TABLE B-19. - PROPELLANT BASIC BORE STRAIN, HORIZONTAL THREE YEAR
STORAGE, SKIRT SUPPORT

Location * (Element Number)	ϵ Basic 1-G Transverse Station 180°* E = 50 (%)
23	3.25
24	3.20
25	3.13
26	3.09
27	3.07
28	3.07
29	3.07
30	3.07
31	3.08
32	3.09
33	3.10
34	3.11
35	3.13
36	3.15
37	3.17
38	3.20
39	3.23
40	3.27
41	3.29
42	3.31
43	3.30
44	3.26
45	3.21
46	3.12
47	2.87
48	2.35
49	1.55

* Station 180° at top
of motor.

Refer to Figure B-9

T = 77°F

TABLE B-20. - PROPELLANT BORE DEFLECTIONS, LATERAL SUPPORT ENTIRE LENGTH OF MOTOR, RADIAL CONTACT ANGLE = 88°F, SUPPORT LENGTH = 1160 IN.

Location (Nodal Point)	ΔX Displ. (in.)	ΔY Disp. (in.)	Location (Nodal Point)	ΔX Displ. (in)	ΔY Displ. (in)
1	0	-1.098	26	1.412	-3.258
2	.113	-1.105	27	1.376	-3.342
3	.226	-1.124	28	1.334	-3.422
4	.338	-1.157	29	1.286	-3.499
5	.448	-1.201	30	1.233	-3.571
6	.555	-1.257	31	1.175	-3.640
7	.660	-1.323	32	1.113	-3.705
8	.761	-1.400	33	1.047	-3.765
9	.857	-1.485	34	.977	-3.821
10	.949	-1.577	35	.905	-3.874
11	1.035	-1.677	36	.830	-3.922
12	1.115	-1.781	37	.752	-3.965
13	1.189	-1.889	38	.673	-4.005
14	1.255	-2.000	39	.592	-4.039
15	1.313	-2.114	40	.510	-4.070
16	1.363	-2.227	41	.426	-4.096
17	1.405	-2.341	42	.342	-4.117
18	1.439	-2.454	43	.257	-4.133
19	1.464	-2.565	44	.172	-4.145
20	1.481	-2.674	45	.0859	-4.152
21	1.489	-2.780	46	0	-4.155
22	1.4886	-2.882			
23	1.481	-2.982			
24	1.465	-3.078			
25	1.442	-3.170			

T = 77°F
E = 700 psi

TABLE B-21. - PROPELLANT BORE DEFLECTIONS, LATERAL SUPPORT ENTIRE LENGTH OF MOTOR, RADIAL CONTACT ANGLE = 120°, SUPPORT LENGTH = 1160 IN.

Location (Nodal Point)	ΔX Displ. (in.)	ΔY Displ. (in.)	Location (Nodal Point)	ΔX Displ. (in.)	ΔY Displ. (in.)
1	0	-.475	26	1.005	-1.799
2	.058	-.478	27	.989	-1.864
3	.116	-.487	28	.968	-1.925
4	.175	-.503	29	.941	-1.985
5	.233	-.525	30	.909	-2.041
6	.291	-.552	31	.872	-2.095
7	.349	-.585	32	.831	-2.145
8	.407	-.624	33	.787	-2.193
9	.465	-.668	34	.738	-2.237
10	.522	-.716	35	.687	-2.279
11	.578	-.769	36	.632	-2.317
12	.633	-.825	37	.575	-2.351
13	.687	-.886	38	.516	-2.382
14	.738	-.950	39	.456	-2.410
15	.787	-1.016	40	.393	-2.434
16	.832	-1.085	41	.330	-2.454
17	.874	-1.156	42	.265	-2.471
18	.911	-1.229	43	.199	-2.484
19	.943	-1.302	44	.133	-2.494
20	.970	-1.376	45	.067	-2.499
21	.991	-1.449	46	0	-2.501
22	1.007	-1.522			
23	1.015	-1.594			
24	1.018	-1.664			
25	1.014	-1.733			

T = 77°F
E = 700 psi

TABLE B-22. - PROPELLANT BORE DEFLECTIONS, LATERAL SUPPORT ENTIRE LENGTH OF MOTOR, RADIAL CONTACT ANGLE = 152°, SUPPORT LENGTH = 1160 IN.

Location (Nodal Point)	ΔX Displ. (in.)	ΔY Displ. (in.)	Location (Nodal Point)	ΔX Displ. (in.)	ΔY Displ. (in.)
1	0	-.048	26	.516	-.568
2	.012	-.049	27	.522	-.604
3	.024	-.052	28	.524	-.640
4	.036	-.056	29	.521	-.675
5	.049	-.062	30	.514	-.709
6	.063	-.070	31	.503	-.742
7	.079	-.079	32	.488	-.774
8	.095	-.090	33	.468	-.804
9	.113	-.103	34	.446	-.833
10	.133	-.117	35	.420	-.859
11	.154	-.133	36	.391	-.884
12	.177	-.151	37	.359	-.906
13	.202	-.170	38	.325	-.927
14	.229	-.191	39	.289	-.945
15	.256	-.214	40	.251	-.961
16	.285	-.239	41	.211	-.974
17	.315	-.266	42	.170	-.985
18	.344	-.294	43	.129	-.994
19	.373	-.324	44	.086	-1.000
20	.401	-.356	45	.043	-1.004
21	.428	-.389	46	0	-1.005
22	.452	-.423			
23	.473	-.459			
24	.491	-.495			
25	.506	-.531			

T = 77°F

E = 700 psi

TABLE B-23. PROPELLANT BORE DEFLECTIONS, LATERAL SUPPORT ENTIRE LENGTH OF MOTOR, RADIAL CONTACT ANGLE = 120°, SUPPORT LENGTH = 100 IN.

Location (Nodal Point)	ΔX Displ. (in.)	ΔY Displ. (in.)	Location (Nodal Point)	ΔX Displ. (in.)	ΔY Displ. (in.)
1	0	-.534	26	1.981	-3.082
2	.184	-.591	27	1.955	-3.216
3	.259	-.655	28	1.917	-3.347
4	.369	-.676	29	1.869	-3.475
5	.476	-.718	30	1.810	-3.600
6	.588	-.765	31	1.741	-3.720
7	.700	-.824	32	1.664	-3.836
8	.813	-.892	33	1.577	-3.947
9	.924	-.969	34	1.483	-4.053
10	1.034	-1.055	35	1.382	-4.153
11	1.143	-1.149	36	1.275	-4.246
12	1.249	-1.250	37	1.162	-4.332
13	1.351	-1.359	38	1.044	-4.411
14	1.449	-1.473	39	.922	-4.482
15	1.542	-1.594	40	.797	-4.545
16	1.629	-1.719	41	.668	-4.598
17	1.708	-1.849	42	.537	-4.643
18	1.780	-1.981	43	.405	-4.678
19	1.843	-2.117	44	.270	-4.703
20	1.896	-2.254	45	.135	-4.718
21	1.938	-2.392	46	0	-4.723
22	1.970	-2.531			
23	1.990	-2.671			
24	1.999	-2.809			
25	1.996	-2.947			

T = 77°F
E = 700 psi

TABLE B-24. - PROPELLANT BORE DEFLECTIONS, LATERAL SUPPORT ENTIRE LENGTH OF MOTOR, RADIAL CONTACT ANGLE = 120°, SUPPORT LENGTH = 200 IN.

Location (Nodal Point)	ΔX Displ. (in.)	ΔY Displ. (in.)	Location (Nodal Point)	ΔX Displ. (in.)	ΔY Displ. (in.)
1	0	-.230	26	.976	-1.528
2	.085	-.256	27	.966	-1.592
3	.120	-.287	28	.950	-1.654
4	.171	-.299	29	.928	-1.715
5	.221	-.321	30	.901	-1.773
6	.274	-.346	31	.869	-1.828
7	.327	-.378	32	.832	-1.882
8	.380	-.414	33	.790	-1.932
9	.433	-.455	34	.745	-1.980
10	.486	-.500	35	.695	-2.025
11	.538	-.550	36	.643	-2.066
12	.590	-.604	37	.587	-2.105
13	.640	-.661	38	.528	-2.139
14	.689	-.721	39	.467	-2.170
15	.735	-.783	40	.404	-2.198
16	.779	-.848	41	.339	-2.221
17	.820	-.915	42	.273	-2.240
18	.857	-.983	43	.206	-2.256
19	.890	-1.052	44	.138	-2.266
20	.918	-1.121	45	.069	-2.273
21	.942	-1.190	46	0	-2.275
22	.960	-1.260			
23	.972	-1.328			
24	.979	-1.396			
25	.981	-1.463			

T = 77°F
E = 700 psi

TABLE B-25. - PROPELLANT BASIC BORE STRAIN, THREE DIMENSIONAL ANALYSIS,
LATERAL SUPPORT 1/3 WEIGHT MOTOR, CONTACT ANGLE = 120°

Location* (Element Number)	εBasic Max Basic Bore Strain (%)	
	Length = 100"	Length = 200"
1	1.2	1.2
9	2.5	2.5
17	3.7	3.7
25	5.0	4.9
33	6.2	6.2
41	7.3	7.2
49	8.4	8.3
57	9.4	9.4
65	10.4	10.4
73	11.3	11.2
81	11.9	11.7
89	12.1	11.9
97	11.8	11.7
105	11.2	11.2
113	10.5	10.4
121	9.6	9.6
129	8.6	8.5
137	7.2	7.1
145	5.6	5.5
153	3.7	3.7

* Refer to Figure B-11 T = 77°F
E = 50 psi

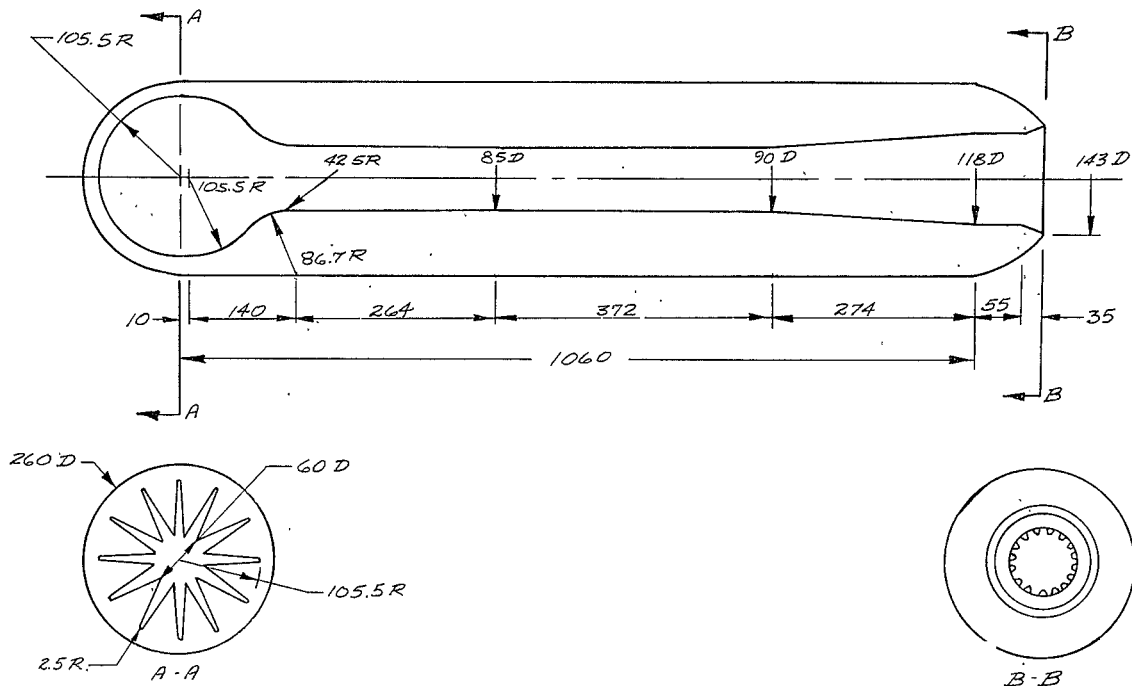


Figure B-1. - Propellant Grain Configuration of 260-in.-dia Motor

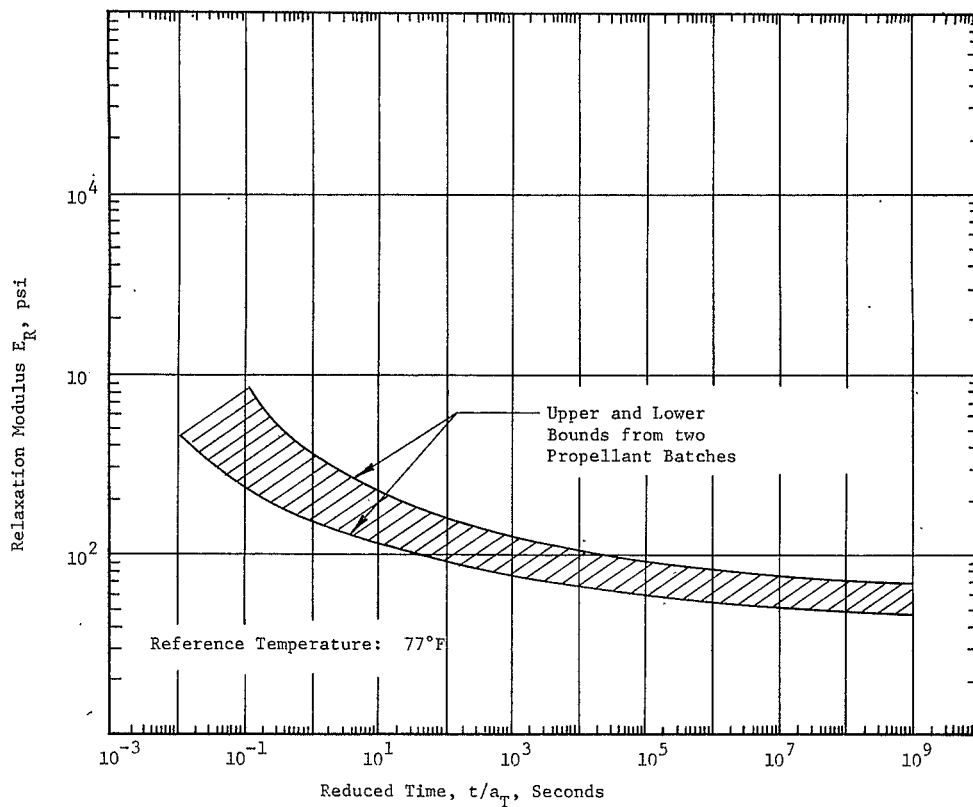


Figure B-2. - Master Relaxation Curve, ANB-3105 Propellant

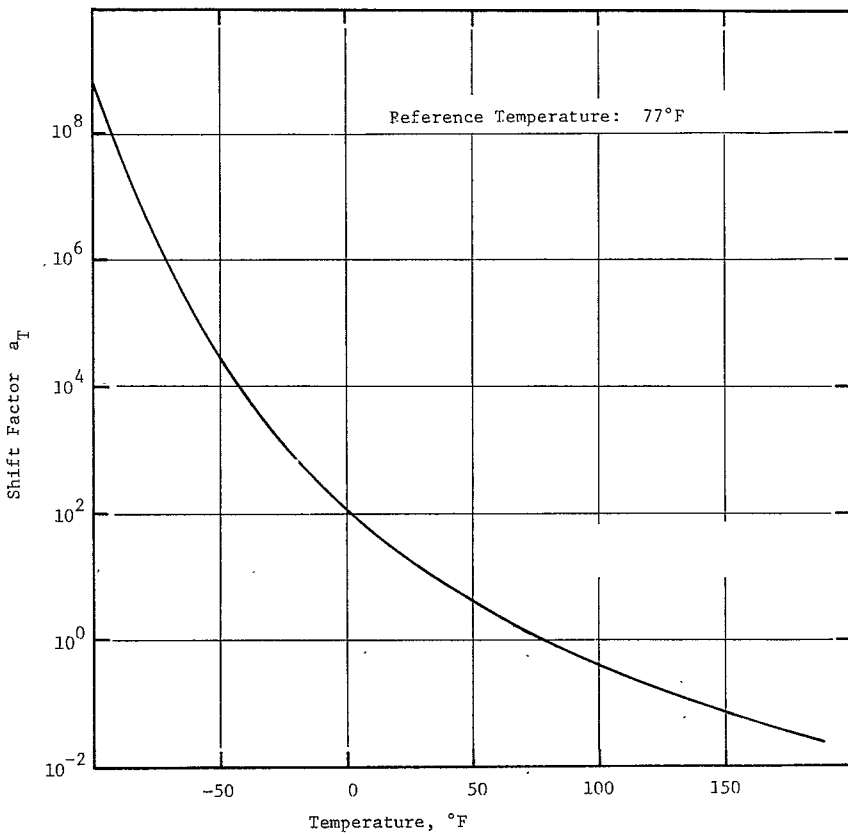


Figure B-3. - Time-Temperature Shift Factor for ANB-3105 Propellant

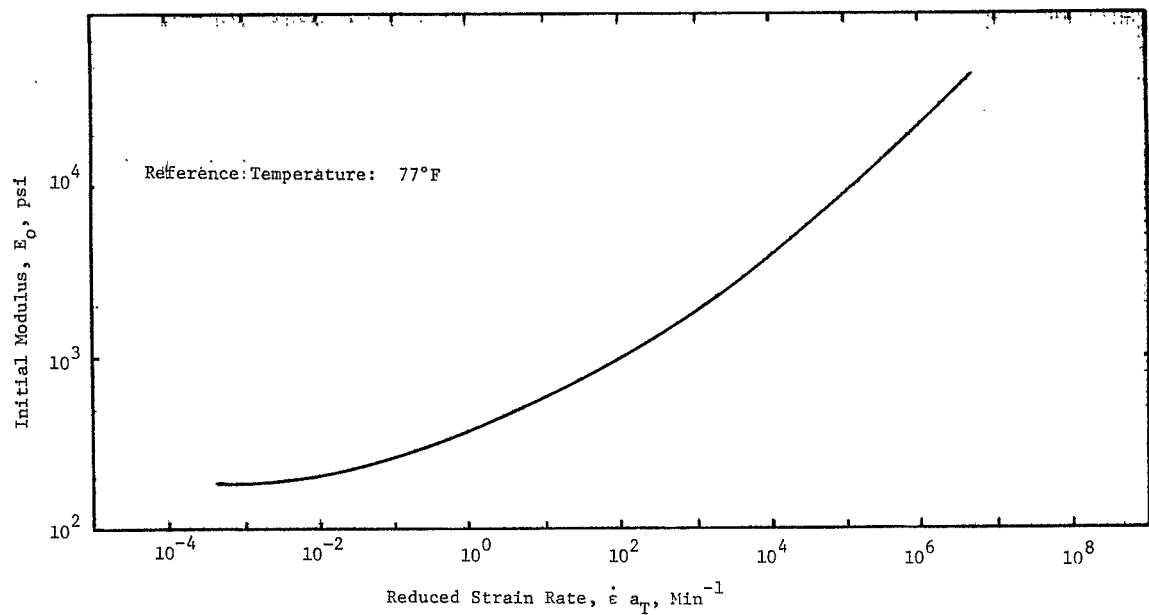


Figure B-4. - Initial Modulus vs Reduced Strain Rate for ANB-3105 Propellant

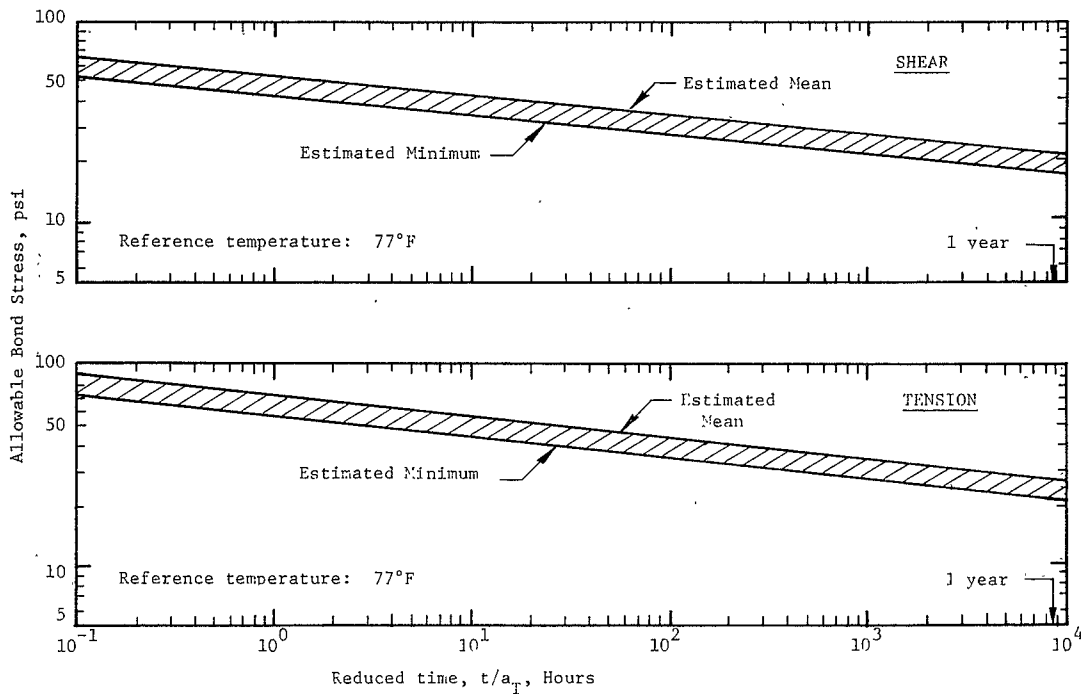


Figure B-5. - Allowable Bond Stresses for ANB-3105 Propellant

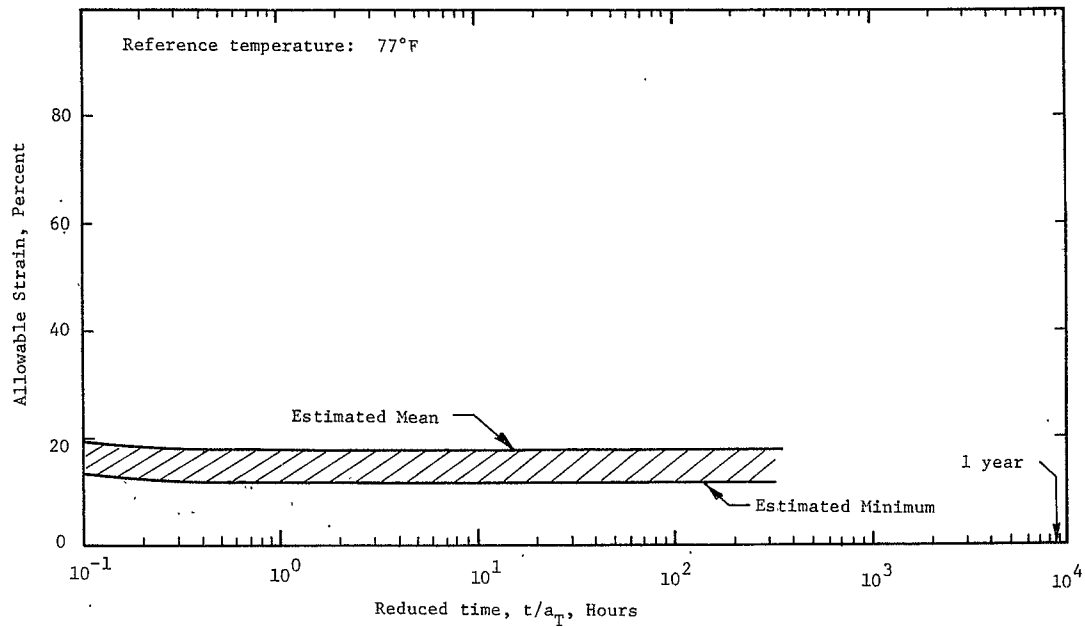


Figure B-6. - Allowable Storage Strain for ANB-3105 Propellant

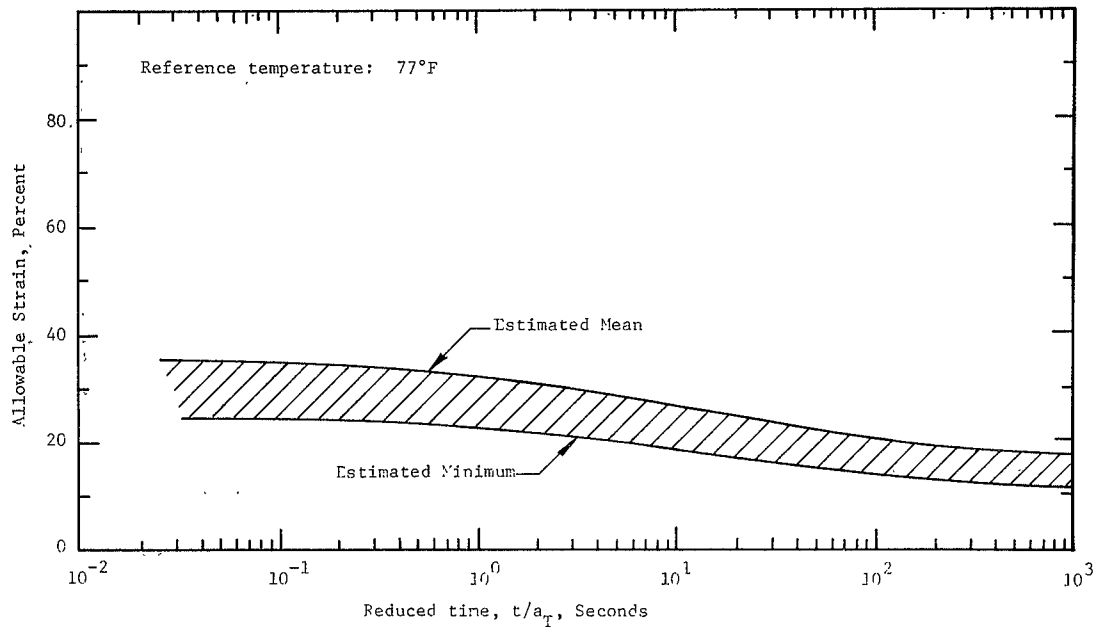


Figure B-7. - Allowable Strain for High Rate Acceleration
Loading for ANB-3105 Propellant

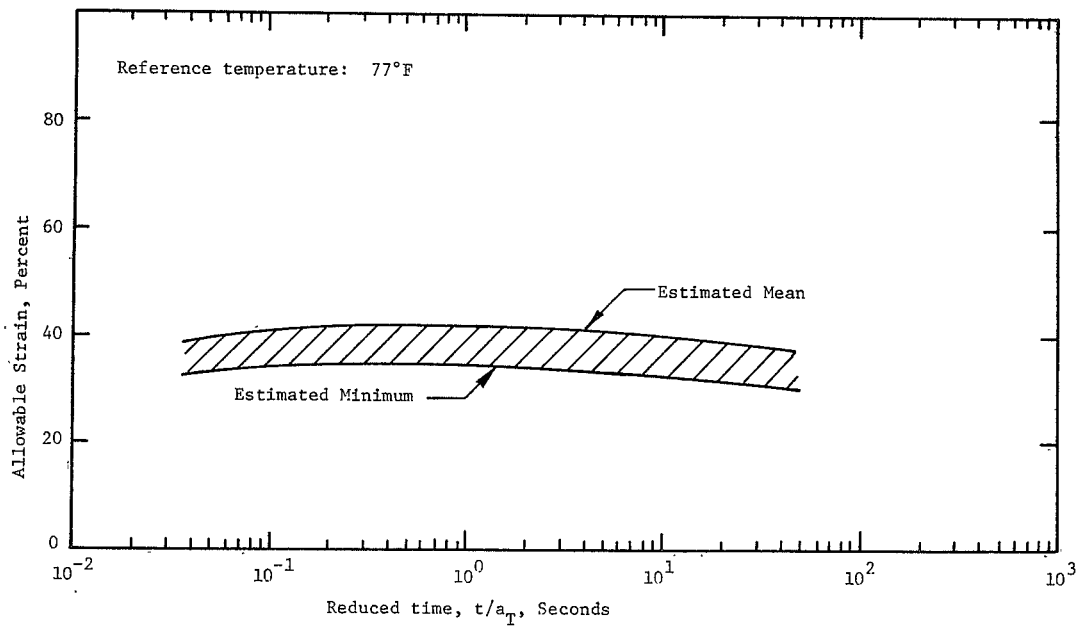


Figure B-8. - Allowable Strain for Firing for ANB-3105 Propellant

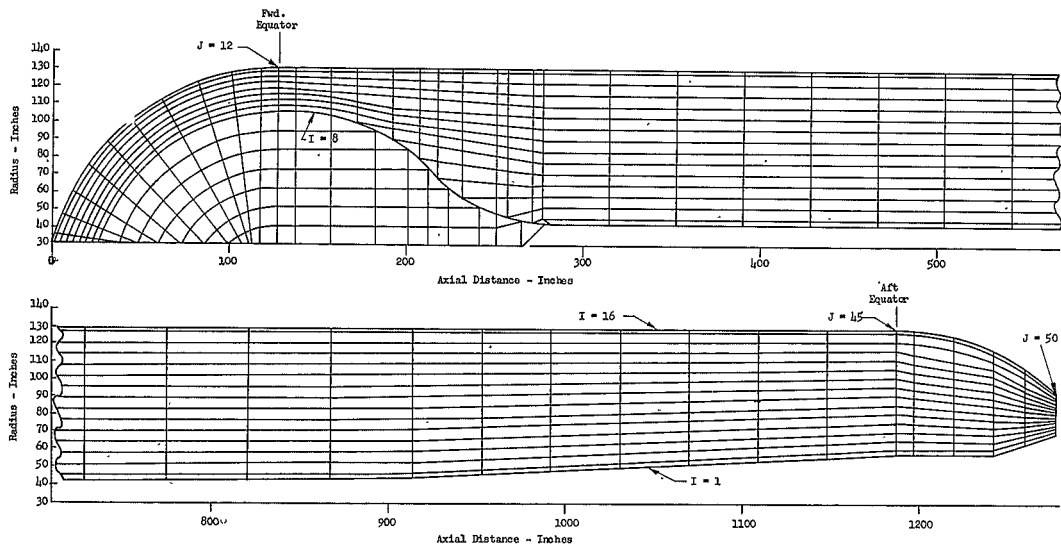


Figure B-9. - Axisymmetrical Analysis Configuration With Fully Bonded Insulation
260-in.-dia Propellant Grain and Chamber Finite Element Grid System

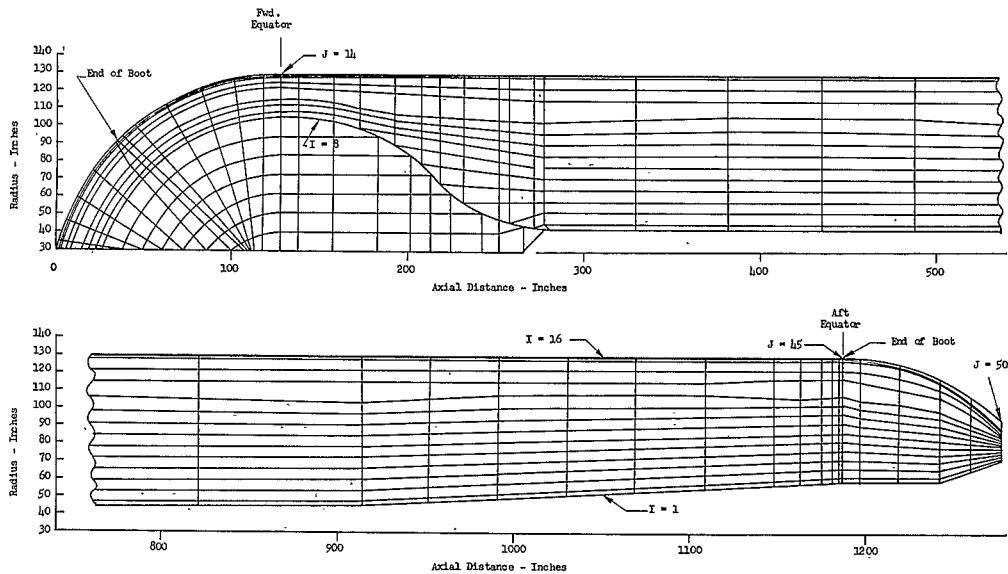


Figure B-10. - Axisymmetrical Analysis Configuration With Booted Insulation,
260-in.-dia Propellant Grain and Chamber Finite Element Grid System

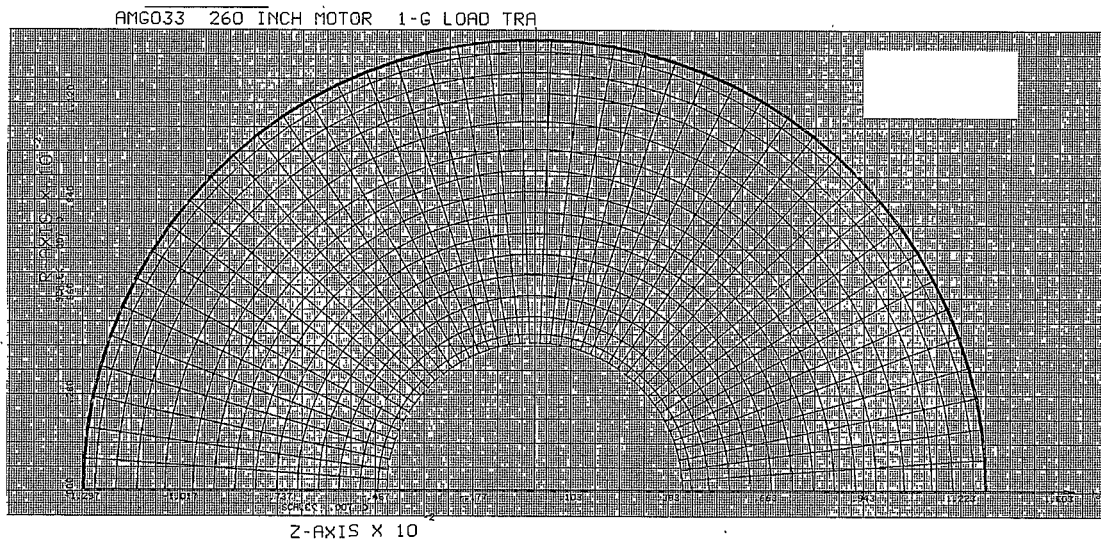
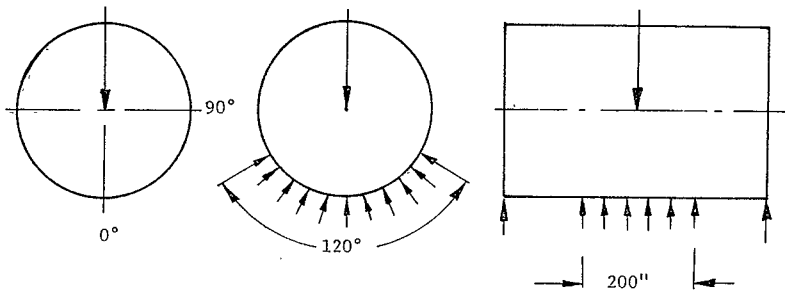


Figure B-11. - Finite Element Grid Used in Plane Strain Analysis of
Propellant Grain Cross Section



120° Central Support over a 200'' Length
 Supported @ Nodal Points 9 and 189 and
 1/3 Weight at Nodal Points 90, 99, 108, 117 and 126

$E_p = 234 \text{ psi}$

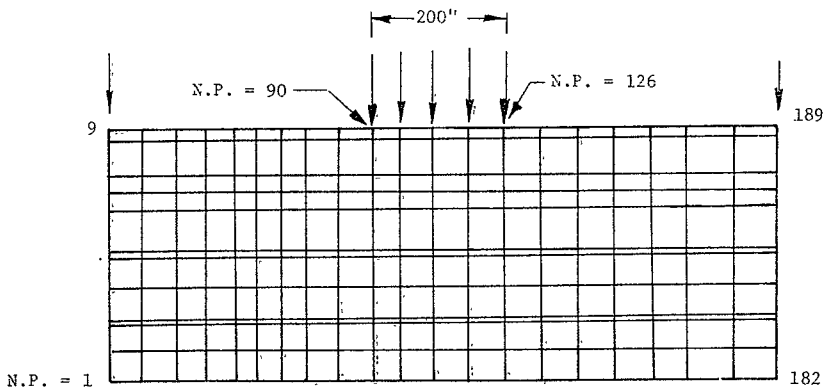


Figure B-12. - Nonaxisymmetric Load Analysis, Configuration
 with Fully Bonded Insulation,
 260-in-dia Stage,
 Simulated Propellant Grain and Chamber
 Finite Element Grid System

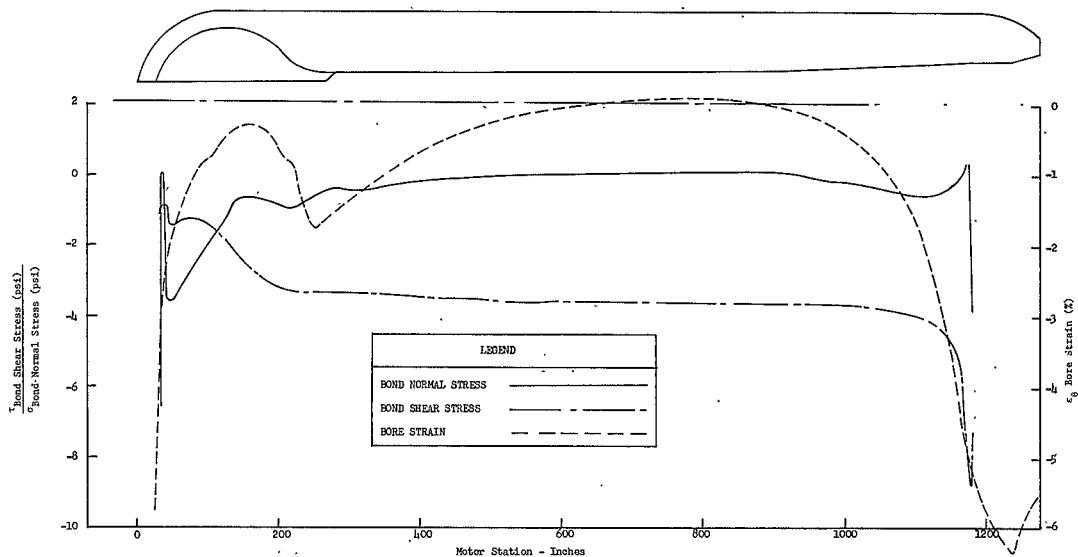


Figure B-13. - 260-in.-dia Motor With Booted Insulation and Skirt Support
 Propellant Bond Stress and Bore Strain Distribution
 for 1-g Axial ($E_p = 50$ psi)

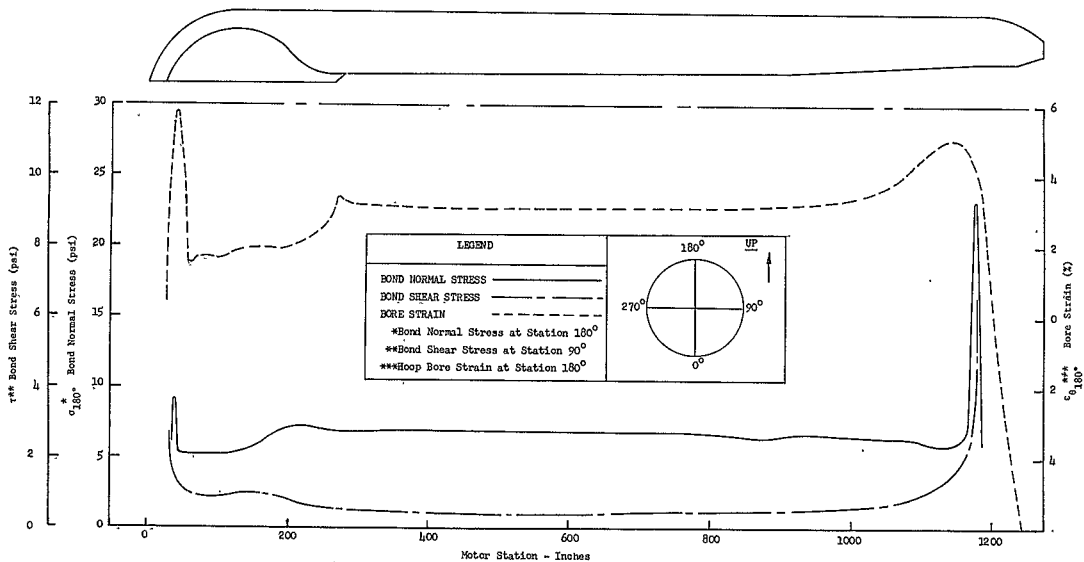


Figure B-14. - 260-in.-dia Motor With Booted Insulation and Skirt Support
 Propellant Bond Stress and Bore Strain Distribution
 for 1-g Transverse Load ($E_p = 50$ psi)

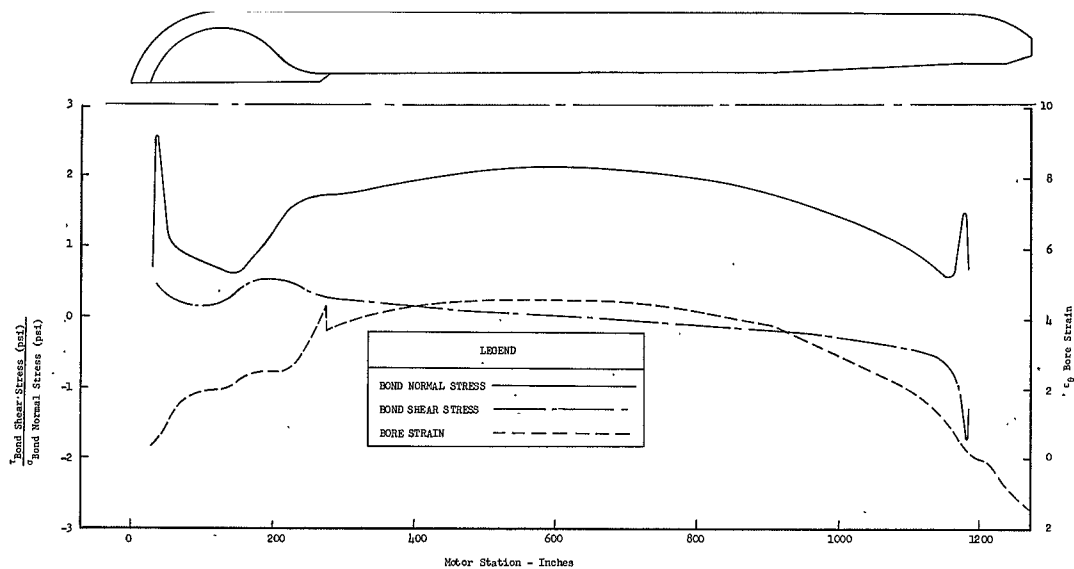


Figure B-15. - 260-in.-dia Motor With Booted Insulation and Skirt Support
 Propellant Bond Stress and Bore Strain Distribution
 Due to Thermal Loading ($\Delta T = -80^{\circ}\text{F}$, $E_p = 70 \text{ psi}$)

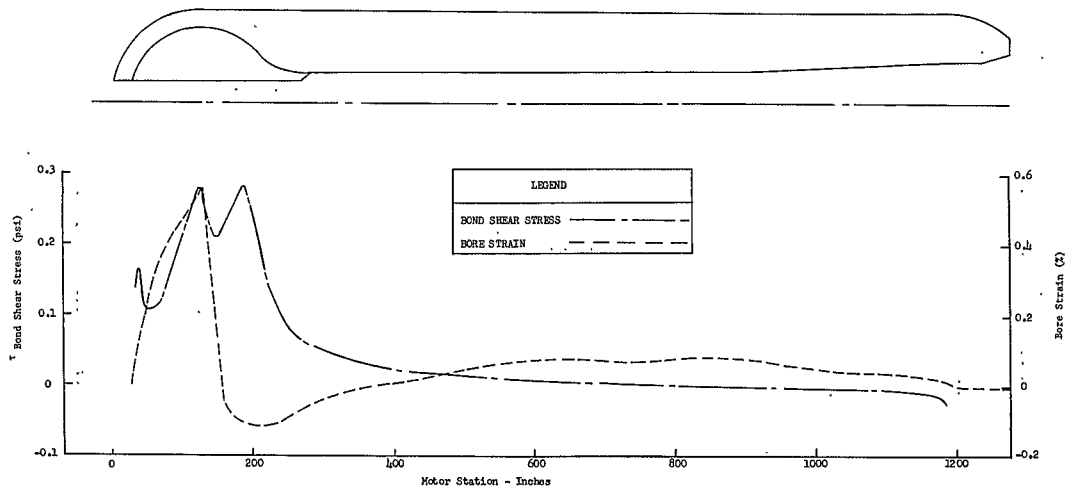


Figure B-16. - 260-in.-dia Motor With Booted Insulation and Skirt Support
 Propellant Bond Shear Stress and Bore Strain Distribution
 for Internal Pressure ($\Delta P = 10$ psi, $E_p = 90$ psi)

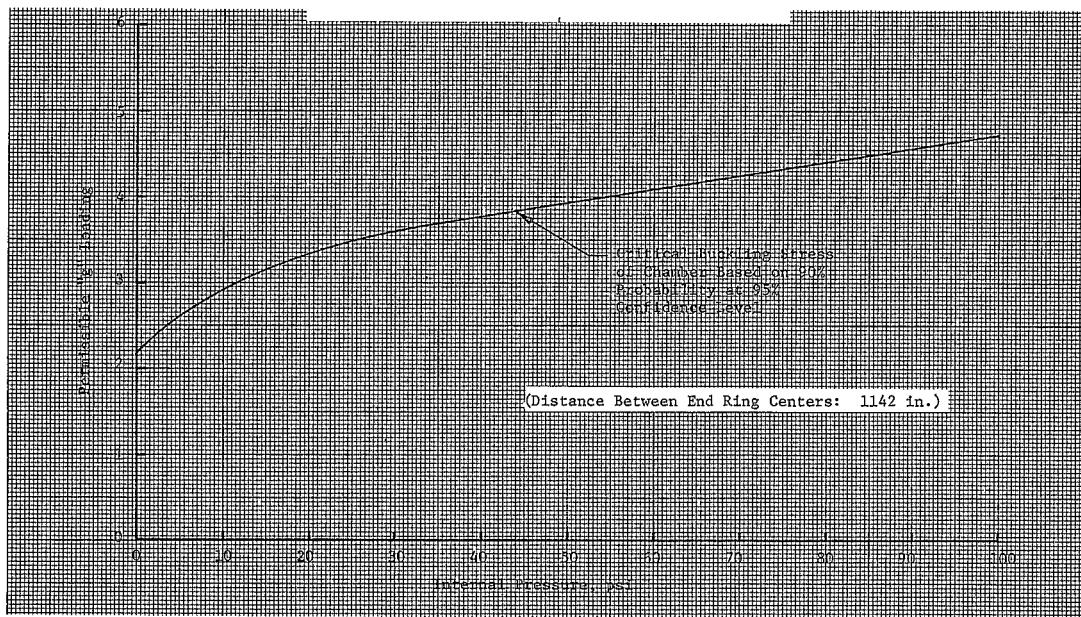


Figure B-17. - Permissible g Load vs Internal Pressure for 260-in.-dia Motor in Horizontal Position and Supported Only by End Rings on Skirts

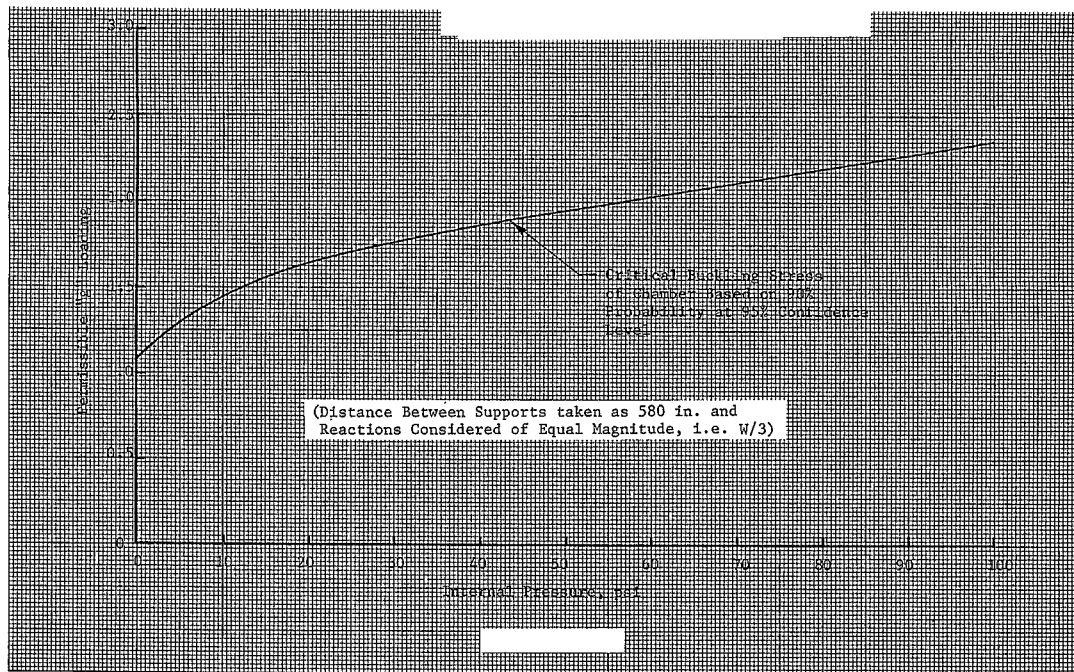


Figure B-18. - Permissible g Load vs Internal Pressure for 260-in.-dia Motor in Horizontal Position With Three Supports

TASK I, HANDLING-METHOD ASSESSMENT AND TRADE STUDY

I. INTRODUCTION

This appendix provides the results of the comparative assessment of the major elements included in the three handling methods identified in Task I and the engineering trade-study accomplished to select the optimum handling method. The major elements of each handling method were evaluated, rather than each of the three handling methods in total, so that the optimum elements of either handling method could be selected in the trade-study to form the optimum handling method.

The assessment criteria and the engineering trade-study are shown in table form. Where applicable, back-up information relative to each assessment criterion are provided following the criterion assessment summary table. The assessment criteria are presented in the tables listed below:

Total Estimated Recurring and Nonrecurring Cost	-	Table C-1
Estimated Cost for Flexibility	-	Table C-2
Risk of Unsuccessful Development	-	Table C-3
Risk of Motor Damage Due to Imposed Loads, Weather and Human Factors	-	Table C-4
Logistics and Schedule Problems	-	Table C-5
Safety Hazards	-	Table C-6
Development Time	-	Table C-7

The results of the comparative assessments were included in the engineering trade-study (Table C-8). The assessment criteria were weighted in the trade-study according to the relative importance of each criterion. The selection of the optimum handling method, based on the trade-study results, is as follows:

I. Introduction (cont)

2000-ton derrick at DCP

Roll-Ramp mobile gantry at KSC

New transport barge

Truck-rail stage transporter

Internal pressure mid-cylinder support (if required)

TABLE C-1 -- TOTAL ESTIMATED RECURRING AND NONRECURRING COSTS
(EXCLUDING DESIGN COSTS)

Item	Tooling, Equipment and Facilities											
	Winch	2000-Ton		Gantry		ARD	New	Roller	Truck-Rail	Midcylinder Support		
	System	Derrick										
	DCP, Only	DCP	KSC	DCP	KSC	Barge	Barge	Transporter	Transporter	Pressure	Bladder	Sling
Total Cost	56.5	90	90	31.9	63.2	90	59.6	90	71.5	90	24.6	42.9

TABLE C-2 - ESTIMATED COST FOR FLEXIBILITY

Item	Tooling, Equipment and Facilities											
	Winch	2000-Ton		Gantry		ARD	New	Roller	Truck-Rail	Midcylinder Support		
	System	Derrick										
	DCP, Only	DCP	KSC	DCP	KSC	Barge	Barge	Transporter	Transporter	Pressure	Bladder	Sling
*Cost Modifications for 1.6M and 5.0M lb Propellant Weight Motors	90.0	83.8	67.4	49.5	90.0	90	62.8	90	67.8	90	20.4	35.7

*Includes nonrecurring cost only.

TABLE C-3 - RISK OF UNSUCCESSFUL DEVELOPMENT SUMMARY TABLE

<u>Item</u>	<u>Tooling, Equipment and Facilities</u>											
	<u>Winch System</u>	<u>2000-Ton Derrick</u>		<u>Gantry</u>		<u>ARD</u>	<u>New</u>	<u>Roller</u>	<u>Truck-Rail</u>	<u>Midcylinder Support</u>		
	<u>DCP, Only</u>	<u>DCP</u>	<u>KSC</u>	<u>DCP</u>	<u>KSC</u>	<u>Barge</u>	<u>Barge</u>	<u>Transporter</u>	<u>Transporter</u>	<u>Pressure</u>	<u>Bladder</u>	<u>Sling</u>
A. State-of-the-Art	90	75	75	75	75	60	90	70	80	90	80	70
B. Number of Major Elements	90	60	40	40	40	-	-	60	80	90	70	90
C. Number of Required Functions	90	70	40	60	60	-	-	90	60	90	60	60
D. Size (Capacity) Required Compared to Existing Items	90	80	80	90	90	70	70	-	-	-	-	-
E. Status of Fabrication Techniques	90	80	80	70	70	80	90	90	90	90	70	70
F. Confidence in Estimated Costs	90	90	70	80	80	60	80	75	75	90	70	70
Total	540	455	385	415	415	270	330	385	385	450	350	360
Avg.	90.0	75.8	64.1	69.1	69.1	67.5	82.5	77.0	77.0	90.0	70.0	72.0

II. RISK OF UNSUCCESSFUL DEVELOPMENT

A. STATE-OF-THE-ART

1. Winch System at DCP (Handling Method No. 3)

Lifting requirement is 2000 tons. Winches at each trunnion are 500 tons at each of the forward trunnions and 1000 tons at each of the aft trunnions. The 1000-ton requirement is well within the winch system requirements of the off-the-shelf 1000-ton stiffleg derrick.

rating = 90

2. 2000-Ton Derrick at DCP and KSC

Stiff-leg derricks of 1000-ton capacity are commercially available from the American Hoist and Derrick Co. Development of the 2000-ton derrick involves the installation of two separate 1000-ton derricks side-by-side and reeving of cables between booms so that the two booms act as one derrick. Critical development item is the demonstration that the individual booms will carry an equal load.

rating = 75

3. Mobile Roll-Ramp Gantry

The Roll-Ramp actuators with required load capacity are commercially available. Also, the wheels, rails and foundation requirements for the mobile aspects of the gantry are available. Critical development item of the gantry is combining stem of actuator to obtain length of travel required to rotate the stage from horizontal to vertical.

rating = 75

II.A. State-of-the-Art (cont)

4. ARD Barge Modifications

Based on available published data, the ARD is expected to have the length, width and draft characteristics required for the 260-in.-dia stage. The critical area within the state-of-the-art is expected to be associated with determining existing deterioration, the "as-built" structural capacities, and the structural integrity of the existing barges.

rating = 60

5. New Barge

The design and fabrication of a new barge is within the existing state-of-the-art.

rating = 90

6. Roller Transporter Concept

The roller transporter is based on the concept of moving heavy objects over rolling members that has been used in many existing commercial applications. Critical areas of development are expected in obtaining smooth and lasting road bed and in being able to make turns.

rating = 70

7. Truck-Rail Transporter

The truck-rail transporter concept is commercially used in many ways; e.g., railroad cars, mobile gantries. The critical area of

II.A. State-of-the-Art (cont)

development is expected to be in the suspension system that will pivot to make gradual turns and that will allow slight independent vertical movement of the wheels to assure equal load distribution.

rating = 80

8. Midcylinder Support, Pressure

Widely used system. State-of-the-art exists and may have only minor difficulty with nozzle seal.

rating = 90

9. Midcylinder Support, Bladder

Sometimes used in full circumference to transport smaller motors of the Polaris size. Difficulty in assuring that expansion of bladder under loads is such that support load distribution to the case is uniform.

rating = 80

10. Midcylinder Support, Sling

Widely used in typically noncritical applications. Difficulty is in establishing the desired preload and then making the sling tension automatically adjustable to provide a uniform support load to the case during various service conditions.

rating = 70

II. Risk of Unsuccessful Development (cont)

B. NUMBER OF MAJOR ELEMENTS

1. Winch System

Elements - foundation, winches, cable system

rating = 90

2. Derrick

Elements - DCP: foundation, winches, cable system and booms. .

rating = 60

Elements - KSC: foundation, winches, cable system, booms,
additional pad foundation, rail support structure, and assembly and disassembly
equipment for derrick storage.

rating = 40

3. Gantry, DCP and KSC

Elements - foundation, trucks, rails, gantry structure,
actuator mechanisms, lift beam and load slings.

rating = 40

4. ARD Barge

Not applicable, ARD and new barge same.

5. New Barge

Not applicable, ARD and new barge same.

II.B. Number of Major Elements (cont)

6. Roller Transporter

Elements - support structure, minimum of 24 sets of rollers, roadway foundation.

rating = 60

7. Truck-Rail Transporter

Elements - support structure, trucks, rails, foundation.

rating = 80

8. Midcylinder Support - Pressure

Elements - gas, forward plug, aft plug, pressure regulator.

rating = 90

9. Midcylinder Support - Bladder

Elements - gas, pressure regulator, bladder, support structure, load transfer structure to cradles.

rating = 70

10. Midcylinder Support - Sling

Elements - sling, attach structure, load transfer structure, load adjusting system.

rating = 90

C. NUMBER OF REQUIRED FUNCTIONS

Winch System

Functions - lift

rating = 90

II.G. Number of Required Functions (cont)

2. Derrick

Functions - DCP, lift and boom.

rating = 70

Functions - KSC, lift, boom, disassemble, and reassemble.

rating = 40

3. Gantry, DCP and KSC

Functions - lift, boom, and transport.

rating = 60

4. ARD Barge

Not applicable, same as for new barge.

5. New Barge

Not applicable, same as for ARD barge.

6. Roller Transporter

Functions - support stage.

rating = 90

7. Truck-Rail Transporter

Functions - support stage, powered movement, and braking.

rating = 60

II.C. Number of Required Functions (cont)

8. Midcylinder Support, Pressure

Functions - regulate prèssuré.

rating = 90

9. Midcylinder Support, Bladder

Functions - structural support and regulate pressure.

rating = 60

10. Midcylinder Support, Sling

Functions - structural support and adjust load.

rating = 60

D. SIZE (CAPACITY) REQUIRED COMPARED TO EXISTING ITEMS

1. Winch System

Available. rating = 90

2. Derrick, DCP and KSC

1000-ton available - required to combine two derricks.

rating = 80

3. Gantry, DCP and KSC

Size available in both capacities and heights.

rating = 90

II.D. Size (Capacity) Required Compared to Existing Items (cont)

4. ARD Barge

Perhaps larger than needed. High sail area will present navigation problem in cross-wind.

rating = 70

5. New Barge

Barges with existing cargo capacity available, but not with load distribution structure required.

rating = 70

6 through 10

Remainder of items (transporters and midcylinder supports) are considered not applicable since similar items are not known to exist.

E. STATUS OF FABRICATION TECHNIQUES

1. Winch System

Currently available.

rating = 90

2. Derrick, DCP and KSC

Fabrication of 1000-ton available -- develop techniques of joining two 1000-ton derricks.

rating = 80

II.E. Status of Fabrication Techniques (cont)

3. Gantry, DCP and KSC

Fabrication of mechanisms available. Fabrication and assembly of stems may require some development.

rating = 70

4. ARD Barge

Existing structure and structural materials may be difficult to ascertain.

rating = 80

5. New Barge

Fabrication technique is completely developed.

rating = 90

6. Roller Transporter

Fabrication technique is available.

rating = 90

7. Truck-Rail Transporter

Fabrication technique is available.

rating = 90

8. Midcylinder Support, Pressure

Fabrication technique available.

rating = 90

II.E. Status of Fabrication Techniques

9. Midcylinder Support, Bladder

Bonding bladder to structure and fabrication of bladder to assure controlled deformation under load may require some development.

rating = 70

10. Midcylinder Support, Sling

Fabrication of load adjusting system may require some development.

rating = 70

F. CONFIDENCE IN ESTIMATED COSTS

1. Winch System

Available components - Support structure may become complex.

rating = 90

2. Derrick

DCP - Actual experience with 300-ton derrick

rating = 90

KSC - Complex because of proximity of derrick foundation to support pedestal foundation and because of necessity to remove and store derrick 30 times.

rating = 70

3. Gantry, DCP and KSC

Complexity may develop with stem

rating = 80

II.F. Confidence in Estimated Costs (cont)

4. ARD Barge

Unknown condition of barge.

rating = 60

5. New Barge

Estimate based on quick-look advanced estimate.

rating = 80

6. Roller Transporter

Difficulties could arise with roller design and fabrication.

rating = 75

7. Truck-Rail Transporter

Difficulties may arise with pivot bearings, if used, and hydraulic suspension system.

rating = 75

8. Midcylinder Support, Pressure

Minor difficulties may occur with leaks.

rating = 90

9. Midcylinder Support, Bladder

Possible bladder material and fabrication problems may occur.

rating = 70

10. Midcylinder Support, Sling

Possible problems in obtaining an automatic load adjusting mechanism.

rating = 70

TABLE C-4 - RISK OF MOTOR DAMAGE DUE TO IMPOSED LOADS, WEATHER AND HUMAN FACTORS

Item	Tooling, Equipment and Facilities											
	Winch System	2000-Ton Derrick		Gantry		ARD	New	Roller	Truck-Rail	Midcylinder Support		
	DCP, Only	DCP	KSC	DCP	KSC	Barge	Barge	Transporter	Transporter	Pressure	Bladder	Sling
A. Stage Loads Imposed	90	60	60	60	60	-	-	70	90	90	70	50
B. Control of Load Input to Stage	90	80	80	70	70	-	-	90	90	90	75	60
C. Damage Potential During Inclement Weather	90	80	80	80	80	70	90	70	90	-	-	-
D. Number of Stage Handling Equipment Operations	90	90	30	75	75	-		50	90	70	70	70
E. Complexity of Operations	80	90	50	70	70	70	90	40	90	90	90	70
F. Complexity of Handling Equipment Required	85	85	40	60	60	60	80	80	70	80	80	60
Total	525	485	340	415	415	200	260	400	520	420	385	310
Avg	87.5	80.8	56.6	69.1	69.1	66.0	86.6	66.6	86.6	84.0	77.0	62.0

III. RISK OF MOTOR DAMAGE

A. STAGE LOADS IMPOSED

1. Winch System

Vertical lift and rotating loads

rating = 90

2. Derrick, DCP and KSC

Vertical lift, rotating loads and tension load from
uncoordinated rotation.

rating = 60

3. Gantry

Vertical lift, rotating loads and tension load from
uncoordinated rotation.

rating = 60

4. ARD Barge

Not applicable - same as New Barge

5. New Barge

Not applicable - same as ARD Barge

6. Roller Transporter

Vertical support - vertical and longitudinal accelerations are
expected to be slightly higher than truck rail because of alignment of roller
pads and external drive force.

rating = 70

7. Truck-Rail Transporter

Vertical support load.

rating = 90

III.A. Stage Loads Imposed (cont)

8. Midcylinder Support, Pressure

Uniform internal pressure causes shear at propellant bond line and inner bore strain. Loads are minor.

rating = 90

9. Midcylinder Support, Bladder

Uniform external band load plus addition case local bending at edge of support.

rating = 70

10. Midcylinder Support, Sling

Nonuniform external band load, depending on shear load developed between sling and case. Local bending stress at edge of support.

rating = 50

B. CONTROL OF LOAD INPUT TO STAGE

1. Winch System

Adjust cable load to maintain equal lift force.

rating = 90

2. Derrick

Equal lift load controlled by reeving drums together.

Tension load during rotation controlled by maintaining cable load within limit values.

rating = 80

3. Gantry

Equal lift load obtained by individual operation or actuators.

Tension load during rotation controlled by maintaining cable load within limit values.

rating = 70

III.B. Control of Load Input to Stage (cont)

4. ARD Barge

Not applicable - same as New Barge.

5. New Barge

Not applicable - same as ARD Barge.

6. Roller Transporter

Control of load input is by taking the time to assure alignment of roller pads and by limiting tug tractor force input.

rating = 90

7. Truck-Rail Transporter

Control of load input is by installing rails properly and by limiting the drive-truck force input.

rating = 90

8. Midcylinder Support, Pressure

Control of load is by regulation of internal pressure.

rating = 90

9. Midcylinder Support, Bladder

Control is by regulation of bladder pressure. No way to control edge bending load.

rating = 75

10. Midcylinder Support, Sling

Control is by automatically adjusting tension load in sling, fairly complex. No way to control edge bending.

rating = 60

III. Risk of Motor Damage (cont)

C. DAMAGE POTENTIAL DURING INCLEMENT WEATHER

1. Winch System

Stage is somewhat sheltered by winch structure. Damage potential during wind is light. Also, stage is always supported at four points.

rating = 90

2. Derrick

Stage can be supported at aft end only and is exposed during sudden high wind gusts. Damage potential is moderate.

rating = 80

3. Gantry

Stage can be supported at aft end only and is exposed during sudden high wind gusts. Damage potential is moderate.

rating = 80

4. ARD Barge

Damage potential is somewhat higher than for New Barge because of the high sail area of the ARD and the potential of running aground in sudden high crosswind gusts.

rating = 70

5. New Barge

Potential of running aground in cross-winds can be reduced since the new barge can be designed with a low sail area.

rating = 90

6. Roller Transporter

Handling of roller pads during periods of wind gusts is potentially hazardous.

rating = 70

III.C. Damage Potential During Inclement Weather (cont)

7. Truck-Rail Transporter

Potential hazards are light as compared to the roller transporter - no real hazards seen.

rating = 90

8. Midcylinder Support, Pressure

Not considered applicable

9. Midcylinder Support, Bladder

Not considered applicable

10. Midcylinder Support, Sling

Not considered applicable

D. NUMBER OF STAGE HANDLING EQUIPMENT OPERATIONS

1. Winch System

Raise vertically, rotate forward end, lower vertically to transporter, move transporter on barge.

rating = 90

2. Derrick

a. DCP

Raise vertically, boom to barge, lower vertically, rotate aft end.

rating = 90

b. KSC

Move stage to pad, rotate stage, raise vertically, boom over pad, lower vertically to pad. Also, using the derrick have to turn transporter around and have to assemble and disassemble after each launch.

rating = 30

III.D. Number of Stage Handling Equipment Operations (cont)

3. Gantry

Raise vertically, move over transporter, lower vertically, rotate, move on barge.

rating = 75

4. ARD Barge

Not applicable, same as New Barge

5. New Barge

Not applicable, same as ARD Barge

6. Roller Transporter

Install and remove roller pads and connect to braking tractors.

rating = 50

7. Truck-Rail Transporter

Actuate drive and braking truck

rating = 90

8. Midcylinder Support, Pressure

Install forward and aft plugs, pressurize, regulate pressure.

rating = 70

9. Midcylinder Support, Bladder

Install bladder, pressurize, regulate pressure

rating = 70

10. Midcylinder Support, Sling

Install sling, adjust preload, regulate load.

rating = 70

III. Risk of Motor Damage (cont)

E. COMPLEXITY OF OPERATIONS

1. Winch System

Complex to operate individual winches.

rating = 80

2. Derrick

Complex to control tension load in stage during rotation.

At KSC, complex to dismantle, store, protect, and reassemble for each launch.

rating = 90 at DCP and 50 at KSC

3. Gantry

Complex to operate minimum of four actuator mechanisms.

rating = 70

4. ARD Barge

May be more complex to navigate in channels than with new barge.

rating = 70

5. New Barge

May be less complex to navigate in channels than ARD Barge.

rating = 90

6. Roller Transporter

Complex to install, position, use and remove roller pads.

rating = 40

7. Truck-Rail Transporter

Truck-rail transporter used with little complexity.

rating = 90

III.E. Complexity of Operations (cont)

8. Midcylinder Support, Pressure

Use of internal pressure involves little complexity of operations.

rating = 90

9. Midcylinder Support, Bladder

Use of bladder involves little complexity of operations.

rating = 90

10. Midcylinder Support, Sling

Adjusting sling load is expected to be somewhat complex.

rating = 70

F. COMPLEXITY OF HANDLING EQUIPMENT REQUIRED

1. Winch System

Basic system is not complex. Protection during any static firing is somewhat complex.

rating = 85

2. Derrick

At DCP, more complex than winch. Not as complex to protect during static firing.

At KSC, very complex to protect during launch.

rating = 85 at DCP and 40 at KSC

3. Gantry

Basic actuation system is considerably more complex than either derrick or winch.

rating = 60

III.F. Complexity of Handling Equipment Required (cont)

4. ARD Barge

ARD barge is expected to be more complex due to reconstruction of the barge and existing features that are not required.

rating = 60

5. New Barge

New barge is not expected to be complex.

rating = 80

6. Roller Transporter

Roller transporter is expected to be somewhat less complex than truck-rail transporter.

rating = 80

7. Truck-Rail Transporter

Truck wheel suspension system complicates the transporter.

rating = 70

8. Midcylinder Support, Pressure

Nozzle plug adds to complexity.

rating = 80

9. Midcylinder Support, Bladder

Expected to be about same complexity as pressure.

rating = 80

10. Midcylinder Support, Sling

Load adjusting mechanism is expected to be complex.

rating = 60

TABLE C-5 - LOGISTICS AND SCHEDULE PROBLEMS SUMMARY TABLE

<u>Item</u>	<u>Tooling, Equipment and Facilities</u>											
	<u>Winch</u>	<u>2000-Ton</u>		<u>Gantry</u>		<u>ARD</u>	<u>New</u>	<u>Roller</u>	<u>Truck-Rail</u>	<u>Midcylinder Support</u>		
	<u>System</u> <u>DCP, Only</u>	<u>Derrick</u> <u>DCP</u>	<u>KSC</u>	<u>DCP</u>	<u>KSC</u>	<u>Barge</u>	<u>Barge</u>	<u>Transporter</u>	<u>Transporter</u>	<u>Pressure</u>	<u>Bladder</u>	<u>Sling</u>
A. Complexity of Operations	80	90	50	70	70	70	90	40	90	90	90	70
B. Number of Major Elements	90	60	40	40	40		-	60	80	90	70	90
C. Number of Stage Handling Equipment Operations	90	90	30	75	75	-		50	90	70	70	70
Total	260	240	120	185	185	70	90	150	260	250	230	230
Average	86.6	80.0	40	61.6	61.6	70	90	50	86.6	83.3	76.6	76.6

IV. LOGISTICS AND SCHEDULE PROBLEMS

A. COMPLEXITY OF OPERATIONS

Same as Assessment on Summary Table C-4, Risk of Motor Damage due to Imposed Loads, Weather and Human Factors, Item No. E.

B. NUMBER OF MAJOR ELEMENTS

Same as Assessment on Summary Table C-3, Risks of Unsuccessful Development, Item No. B.

C. NUMBER OF STAGE HANDLING OPERATIONS

Same as Assessment on Summary Table C-4, Number of Stage Handling Equipment Operations, Item No. D.

TABLE C-6 - SAFETY HAZARDS

<u>Item</u>	<u>Tooling, Equipment and Facilities</u>											
	<u>Winch</u>	<u>2000-Ton</u>		<u>Gantry</u>		<u>ARD</u>	<u>New</u>	<u>Roller</u>	<u>Truck-Rail</u>	<u>Midcylinder Support</u>		
	<u>System</u> <u>DCP, Only</u>	<u>DCP</u>	<u>KSC</u>	<u>DCP</u>	<u>KSC</u>	<u>Barge</u>	<u>Barge</u>	<u>Transporter</u>	<u>Transporter</u>	<u>Pressure</u>	<u>Bladder</u>	<u>Sling</u>
A. Design Reliability	87.5	80	57.5	67.5	67.5	60	85	75	75	85	80	65
B. Operational Simplicity	80	90	50	70	70	70	90	40	90	90	90	70
C. Stage Loads Imposed	90	60	60	60	60	-	-	70	90	90	70	50
Total	257.5	230	167.5	197.5	197.5	130	175	185	255	265	240	185
Average	85.8	76.6	55.8	65.8	65.8	43.3	87.5	61.6	85.0	88.3	80	61.6

V. SAFETY HAZARDS

A. DESIGN RELIABILITY

Average of Assessments "State-of-the-Art" from Summary Table C-3, Item A and "Complexity of Handling Equipment Required" from Summary Table C-4, Item F.

B. OPERATIONAL SIMPLICITY

Same as Assessment on Summary Table C-4, Item E, Complexity of Operations.

C. STAGE LOADS IMPOSED

Same as Assessment on Summary Table C-4, Item A, Stage Loads Imposed.

TABLE C-7 - DEVELOPMENT TIME SUMMARY TABLE
(Sheet 1 of 3)

Item	Tooling, Equipment and Facilities											
	Winch .	2000-Ton		Gantry		ARD	New	Roller	Truck-Rail	Midcylinder Support		
	System	Derrick										
	DCP, Only	DCP	KSC	DCP	KSC	Barge	Barge	Transporter	Transporter	Pressure	Bladder	Sling
Development Schedule (Including Design, Fabrication and Activation)	62	80	76	56	56	60	60	78	78	90	76	76

TABLE C-7 - DEVELOPMENT SCHEDULE (DESIGN INCLUDES DEVELOPMENT AND DESIGN)

(Sheet 2 of 3)

1.	Winch System		
	Design	-	9 mo
	Construct	-	14 mo
	Activate	-	2 mo
	Total	-	27 mo
	Rating	=	62
2.	2000-Ton Derrick		
	a. DCP		
	Design	-	2 mo
	Construct	-	12 mo
	Activate	-	4 mo
	Total	-	18 mo
	Rating	=	80
	b. KSC		
	Design	-	3 mo
	Construct	-	12 mo
	Activate	-	5 mo
	Total	-	20 mo
	Rating	=	76
3.	Gantry - DCP and KSC		
	Design	-	8 mo
	Construct	-	16 mo
	Activate	-	6 mo
	Total	-	30 mo
	Rating	=	56
4.	ARD Barge		
	Design	-	10 mo
	Construct	-	16 mo
	Activate	-	2 mo
	Total	-	28 mo
	Rating	=	60
5.	New Barge		
	Design	-	10 mo
	Construct	-	16 mo
	Activate	-	2 mo
	Total	-	28 mo
	Rating	=	60

TABLE C-7 - DEVELOPMENT SCHEDULE (DESIGN INCLUDES DEVELOPMENT AND DESIGN)

(Sheet 3 of 3)

6.	Roller Transporter		
	Design	-	6 mo
	Construct	-	12 mo
	Activate	-	1 mo
	Total	-	19 mo
	Rating	=	78
7.	Truck-Rail Transporter		
	Design	-	6 mo
	Construct	-	12 mo
	Activate	-	1 mo
	Total	-	19 mo
	Rating	=	78
8.	Midcylinder Support - Pressure		
	Design	-	6 mo
	Construct	-	6 mo
	Activate	-	1 mo
	Total	-	13 mo
	Rating	=	90
9.	Midcylinder Support - Bladder		
	Design	-	8 mo
	Construct	-	10 mo
	Activate	-	2 mo
	Total	-	20 mo
	Rating	=	76
10.	Midcylinder Support - Sling		
	Design	-	8 mo
	Construct	-	10 mo
	Activate	-	2 mo
	Total	-	20 mo
	Rating	=	76

TABLE C-8 - HANDLING METHOD TRADE STUDY

Item	Weight; %	Tooling, Equipment and Facilities											
		Winch	2000-Ton		Gantry		ARD	New	Roller	Truck-Rail	Midcylinder Support		
		System DCP, Only	Derrick DCP	KSC	DCP	KSC	Barge	Barge	Transporter	Transporter	Pressure	Bladder	Sling
1. Estimated Cost	100	56.5	90	90	31.9	63.2	90	59.6	90	71.5	90	24.6	42.9
2. Estimated Cost for Modifications to Handle 1.6 and 5.0M LB W _p Motors	40	36.0	33.5	26.9	19.8	36.0	36.0	25.1	36.0	27.1	36.0	8.2	14.3
3. Risk of Motor Damage	95	83.1	76.7	53.8	65.6	65.6	63.2	82.2	63.2	82.2	79.8	73.1	58.8
4. Safety Hazards	90	77.0	68.9	50.2	59.2	59.2	38.9	78.8	55.5	76.5	79.4	72.0	55.5
5. Risk of Unsuccessful Development	80	72.0	60.6	51.3	55.3	55.3	54.0	66.0	61.6	61.6	72.0	56.0	57.6
6. Logistics and Schedule Problems	70	60.6	56.0	28.0	43.2	43.2	49.0	63.0	35.0	60.6	58.2	53.7	53.7
7. Development Time	60	37.2	48.0	45.6	33.6	33.6	36.0	36.0	46.8	46.8	54.0	45.6	45.6
Totals		422.4	433.7	345.8	308.6	356.1	367.1	414.7	388.1	426.3	469.4	333.2	329.4
Selections			X			X		X		X	X		

OVERLAND TRANSPORTATION OF 260-IN.-DIA.
MOTOR SEGMENTS AT KSC-MILA AND CKAFS

I. INTRODUCTION

The proposed storage facility location and its relationship to LC-37B was reviewed with the thought of potential overland routes for movement of the 260-in.-dia. segments.

Three potential overland routes were evaluated, and the results of this analysis are presented as follows:

II. PRIMARY ROUTE (Figure D-1)

It is recommended that the solid segments be transported by barge to the solid rocket motor storage area adjacent to the Central Telemetry Station (Figure D-1, Point B). The segments would then be transferred by barge as required to a new LC-37 barge landing (Figure D-1, Point F). The segments would then be transferred using a newly designed eight-wheel road vehicle rated at 230,000 lb. per tire. The actual load per tire would not exceed 120,000 lb. This vehicle would transfer the segments from the LC-37 barge landing to the assembly point at the launcher (Figure D-1, Point G). The required 5000-ft roadway would be fabricated and designed to the same specifications as the LC-39 crawler way. The selective grading of the LC-39 roadway will support 100 psi at the crawler treads. The gross (ROM) cost estimate of this concept is as follows:

<u>Item</u>	<u>Each</u>	<u>Cost</u>
Barge - two required	\$1,500,000	\$3,000,000
Barge Ramp - LC-37	2,000,000	2,000,000
5000 ft. Roadway to LC-37 Launch Pad	1,200,000	1,200,000
Land Transporter - two req'd	400,000	800,000
		<u>\$7,000,000</u>

III. ALTERNATE ROUTE 1 (Figure D-2)

In accordance with Alternate Route 1, the segments would be stored within the storable holding area adjacent to the Central Telemetry Station (Figure D-2, Point B). The segments would be loaded in the barge and transported via the Banana River Canal to Point D of Figure D-2, where they would be off-loaded at Point E at the AF hangar barge ramp. A special transporter would then be utilized to transfer the 658,000 lb segment to LC-37B. The gross weight of the segment plus the transporter is estimated to be 908,000 lb. The maximum load permitted by Class B, limited access traffic, utilizing an eight wheel, double axle bogie, is 70,000 lb. Fourteen such bogies (or 112 wheels and tires) would be required to transport the segment from E to J to G (Figure D-2) using the Cape Road. The utilization of 14 bogies and 112 wheels and tires on one transporter is not feasible. If the vehicle could be designed and fabricated, the cost of the carrier would be prohibitive and the turn radius would require the rework of four turns along the proposed route. All power lines and telephone utilities would require relocation.

IV. ALTERNATE ROUTE 2 (Figure D-3)

In accordance with Alternate Route 2, the storable segments would also be held at Point B (Figure D-3) following the transport barge unloading operation. The segments would then be loaded on a pneumatic-tired transporter and moved to the assembly point at LC-37B over route B-H-I-E-J-G (Figure D-3). The route from I to E over the east NASA Causeway requires traversing a bridge that is limited to a 104,000 lb loading per the American Association of Highway Officials Manual. The bridge was designed to Condition H-20-S-16-44. Since the present vehicle is nine times the permissible vehicle weight, it would be necessary to redesign and rebuild the present causeway bridge. The cape roadways would again impose the same limitations described in Alternate Route 1 discussion.

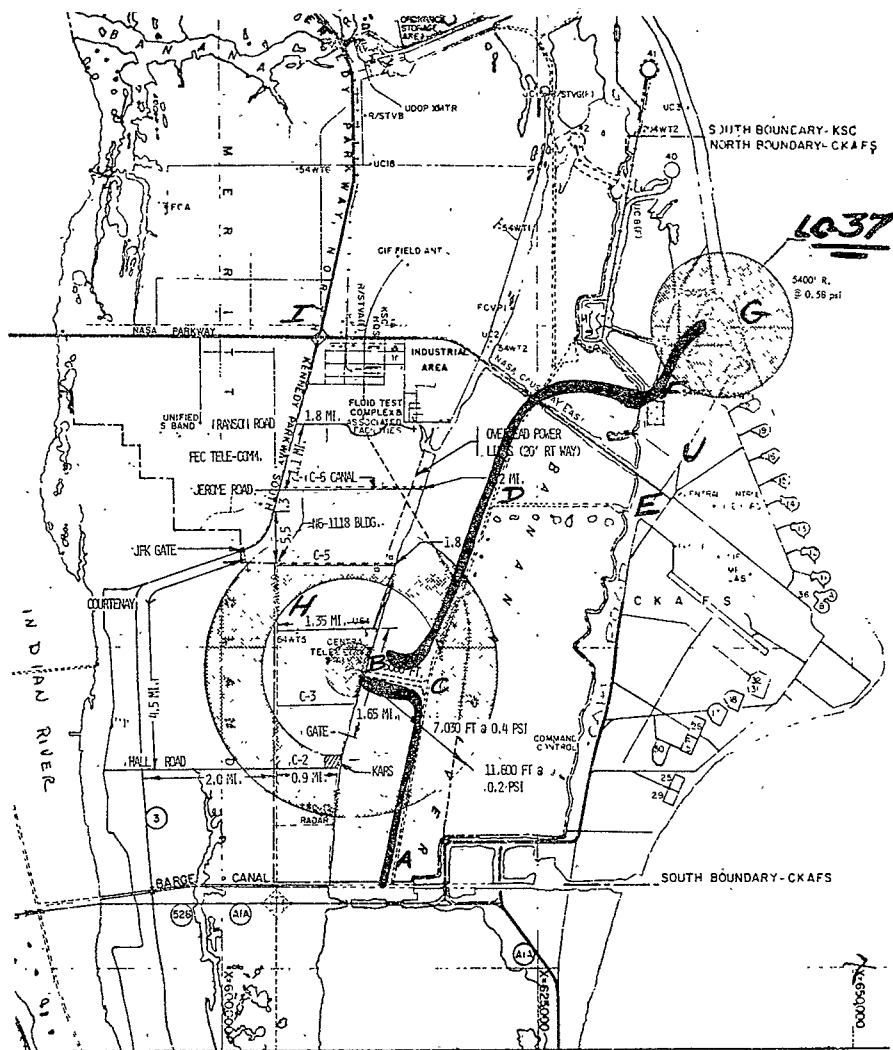


Figure D-1. - Primary Route - Recommended Relocation of Storage and Checkout Facility

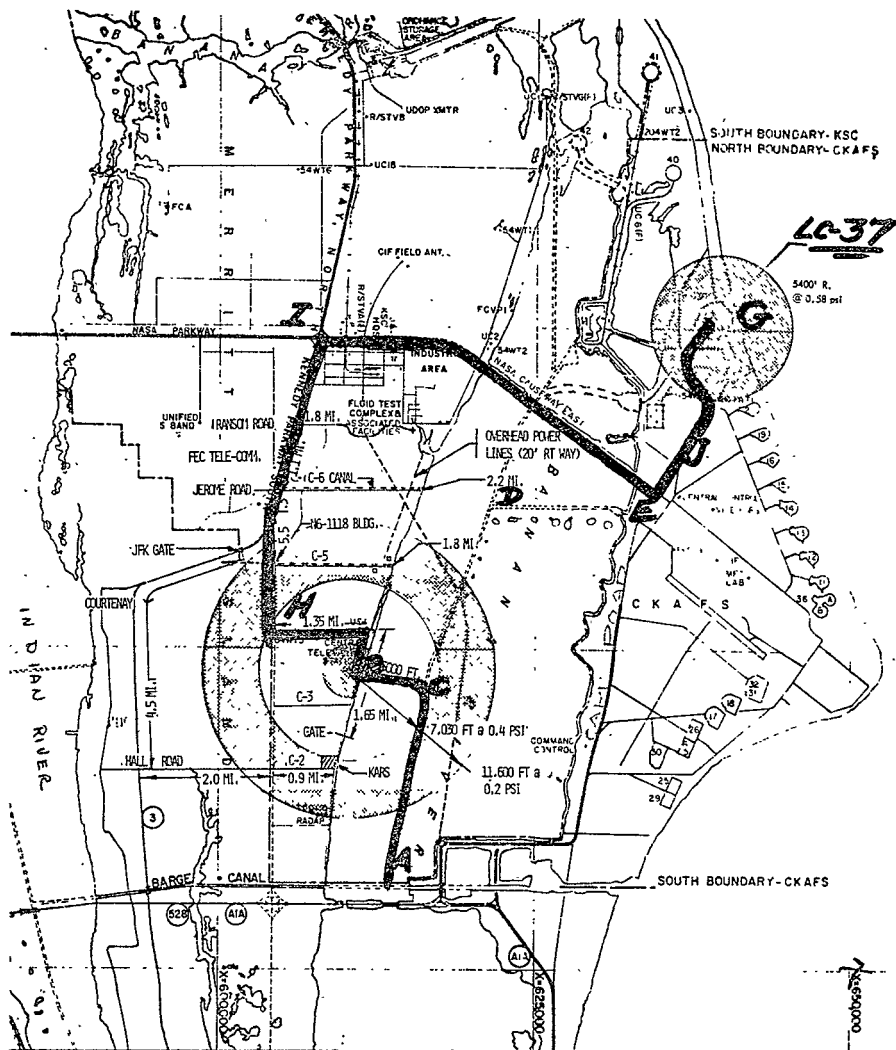


Figure D-3. - Alternate Route 2 - Recommended Relocation of Storage and Checkout Facility

DYNAMIC ANALYSIS OF THE 260-IN.-DIA STAGE
IN A BARGE-TRANSPORTATION ENVIRONMENT

I. INTRODUCTION

This report describes the dynamic analyses that were conducted as a part of the study of storage and handling of the 260-in.-dia solid rocket motor authorized by Contract NAS3-12052.

The overall objective of the dynamic analysis program was to evaluate the proposed barge transportation methods with respect to structural dynamic considerations and to recommend a method that would result in successful towed barge shipments of the 260-in.-dia motor.

The analyses were conducted for vibratory excitation environments for both the longitudinal and transverse axes. In all phases of the analyses it was assumed that the motor would be supported in a horizontal attitude on a rigid barge by rigid support rings bolted to the forward and aft motor skirts. The four barge transportation methods of the 260-in.-dia motor that were considered in this dynamic analysis program were:

- A. Internal Pressurization of the Motor
- B. Pneumatic Support of the Motor
- C. Structural Support at the Center of the Motor
- D. No Intermediate Support or Internal Pressurization

Emphasis was directed toward a comprehensive analytical determination of the propellant dynamic response characteristics and propellant dynamic stress. The method of dynamic analysis used in the study was based on a lumped-mass representation of the motor and propellant and a linear viscoelastic characterization of the propellant. Direct analog (force-current electromechanical analogy) circuit representations of the lumped-mass models of the motor were

I. Introduction (cont)

formed and the systems of linear algebraic equations derived from the analog circuits were solved at each selected discrete frequency on an IBM System 360/65 computer.

II. SUMMARY

The four barge transportation methods identified for the 260-in.-dia motor were evaluated with respect to the longitudinal and transverse axis vibration environments expected during barge transportation of the motor.

The results of the analyses showed the transverse axis dynamic loads to be considerably greater than the longitudinal axis loads during barge transportation of the motor.

The excitation frequencies associated with the towed barge transportation vibration environment are expected to occur at a frequency range of 0.1 to 9 cps (1). The calculated fundamental longitudinal and transverse axis resonant frequencies of the motor vary from 1.77 to 7.0 cps.

The results of the analyses showed that internal pressurization of 10 psi for Handling Method No. 1 had a negligible effect on the transverse axis structural stiffness characteristics of the motor. No significant change in either the fundamental transverse axis resonant frequency or dynamic amplification factor was calculated for the case in which the motor was internally pressurized to 10 psi. The capability of the motor to withstand the vibration environments expected during barge transportation would not be improved through internal pressurization of the motor.

* The list of references for this analysis are presented in Section VI of this appendix.

II. Summary (cont)

The addition of the intermediate pneumatic support (Handling Method No. 2) of the motor was shown to have a negligible effect on the dynamic response characteristics of the motor. The extremely low spring rate of the proposed pneumatic support system did not have a significant effect on the first transverse axis resonant frequency of the motor. The use of an intermediate pneumatic support system as identified in this study could not be recommended for barge transportation of the 260-in.-dia motor.

The major effort of this study was directed toward a structural dynamic evaluation of the effect of a structural support (Handling Method No. 3) installed at the center of the motor. Parametric studies were performed in the transverse axis of the motor for a series of structural support spring rates in the range of 2 to 12 million lb/in. The highest spring rate of 12 million lb/in. was considered to be the most effective and was used throughout this study. A value of 8% critical damping was assumed in this analysis for the intermediate motor structural support. The principal results obtained from this analysis are listed in comparative form in Table E-1 for the unsupported and supported motor configurations.

The results of the analysis show that the addition of an intermediate structural support has a negligible effect on the longitudinal axis dynamic response characteristics and on the maximum calculated dynamic propellant stresses.

The addition of the intermediate structural support produced the following changes in the transverse axis dynamic response characteristics of the motor as shown in Table E-1.

A. Increase in the fundamental transverse axis resonant frequency from 4.5 to 7.0 cps.

B. Decrease in the dynamic amplification factor at the transverse axis resonant frequency from 4.65 to 3.70 cps.

II. Summary (cont)

C. Small decreases in dynamic stress/g amplitudes for the maximum propellant-liner bond direct (25.6 to 20.5 psi/g) and shear (5.2 to 3.2 psi/g) stresses.

Although the changes in transverse axis dynamic response characteristics resulting from addition of the intermediate structural support are favorable changes, the reductions in propellant-liner-bond dynamic stresses are not of sufficient magnitudes to justify a recommendation for using the intermediate structural support.

It should be noted that an accurate definition of the vibration environment expected during barge transportation of the 260-in.-dia motor is not available at the present time. Barge transportation environmental data that were available during this study were the vibratory excitation frequencies and acceleration input levels recorded during the towed-barge shipment of the Saturn IV-5 vehicle (1). These data are not considered directly applicable to barge transportation of the 260-in.-dia motor, which weighs approximately 4 million lb. The occurrence of vibratory input levels greater than ± 1.0 g at frequencies in the range of 0.10 to 10.0 cps is considered to be highly improbable during barge transportation of the 260-in.-dia motor.

III. CONCLUSIONS

The objectives of the dynamic analysis were accomplished successfully.

The results of the analysis show that the 260-in.-dia motor, unpressurized and without an intermediate structural support, is capable of withstanding the vibration environments expected during towed-barge transportation.

IV. TECHNICAL DISCUSSION

A. DYNAMIC MODEL REPRESENTATIONS

IV.A. Dynamic Model Representations (cont)

1. General

The analytical configurations of the 260-in.-dia motor considered in this analysis were selected to represent the methods of structural support and vibratory excitation that will exist during towed barge transportation of the motor.

In all phases of the analysis it was assumed that the motor would be supported in a horizontal attitude on a rigid barge by rigid support rings bolted to the forward and aft motor skirts. The method of analysis and its related computer program (AGC #55000) would permit a flexible barge representation. It was not possible to obtain any valid transverse axis structural stiffness data for the barge considered in this 260-in.-dia motor study and the barge was assumed to be a rigid support platform. The two motor skirt support rings provided a pin-pin restraint condition on the motor with respect to the barge. A schematic drawing of the barge transportation configuration is shown in Figure E-1.

The structural support at the motor c.g. was represented as a linear elastic spring with spring rates ranging from 2 to 12 million lb/in. and a linear viscous damper with an 8% critical damping value. A spring rate of 12 million lb/in. was the maximum permissible value that could be considered in this analysis. The final results given in this report for the motor condition with the added structural support system were obtained using the maximum spring rate of 12 million lb/in.

2. Lumped Mass Representation of the Motor

a. Motor Case and Propellant

The detailed mass and geometrical data used in the dynamic model representation of the 260-in.-dia motor were obtained from Reference (2).

IV.A. Dynamic Model Representations (cont)

The weights of the principal motor components used in this analysis are listed in Table E-2.

The dynamic analysis for the 260-in.-dia motor is based on a lumped-mass representation of the motor. In this analysis the motor was subdivided into an appropriate number of cylindrical-type segments formed by making a series of vertical cuts at specified distances along the axis of the motor. A propellant wedge running along the axis of the motor and including the upper-half of the motor case and propellant is formed such that the forward and aft flat surfaces are 1-radian sections symmetrically centered about a vertical centerline of the motor. Figure E-2 shows the basic 1-radian propellant wedge element and the coordinate system that was used in this analysis. The generation angle of the elemental propellant wedge was taken to be 1-radian only as a convenience in computation. The forward and aft faces of each elemental propellant wedge were subdivided radially by a series of circular arcs. The mass of each propellant wedge is considered to be concentrated at the center of gravity of each elemental propellant wedge.

In this dynamic analysis, 11 vertical reference planes, 106 in. apart, were established along the longitudinal axis of the motor. Provisions were made for the location of as many as nine data read-out points located in a radial direction on each 1-radian wedge surface at each of the vertical planes. Additional data read-out points were established on the closures and on the nozzle.

b. Motor Closures

The forward and aft closures are represented in the analytical model by a series of truncated cones with mass and stiffness distributions of the actual motor closures.

IV.A. Dynamic Model Representations (cont)

c. Nozzle

For the 260-in.-dia motor dynamic analysis, the nozzle was represented as a single lumped mass that was directly attached to the flexible aft closure.

3. Analytical Characterization of the Motor Propellant

The dynamic mechanical properties of the motor propellant that were incorporated into the analytical dynamic model of the 260-in.-dia motor were derived from test data obtained from laboratory tests of specimens of ANB-3105 propellant. The propellant was characterized in the 260-in.-dia motor dynamic analysis by the four following quantities:

- a. Shear storage modulus (G') for a frequency range of 1 to 100 cps.
- b. Shear loss tangent G''/G' for a frequency range of 1 to 100 cps.
- c. Propellant density of 0.0625 lb/cu in.
- d. Poisson's ratio assumed to be a real quantity with a value of $1/2$.

The shear storage modulus and loss tangent distribution used to characterize the motor propellant were derived from laboratory vibration tests of propellant disc specimens and propellant reed specimens. The shear storage modulus and shear loss tangent distributions that were used to define the dynamic-mechanical properties of the motor propellant in this dynamic analysis are shown in Figures E-3 and -4, respectively, and the stress allowables for this propellant are given in Figure E-5. It should be noted that all

IV.A. Dynamic Model Representations (cont)

propellant mechanical property data were determined at a test temperature of 77°F. Detailed descriptions of the test methods used to conduct the propellant disc tests are given in Reference (3), and a discussion of the vibrating propellant reed test is given in Reference (4).

B. METHOD OF ANALYSIS

A detailed discussion of the analytical dynamic method and its related IBM System 360/65 computer program that was used in the dynamic analysis of the 260-in.-dia motor is given in Reference (5). A very brief description of this analytical dynamics method is given in the following paragraph.

A 1-radian wedge extending from the forward closure to the aft closure of the motor case is formed. This basic propellant wedge is subdivided axially to form a specified number of shorter wedges by making a specified number of vertical slices along the axis of the motor. In this particular analysis, nine vertical slices or vertical reference planes were established. The flat forward and aft surfaces of the incremental wedges were subdivided by a series of seven circular arcs to form a series of small incremental propellant wedges. The actual mass and elastic properties are determined for a propellant wedge whose length is twice the distance between the vertical reference planes. The calculated mass and elastic properties are assumed to be concentrated at the center of gravity of the wedge, and the areas of the surfaces of the incremental wedges are known quantities. The strain-displacement and stress-strain relations for both direct and shear stresses, together with the assumption that Poisson's ratio is 1/2, were written for each incremental wedge. Since the longitudinal axis analysis is an axisymmetric problem, only radial and axial displacements are involved. The transverse axis analysis is a non-axisymmetric problem and radial, axial, and circumferential displacements are involved. In general, the transverse axis analysis presents a problem of much greater complexity than that experienced in the longitudinal axis analysis. The strain-displacement and

IV.B Method of Analysis (cont)

stress-strain relations derived for the incremental propellant wedges are then written in finite difference form and electrical circuits are synthesized to satisfy the strain-displacement and stress-strain relations (in finite difference form) using the following electromechanical analogies:

Force - Current

Velocity - Voltage

Mass and Inertia - Capacitance

Structural Stiffness - Inverse of Inductance

Viscous Damping - Inverse of Resistance

Mechanical Coupling - Transformers

The constraints acting on a propellant incremental wedge as a result of motor case and closure geometry, adjacent wedges, or motion constraints are introduced into the circuit diagrams that represent accurate analogies of the strain-displacement and stress-strain relations so that the total resulting circuit diagram for a given propellant wedge satisfies all stress, strain, displacement, and constraint conditions.

The analytical model of the 260-in.-dia motor for the longitudinal and transverse axis steady-state dynamics analysis consists of two basic analog circuit diagrams: one for the longitudinal axis analysis, and one for the transverse axis analysis. The analytical model for the longitudinal axis analysis is represented in the form of two different, but not independent, analog circuit diagrams. Figure E-6 is the longitudinal axis circuit diagram for axial (Z) response, and Figure E-7 is the longitudinal axis circuit diagram for radial (R) response. Each circuit diagram shows the number and orientation of capacitors (masses), inductors (elastic and viscoelastic elements), and transformers (constraints) used to represent the dynamic response behavior of the actual motor in the axial and radial coordinates. The analog circuit diagram for the longitudinal axis analysis is presented as two separate circuit diagrams for ease and convenience in drawing and understanding the analytical

IV.B. Method of Analysis (cont)

analog model representation of the motor. When the longitudinal axis input data are properly assembled in the computer, the analytical model that the computer solves is one very complex circuit diagram consisting of the two circuit diagrams shown in Figures E-6 and -7. Three separate, but not independent, circuit diagrams are used to represent the dynamic model representation of the motor in the transverse axis analysis. Figures E-8, -9, and -10 are the transverse axis circuit diagrams for radial, axial, and circumferential responses, respectively. In a longitudinal axis analysis, the two circuit diagrams with proper numerical values assigned to electrical circuit elements to represent the mass properties, the structural damping, the elasticity, the viscoelastic properties of the propellant mass, the mass coupling, and the constraint conditions are entered into the computer. A sinusoidal unit displacement function is applied to the excitation input point of the model at one selected discrete frequency. The computer program then performs a summation of currents at every node of the circuit diagram and forms a set of N linear algebraic equations in N unknowns. With the use of special computer program routines, a solution of the set of linear algebraic equations is obtained for the one discrete excitation frequency being considered. The vector of the node displacements is determined and the remaining unknowns of the system may be found. In reference to the actual structural motor, the solution establishes the displacements of the nodes and the forces in the circuit elements used in the analog circuit model of the motor. Also, the shear stresses are determined immediately from the displacement and force solution for the nodes of the circuits. The direct stresses are obtained with the use of an auxiliary computer program that sums forces within elements and associates the forces with appropriate areas within the model. In the longitudinal axis dynamic analysis of the 260-in.-dia motor, the IBM System 360 computer required 9 minutes of computer time to obtain the solution of the circuits for the first discrete frequency of each study, and 1.3 minutes of computer time for each additional discrete frequency entered. In the transverse axis analysis, 19 minutes of computer time were required to obtain a solution of the circuits for the first entered discrete frequency, and 3.7 minutes were

IV.B. Method of Analysis (cont)

required for each additional discrete frequency. Additional computer time is required to print out stress magnitudes at a selected discrete frequency.

A definition of the symbols used in the analog circuit diagrams in the 260-in.-dia motor dynamic analysis is given in Figure E-11.

The number and locations of the axial and radial data read-out points within the longitudinal axis dynamic model are shown in Figure E-12. Similarly, the number and locations of the radial, axial, and circumferential data read-out points within the transverse axis dynamic model are shown in Figure E-13.

V. ANALYSIS RESULTS

A. LONGITUDINAL AXIS ANALYSIS

1. Resonance Response Analysis

A rigid body analysis was conducted in the longitudinal axis of the motor at a discrete excitational frequency of 0.1 cps to ensure that the analog circuit representation was properly entered into the computer program and that the program was operating satisfactorily. A satisfactory rigid body check at the discrete excitational frequency of 0.1 cps was obtained.

The initial resonance response analysis was conducted over a frequency range of 0.1 to 10 cps. A series of 20 selected discrete frequencies in the frequency range of 0.3 to 10 cps was entered into the computer and the acceleration responses of all nodes of the longitudinal axis analog circuit were determined for each discrete excitational frequency. The ± 1.0 g sinusoidal input function was applied in phase at each of the two motor support rings at nodes 1001 and 2002 (Figure E-6). This initial analysis showed the existence of a significant longitudinal axis resonance response of the propellant in the

V.A. Longitudinal Axis Analysis (cont)

frequency range of 1.6 to 2.0 cps. Detailed resonance response analyses performed in this narrow frequency band showed a resonance response peak at 1.77 cps. A maximum dynamic amplification factor of 2.79 was calculated at propellant node 1024 on the propellant bore near the center of the motor. The resonance response plot of propellant node 1024 is shown in Figure E-14.

Additional analyses conducted in the frequency range of 10 to 50 cps did not reveal any other propellant resonance responses in this extended frequency range. Analytical emphasis was directed to the 0.1 to 10 cps frequency range since the range of excitational frequencies associated with large transportation vibration environments are expected to be from 0.1 to 9 cps.

Resonance response plots similar to the plot shown in Figure E-14 could be made for each data read-out point included in the longitudinal axis circuit diagram (Figure E-12).

2. Modal Analysis

The longitudinal axis resonance response analysis revealed only one significant resonance response in the frequency range of 0.1 to 10 cps, the 1.77 cps resonance response that is characterized in Figure E-14.

The mode shape of the motor at the 1.77 cps resonant frequency is shown in Figure E-15. The acceleration response amplitudes of selected data read-out points of the longitudinal axis configuration for ± 1.0 g sinusoidal input functions applied axially to the motor support rings at the 1.77 cps resonant frequency are described numerically and graphically in Figure E-15. Each directed arrow symbol shown in Figure E-15 is drawn to scale so that the relative acceleration response amplitudes throughout the motor can be observed on a comparative basis at the excitational frequency of 1.77 cps. Phase angle relationships for all data read-out modes are shown in Figure E-15. The mode

V.A. Longitudinal Axis Analysis (cont)

shape plot of Figure E-15 shows the 1.77 cps mode to be a longitudinal axis propellant shear mode of the motor. The Figure E-15 plot shows the motor case nodes to be nearly in phase with the ± 1.0 g input functions and shows the propellant nodes to be approximately 90 degrees out-of-phase with respect to the ± 1.0 g input functions.

It should be noted that the dynamic response behavior of a complex heavily damped structure is quite different from the known and classical responses of highly damped single degree-of-freedom systems.

3. Dynamic Stress Analysis

Peak direct axial stresses and peak shear stresses were calculated at selected data read-out points for ± 1.0 g acceleration input levels applied at the motor support rings at the axial propellant resonant frequency of 1.77 cps. A graphic display of the peak axial direct (tension-compression) dynamic stresses calculated for the selected data read-out points is shown in Figure E-16, and a similar display of the corresponding peak dynamic shear stresses is shown in Figure E-17. Again it should be noted that arrow symbols of Figures E-16 and -17 are drawn to scale to show relative maximum stress amplitudes throughout the motor propellant for ± 1.0 g acceleration input functions applied axially at the support rings at 1.77 cps; the sense of the arrow symbols has no particular significance in this application.

The dynamic stress distributions presented in Figures E-16 and -17 show peak dynamic direct and shear stresses of 16.5 psi/g and 8.7 psi/g, respectively. These maximum stresses occur at the aft equator of the motor in the propellant-liner bond.

B. TRANSVERSE AXIS ANALYSIS

V.B. Transverse Axis Analysis (cont)

1. Resonance Response Analysis

A rigid-body check test was conducted at a discrete excitation frequency of 0.10 cps to determine if the transverse axis analog circuits were properly installed on the computer and if the computer program was operating satisfactorily. The rigid-body check test was completed satisfactorily.

A resonance response analysis was conducted in a frequency range of 0.1 to 10 cps for the unpressurized motor without a central structural support. A ± 1.0 g input sinusoidal function was applied in-phase at each motor support ring.

The results of this analysis showed a resonant frequency of 4.1 cps and a corresponding maximum dynamic amplification factor of 4.65 at case node 1028. The response plot of node 1028 is shown in Figure E-18. The response plot of propellant node 2044, located on the motor bore at the center of the motor, is shown in Figure E-19.

This analysis was repeated with an assumed structural support at the center of the motor. The vertical spring rate of the central structural support was 12 million lb/in. The results of this analysis are shown for case node 1028 and propellant node 2044 in Figures E-20 and -21, respectively.

Comparisons of the plots given in Figures E-18 through -21 show the following:

Motor Config.	<u>Case Node 1028</u>		<u>Case Node 2044</u>	
	<u>Res Freq (cps)</u>	<u>D.A.F.</u>	<u>Res Freq (cps)</u>	<u>D.A.F.</u>
Without Support	4.5	4.65	4.5	2.07
With Support	7.0	3.47	7.0	3.63

V.B. Transverse Axis Analysis (cont)

At this phase in the analysis a parametric study was conducted in the transverse axis of the motor by varying the spring rates of the central support structure over a range of 2 to 12 million lb/in. A value of 8% critical damping was assumed for the central structural support system. The spring rate of the central structural support was restricted to an upper limit of 12 million lb/in. because of local buckling considerations of the motor case.

The addition of the central support structure was made on the basis that it might produce the following desirable dynamic effects on the transverse axis dynamic response characteristics of the motor:

a. Increase the fundamental transverse axis resonant frequency of the motor to a value that would be above the 0.1 to 9 cps frequency range associated with expected large transportation environments.

b. Reduce the maximum acceleration response amplitudes and maximum dynamic propellant liner bond stresses significantly below the values obtained from the unsupported motor analysis.

The results of this analysis are summarized in Table E-1. These data show increase from 4.5 to 7.0 cps when the results of the unsupported motor analysis are compared with the results of the supported motor obtained using the maximum central support spring rate of 12 million lb/in.

The reduction in maximum dynamic stress in the propellant-liner bond from 25.6 to 20.5 psi/g was small and would not justify the addition of the central support.

2. Modal Analysis

The results of the modal analysis for the unsupported and centrally supported motor configurations are shown in the mode shape plots given in Figures E-22 and -23, respectively. Comparison of the two mode shape plots

V.B. Transverse Axis Analysis (cont)

shows the small effect that a 12 million lb/in. support spring has on the transverse axis response amplitudes on the motor and within the propellant.

3. Dynamic Stress Analysis

The maximum dynamic direct and shear stresses in the propellant and propellant-liner bond were calculated for the unsupported and centrally supported motor configurations. Plots of the maximum dynamic direct stresses of the unsupported motor at 7.0 cps are shown in Figures E-24 and -26, respectively and in the maximum dynamic shear stresses in Figures E-25 and -27, respectively. A comparison of both the dynamic direct and shear stresses for the unsupported and centrally supported motor configurations shows small differences between the two support conditions.

C. STRUCTURAL DYNAMIC EVALUATIONS

1. General

At the completion of the dynamic analysis program an evaluation was performed to assess the capability of the 260-in.-dia motor to withstand the vibration input environment that could occur during towed stage transportation.

A comprehensive search was made from the beginning of the barge transportation study to obtain valid and meaningful input vibration environmental data that would be applicable to barge transportation of a motor in the 4 million lb class and, that could be used in this particular structural dynamic evaluation. The only published data obtained on this subject are given in Reference (1), which is a Douglas Aircraft Co. Report (No. SM44783) that lists measured input acceleration levels and corresponding excitational frequencies recorded during barge transportation of the Saturn S-IV-5 stage. The weight of the empty Saturn S-IV-5 stage is about 24,000 lb. It is estimated

V.C. Structural Dynamic Evaluations (cont)

that the weight of support structures, protective containers, instrumentation, etc. would be 5,000 to 6,000 lb, and the total transported weight of the S-IV-5 stage and supplemental shipping equipment would be approximately 30,000 lb. The weight of the 260-in.-dia stage is 3,985,295 lb (Table E-2).

Reference (1) explains that the vibration environment generated during barge transportation is dependent on the size and draft of the barge and the sea state. The maximum input acceleration levels and excitational frequencies recorded during the Saturn S-IV-5 study are summarized below:

<u>Motor Axis</u>	<u>Excitation Frequency Range, cps</u>	<u>Max Accel Levels Recorded, \pm g</u>
Longitudinal	0.1 - 9.0	0.51
Transverse	0.1 to 9.0	1.24

It is believed that the maximum acceleration input levels that would occur during barge transportation of the 260-in.-dia motor would be considerably less than those listed in the table above. The consideration is that the maximum acceleration levels expected during barge transportation of the 260-in.-dia motor would not exceed ± 0.50 g in the longitudinal direction and ± 1.0 g in the transverse axis direction. It is believed that the excitational frequency range for the motor shipment would be 0.1 to 9.0 cps.

It should be noted that the maximum acceleration input levels of ± 0.51 and ± 1.24 g (1) are isolated peak values with a small probability of occurrence during an operational shipment.

Since it was not possible to obtain vibration environmental data that are applicable to shipments of the 260-in.-dia motor, this structural dynamics evaluation of the unsupported, unpressurized 260-in.-dia stage was conducted using very conservative acceleration input levels of 1.0 and 0.85 g in the longitudinal axis and 1.0 and 1.25 g in the transverse axis.

V.C. Structural Dynamic Evaluations (cont)

2. Longitudinal Axis Evaluation

The longitudinal axis structural dynamics evaluation of the 260-in.-dia motor was conducted using the assumption that the motor would be subjected to an input acceleration level of ± 0.85 g at its resonant frequency of 1.7 cps for a total duration of 60 minutes during each operational motor shipment.

The maximum dynamic propellant-liner stresses calculated for the longitudinal axis configuration at 1.77 cps are as follows:

Longitudinal Axis Evaluation - Dynamic Stresses
Resonant Frequency - 1.77 cps

Input Level at Barge, \pm g	Max Prop.-Liner Direct Stress, psi	Prop.-Liner Direct Stress Allowable, psi, 1-hr	Max Prop.-Liner Shear Stress, psi	Prop.-Liner Shear Stress Allowable, psi, 1-hr
1.0	16.5	61.0	8.7	44.0
0.85	14.0	61.0	7.4	44.0

The dynamic stress allowable data plots of Figure E-5 show the following:

<u>Time, hr</u>	<u>Prop.-Liner Direct Stress Allowable, psi</u>	<u>Prop.-Liner Shear Stress Allowable, psi</u>
0.1	80	56
1.0	61	44
10.0	47	34
50.0	39.5	29.5

V.C. Structural Dynamic Evaluations (cont)

This extremely conservative evaluation shows that the 260-in.-dia motor, unpressurized and without a central support, is capable of withstanding longitudinal axis vibration input levels greater than the levels expected during towed barge transportation.

3. Transverse Axis Evaluation

The transverse axis structural dynamic evaluation of the 260-in.-dia motor was conducted using the assumption that the unpressurized motor, without central support, would be subjected to an acceleration input level of ± 1.25 g at its resonant frequency of 4.5 cps for a duration of 60 minutes during each operational motor shipment.

The maximum dynamic propellant-liner bond stresses calculated for the transverse axis configuration at 4.5 cps are as follows:

Transverse Axis Evaluation - Dynamic Stresses
Resonant Frequency 4.5 cps

<u>Input Level</u> <u>at Barge,</u> <u>\pm g</u>	<u>Max Prop.-Liner</u> <u>Direct Stress,</u> <u>psi</u>	<u>Prop.-Liner</u> <u>Direct Stress</u> <u>Allowable,</u> <u>psi, 1-hr</u>	<u>Max Prop.-Liner</u> <u>Shear Stress,</u> <u>psi</u>	<u>Prop.-Liner</u> <u>Shear Stress</u> <u>Allowable,</u> <u>psi, 1-hr</u>
1.0	25.6	61.0	5.2	44.0
1.25	32.0	61.0	6.5	44.0

The static direct stress in the propellant-liner bond at the center of the motor resulting from the static 1-g body forces was calculated during the static stress analysis (see Appendix B) of the motor. In this analysis the motor was assumed to be in a horizontal attitude, unpressurized, and without a central structural support. The maximum static direct stress calculated in the propellant-liner bond at the center of the motor in this analysis was 7.0 psi.

V.C. Structural Dynamic Evaluations (cont)

The total maximum direct stress (1-g static stress plus dynamic stress at the conservative ± 1.25 g input) predicted in the propellant-liner bond during barge transportation is 39.0 psi. Since, the direct stress allowable for a loading duration of 1 hour is 61.0 psi, failure of the propellant-liner bond would not be expected at a stress level of 39.0 psi. The stress allowable data listed in Figure E-5 show a direct stress-to-failure level of 39.5 psi for 50 hours of applied loading.

It should be noted here that the above structural dynamic evaluations are extremely conservative because of the assumption that the motor is excited at its resonant frequency at a maximum input level for the time period assumed in this evaluation.

The above analyses show that the unpressurized 260-in.-dia motor, without a central structural support, is capable of withstanding the vibration environment expected during towed barge transportation.

VI. REFERENCES

1. Douglas Santa Monica Report No. 44783, Vibration Environment of the Saturn S-IV-5 Stage During Surface Transportation to the Sacramento Field Station and Air Transportation to the Atlantic Missile Range, September 1965.
2. Douglas Missile and Space Systems Division Report No. SM-51896 Vol II, Saturn I-B Improvement Study (Solid First Stage) Phase II, Final Detailed Report, 30 March 1966
3. T. Depkovich and L. Peterson, A Study of the Dynamic Behavior of Minuteman Propellants Using Propellant Disk Vibration Tests, AGC Report TM 224 SRP, 20 June 1963.
4. G. J. Kostyrko, Development and Use of a Free Vibrating Reed Test for Evaluation of Solid Propellants, AGC Report TM 228 SRP, August 1963.
5. T. Depkovich and L. Peterson, Dynamic Analysis of Minuteman Wing VI Second Stage Motor 52TH-1, AGC Report TR:4640:64-023, September 1964.

Longitudinal Axis Analysis

	Fund. Resonant Frequency (cps)	Max. Dyn. Amplification Factor (\pm 1-G Input)	Max. Prop-Liner Dynamic Direct Stress/G	Prop-Liner Direct Stress Allowable (psi, 1.0 hour)	Max. Dyn. Prop-Liner Shear Stress/G	Prop-Liner Shear Stress Allowable (psi, 1.0 hour)
No Intermediate support	1.77	2.79	16.5	61.0	8.7	44.0

Transverse Axis Analysis

No Intermediate support	4.5	4.65 (1)	25.6	61.0	5.2	44.0
With Intermediate support (3)	7.0	3.70 (2)	20.5	61.0	3.2	44.0

(1) Center of Motor Case

(2) 318" Forward of the Aft Equator

(3) Spring Rate of 12 million pounds per inch

TABLE E-1. - SUMMARY OF PRINCIPAL ANALYSIS RESULTS

TABLE E-2. - BARGE TRANSPORTATION CONFIGURATION WEIGHTS SUMMARY

<u>Insulated Chamber</u>			227,137 lb
Steel Case		199,445	
Fwd. Head	21,550		
Cylinder	162,600		
Aft Head	15,295		
Insulation (V-44)		26,012	
Liner (SD 850-2)		1,680	
<u>Nozzle and Cone Assembly</u>			56,722
Nozzle Assembly		19,811	
Steel Shell	8,045		
Support Structure	3,293		
Carbon Cloth-Phenolic	4,504		
Silica Cloth-Phenolic	1,665		
Insulation (V-44)	2,304		
Forward Exit Cone Assembly		14,621	
Honeycomb Structure	6,561		
Carbon Cloth-Phenolic	3,130		
Silica Cloth-Phenolic	4,930		
Aft Exit Cone Assembly		22,290	
Honeycomb Structure	5,040		
Silica Cloth-Phenolic	16,580		
Exit Plane Insulation	670		
<u>Equipment and Instrumentation</u>			13,187
Roll Control		571	
Thrust Vector Control		9,748	
Misc. Equip. & Elect. Systems		2,868	
<u>Structures</u>			8,249
Aft Cone		6,901	
Base Heat Protection		1,100	
Raceway Tunnel		248	
<u>Handling Rings</u>			280,000
Forward Ring		120,000	
Aft Ring		160,000	
<u>Propellant</u>			<u>3,400,000</u>
Total			3,985,295

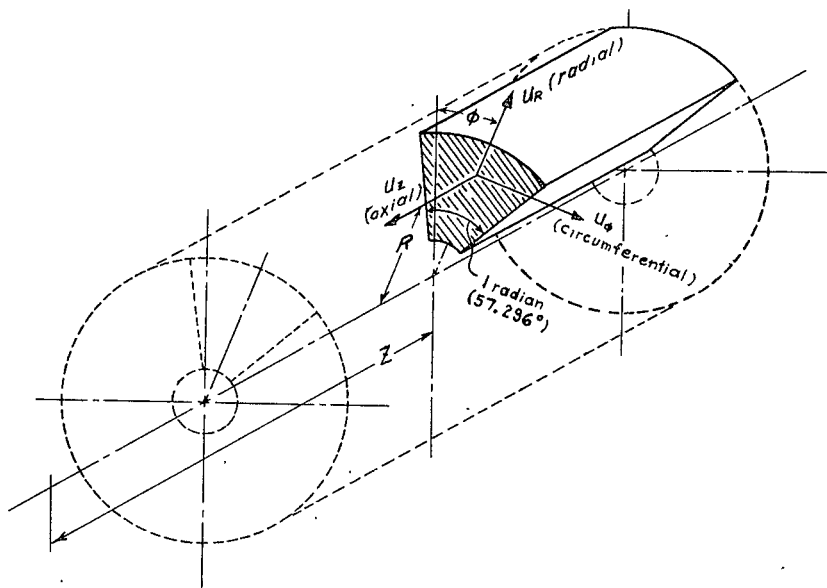


Figure E-2. - Coordinate System and One Radian Propellant Wedge

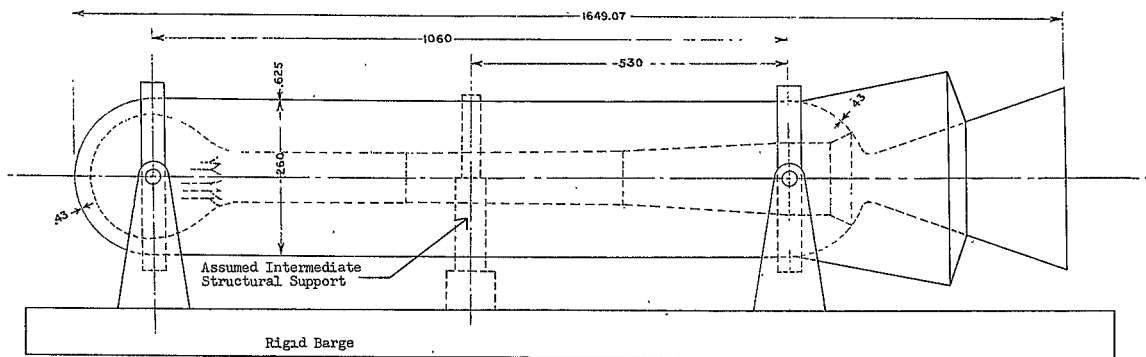


Figure E-1., - Analytical Configuration Concepts - Towed Barge Transporter

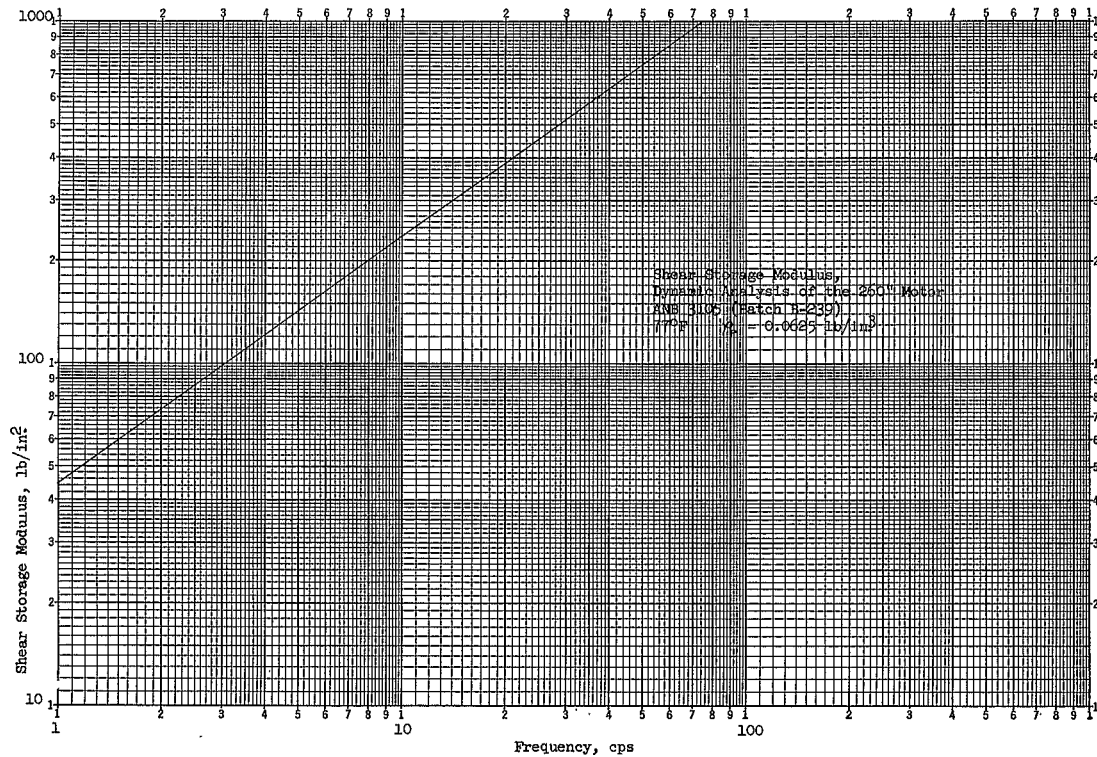


Figure E-3. - Shear Storage Modulus of ANB-3105 Propellant (Batch B-239)

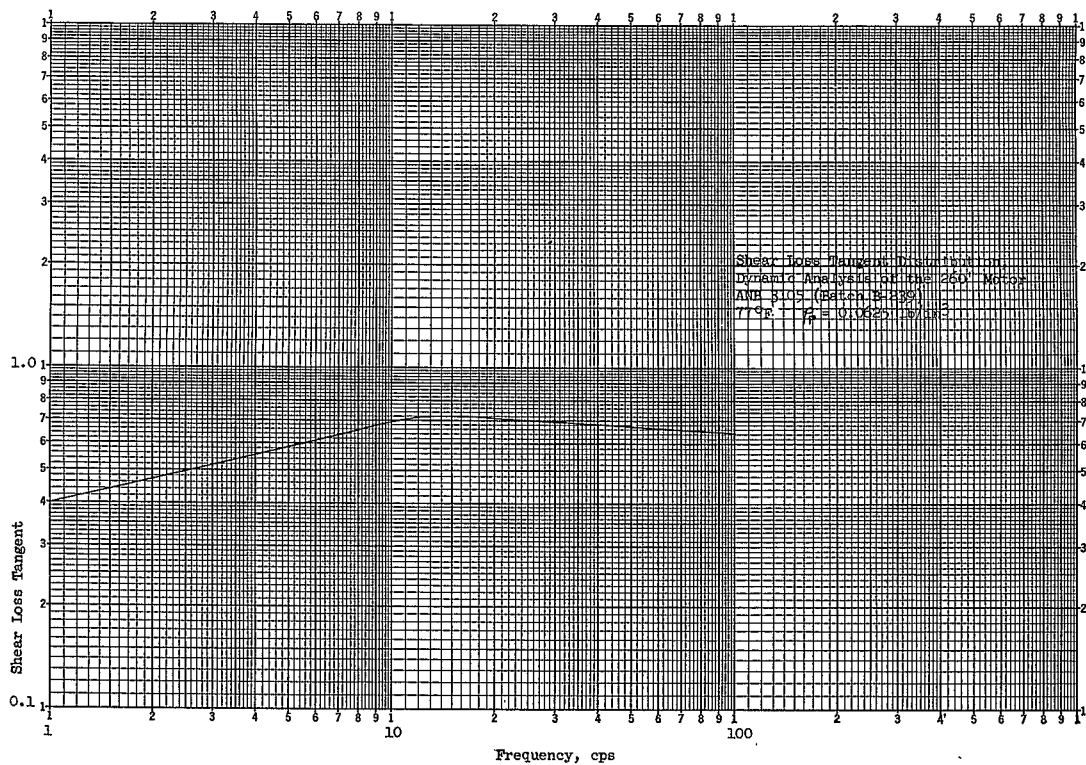


Figure E-4. - Shear Loss Tangent Distribution of ANB-3105 Propellant (Batch B-239)

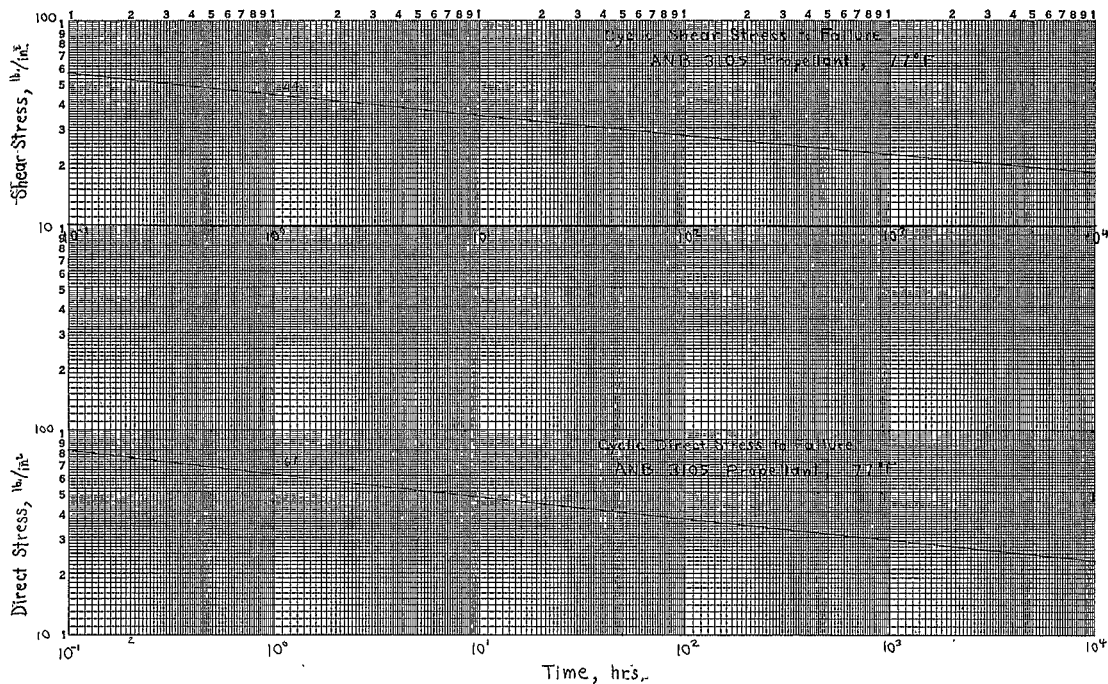


Figure E-5. - Allowable Interface Bond Stresses for ANB-3105
 Propellant/SD-850-2 Liner System

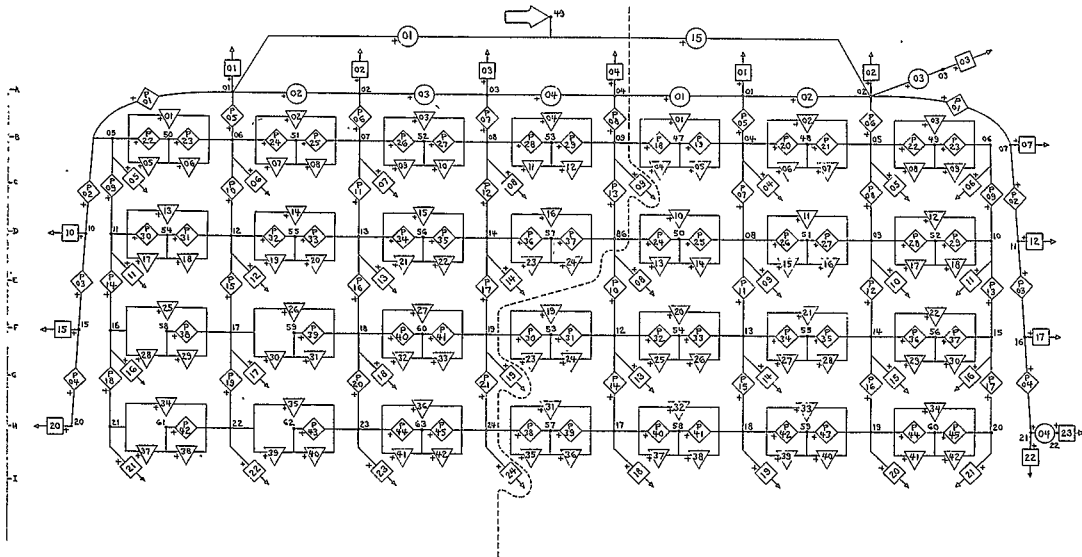


Figure E-6. - Longitudinal-Axis Circuit Diagram for Axial (Z) Response

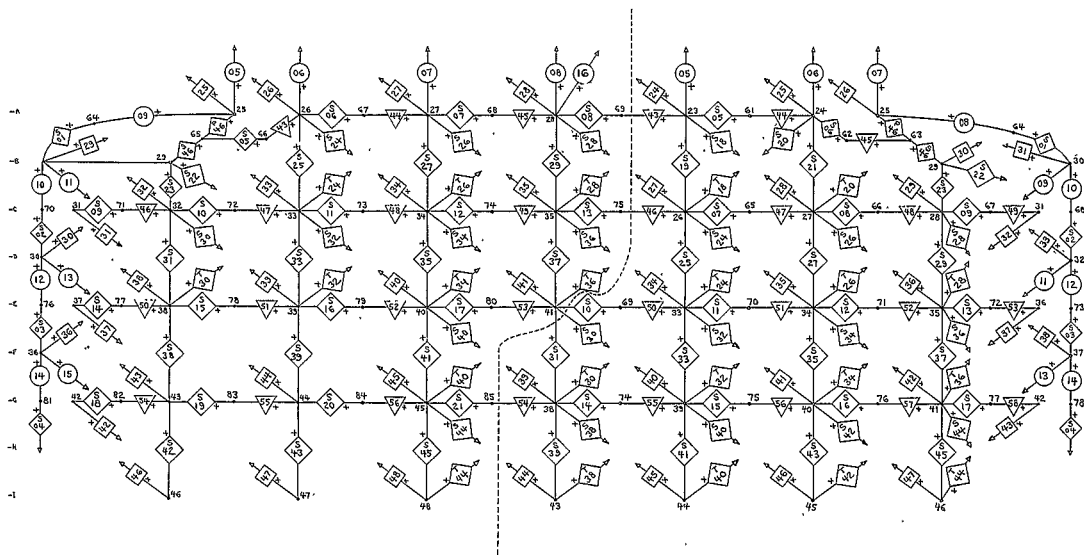


Figure E-7. - Longitudinal-Axis Circuit Diagram for Radial (R) Response

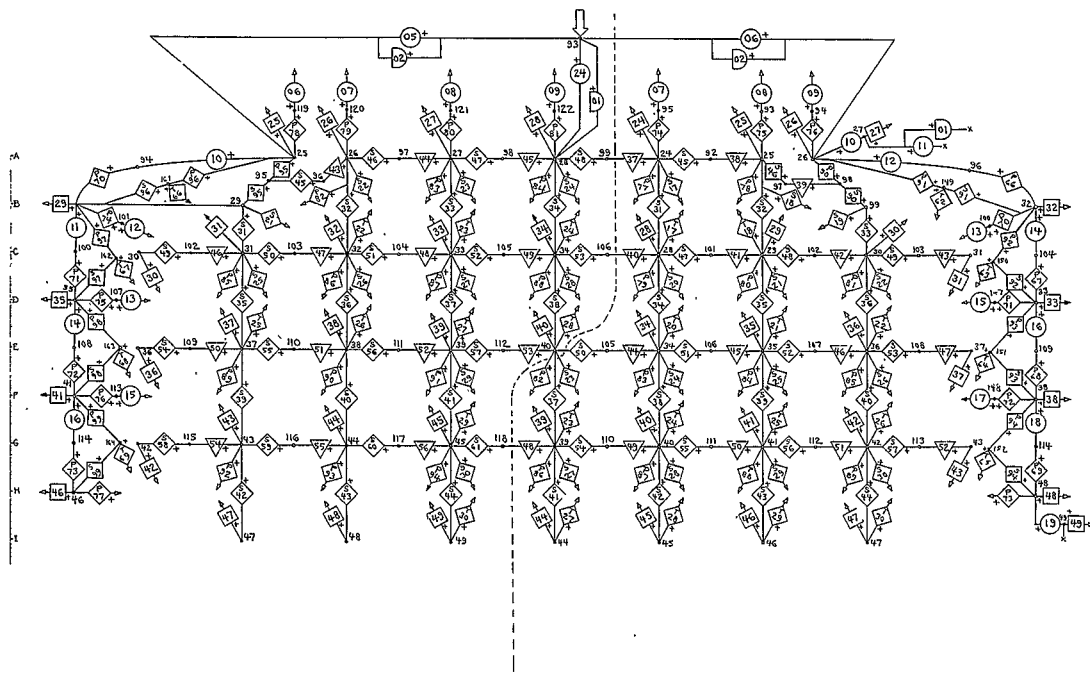


Figure E-8. - Transverse-Axis Circuit Diagram for Radial (R) Response'

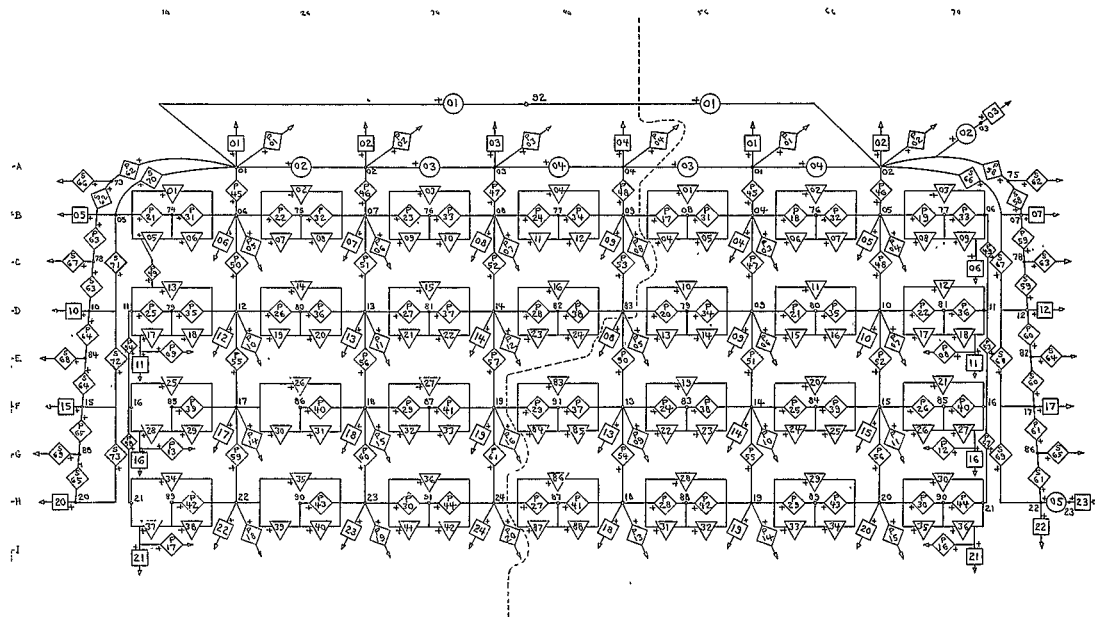


Figure E-9. - Transverse-Axis Circuit Diagram for Axial (Z) Response

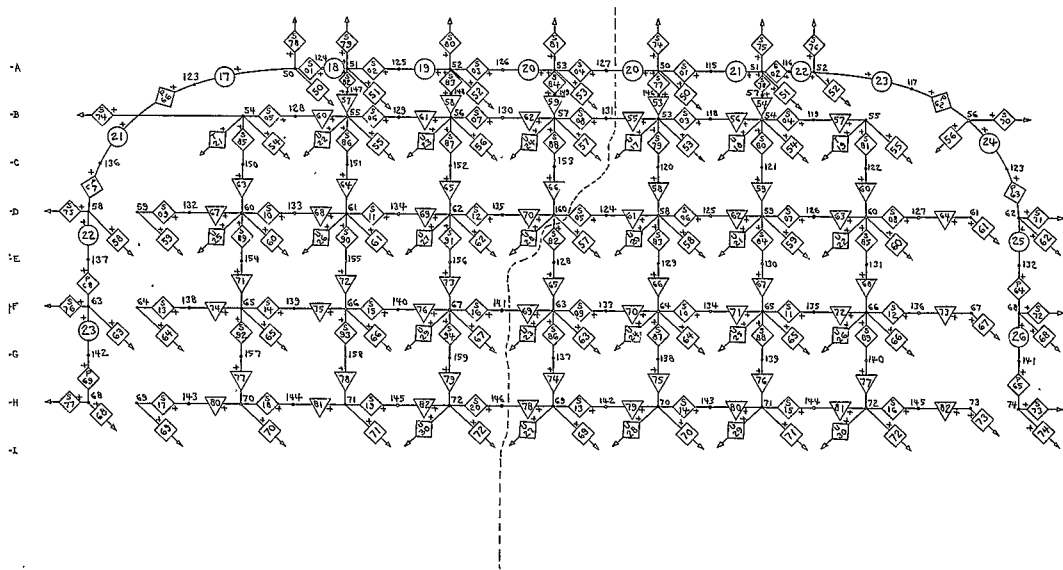


Figure E-10. - Transverse-Axis Circuit Diagram for Circumferential (ϕ) Response

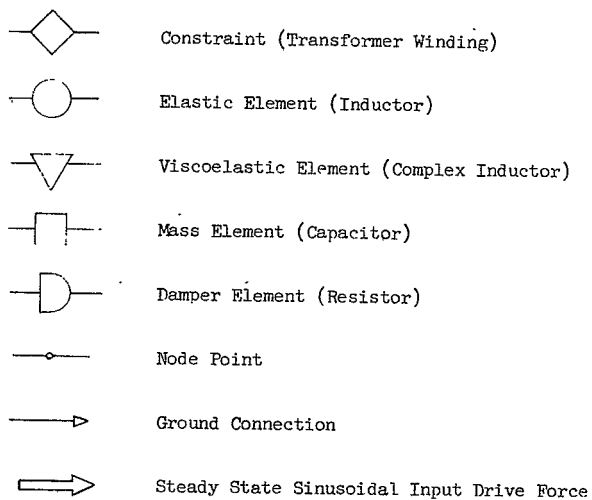


Figure E-11. - Circuit Diagram Symbols

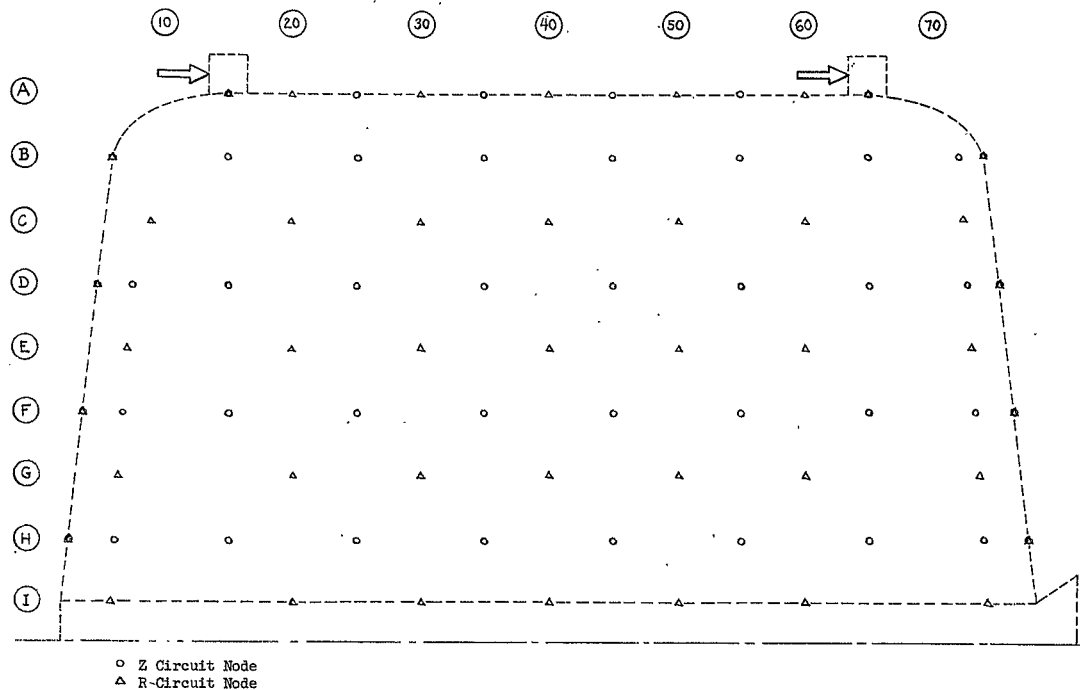


Figure E-12. - Dynamic-Model Data Readout and Excitation Points,
Longitudinal-Axis Analysis

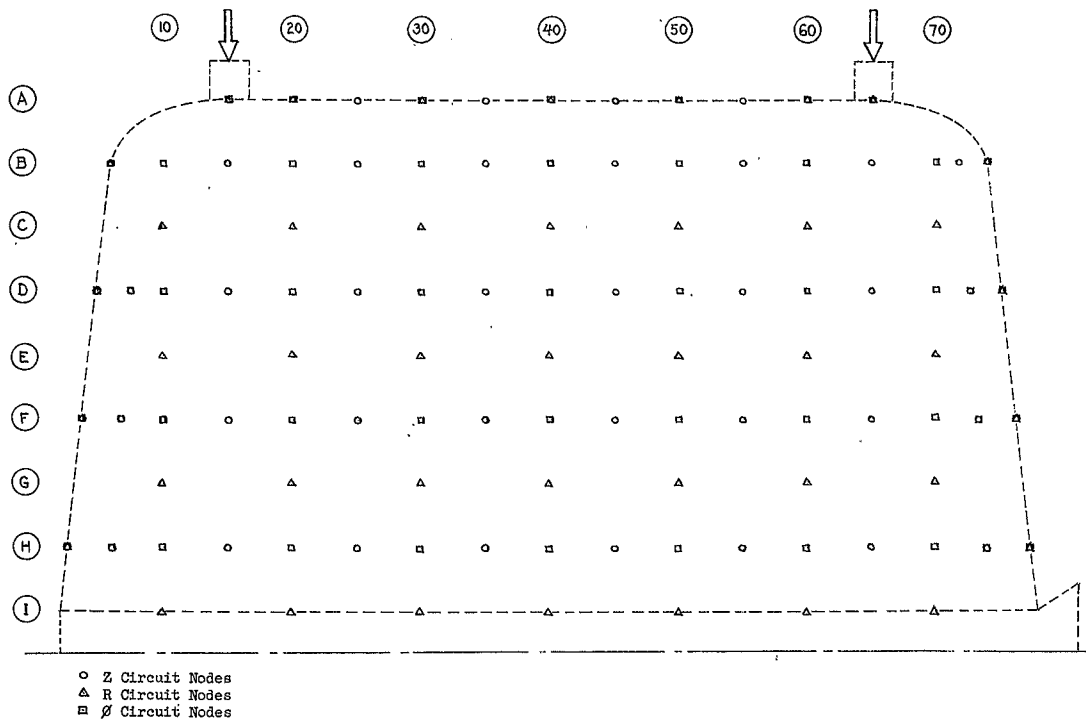


Figure E-13. - Dynamic-Model Data Readout and Excitation Points,
Transverse-Axis Analysis

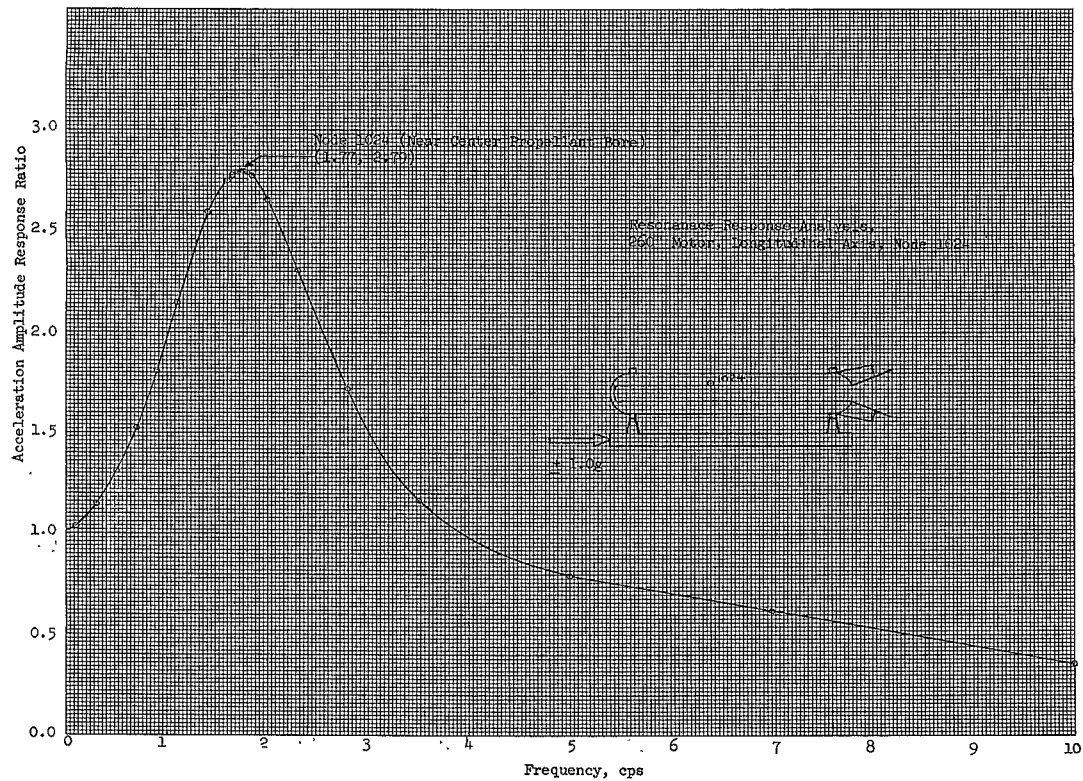


Figure E-14. - Resonance Response Analysis, Longitudinal Axis, Node 1024

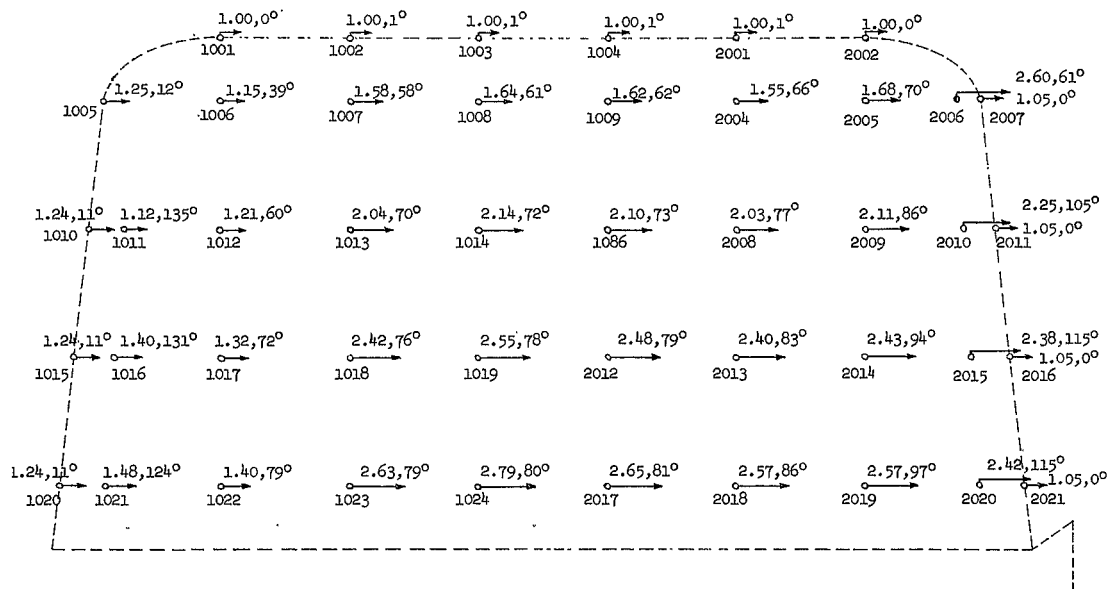


Figure E-15. - Longitudinal-Axis Mode Shape at 1.77 cps

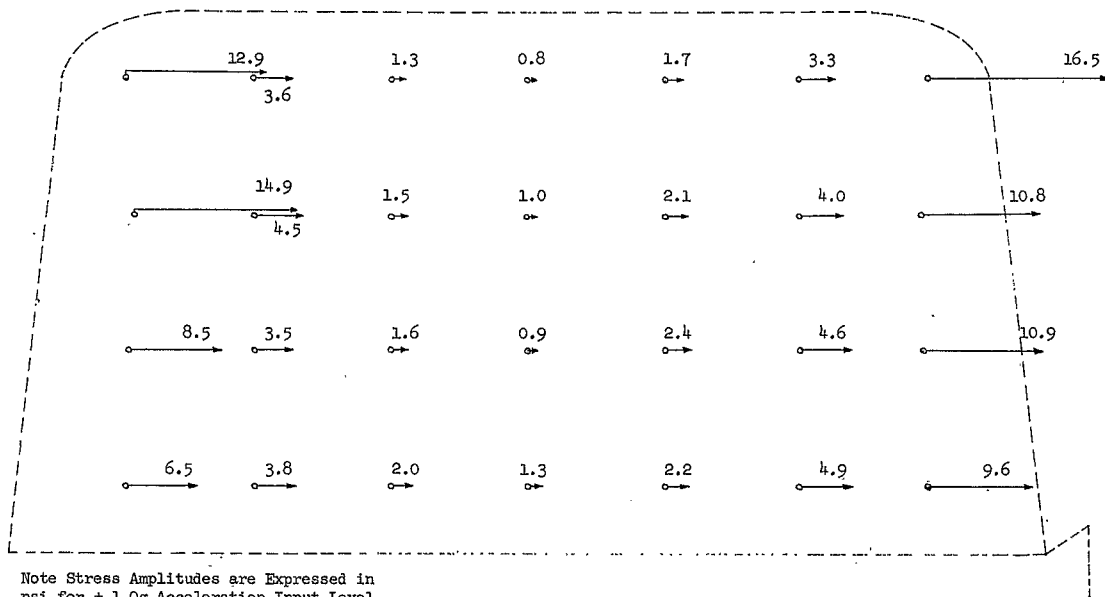


Figure E-16. - Longitudinal-Axis Dynamic Stress Analysis, Distribution
of Peak Direct Axial Stresses at 1.77 cps

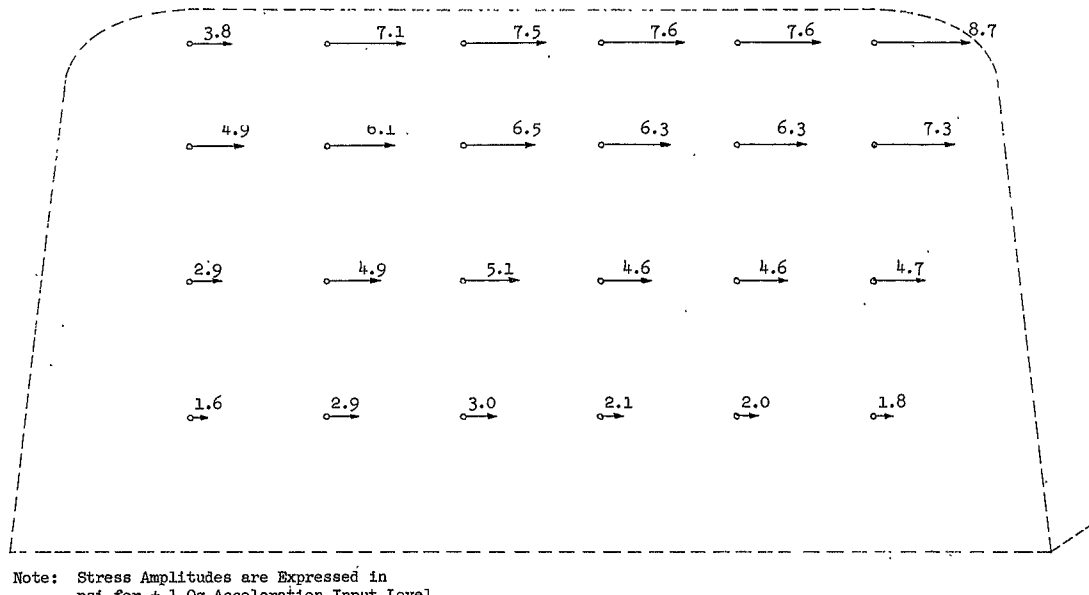


Figure E-17. - Longitudinal-Axis Dynamic Stress Analysis, Distribution
of Peak Shear Stress at 1.77 cps

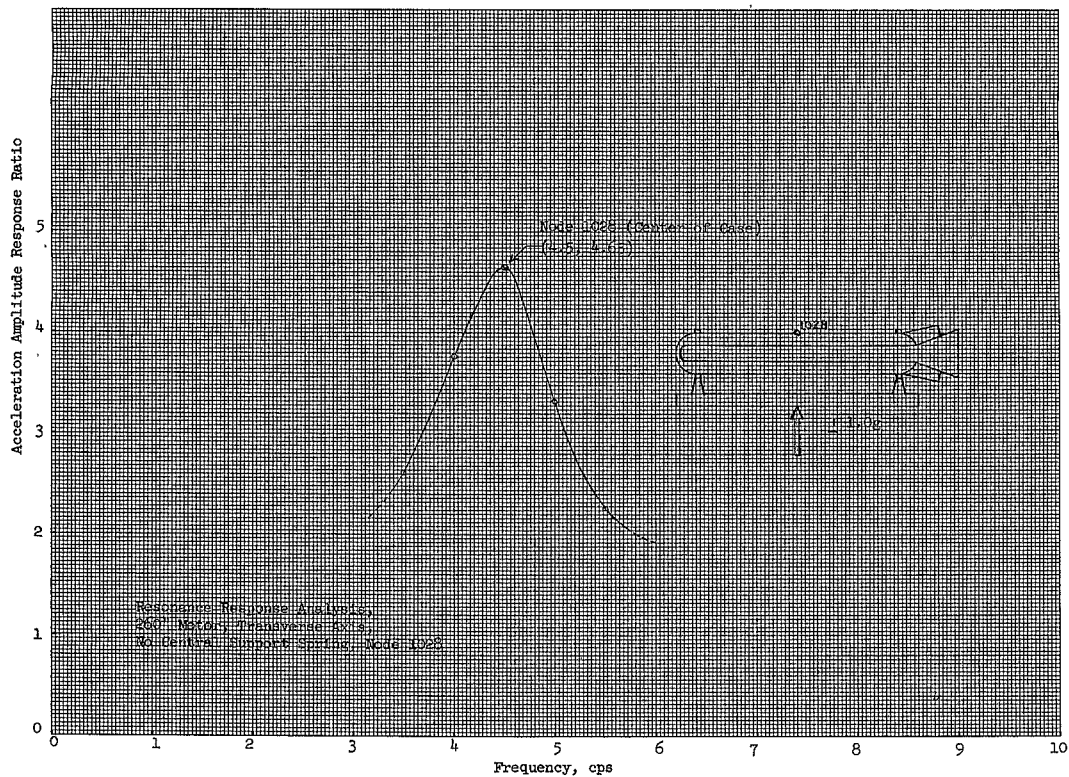


Figure E-18. - Resonance Response Analysis of 260-in-dia Motor,
Transverse Axis, No Central Support Spring, Node 1028

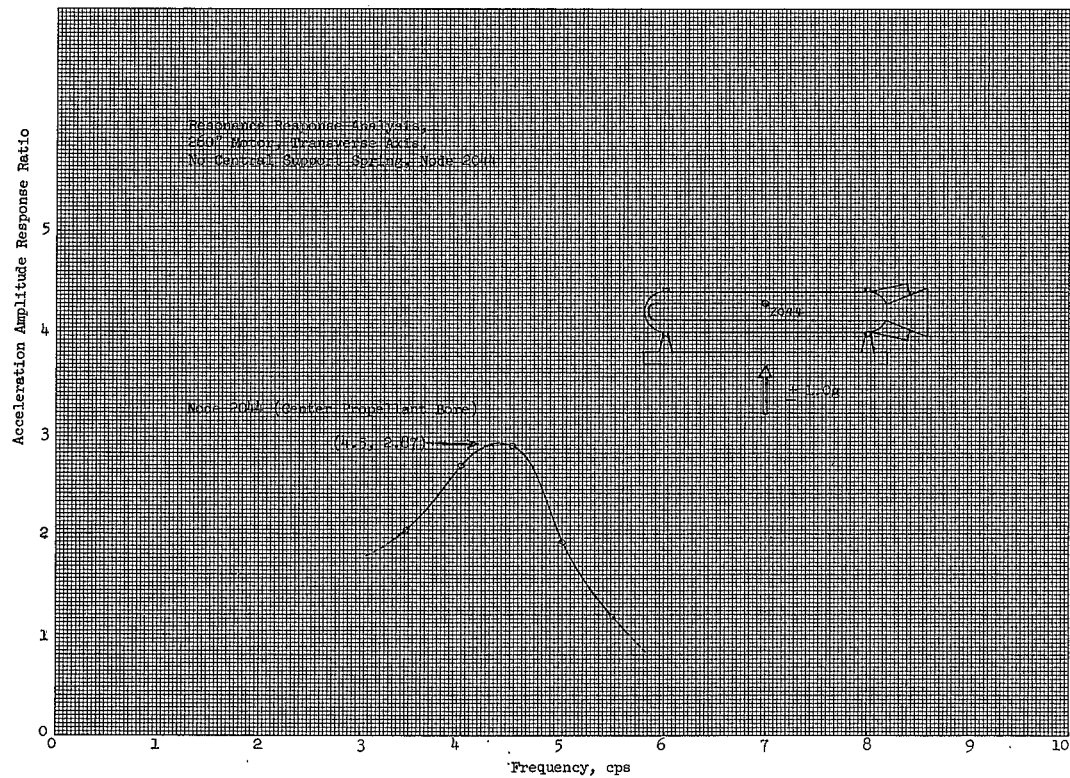


Figure E-19. - Resonance Response Analysis of 260-in.-dia Motor,
Transverse Axis, No Central Support Spring, Node 2044

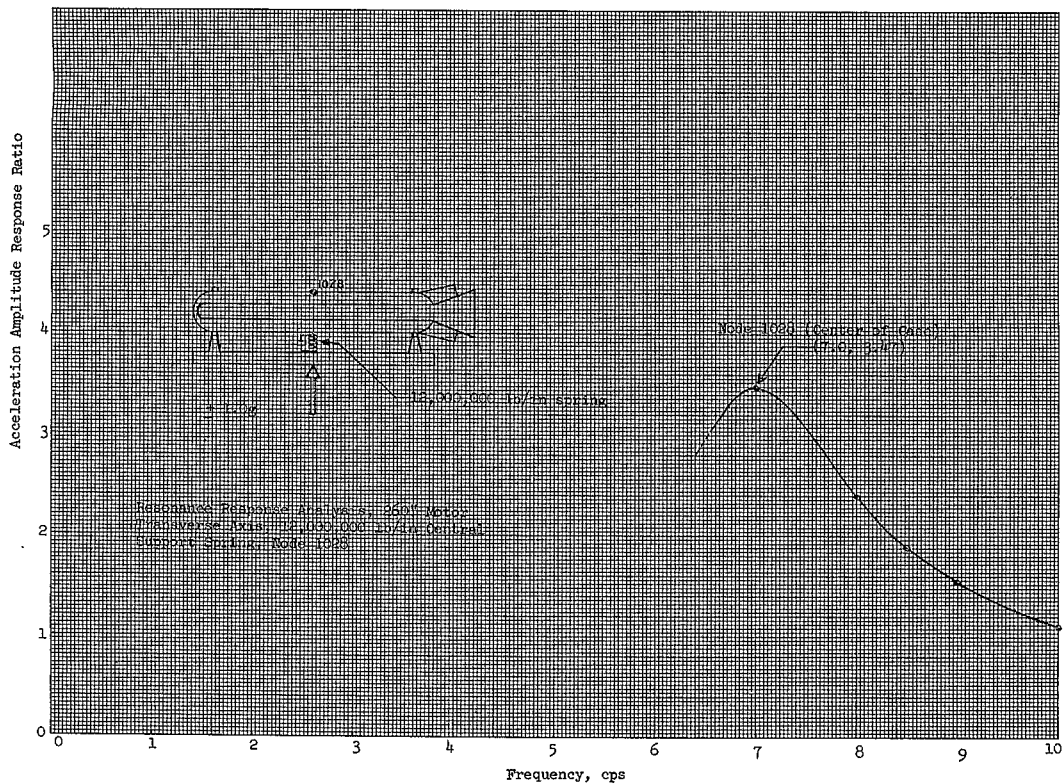


Figure E-20. - Resonance Response Analysis of 260-in.-dia Motor, Transverse Axis, 12,000,000 lb/in. Central Support Spring, Node 1028

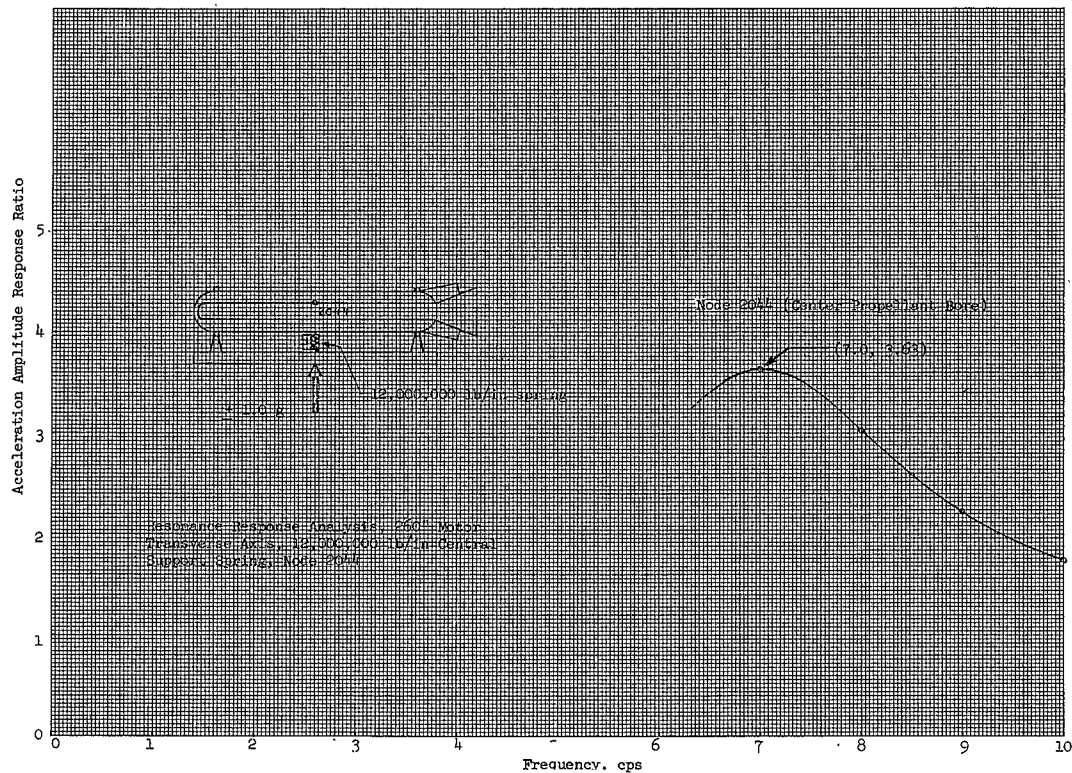


Figure E-21. - Resonance Response Analysis of 260-in.-dia Motor,
 Transverse Axis, 12,000,000 lb/in. Central Support
 Spring, Node 2044

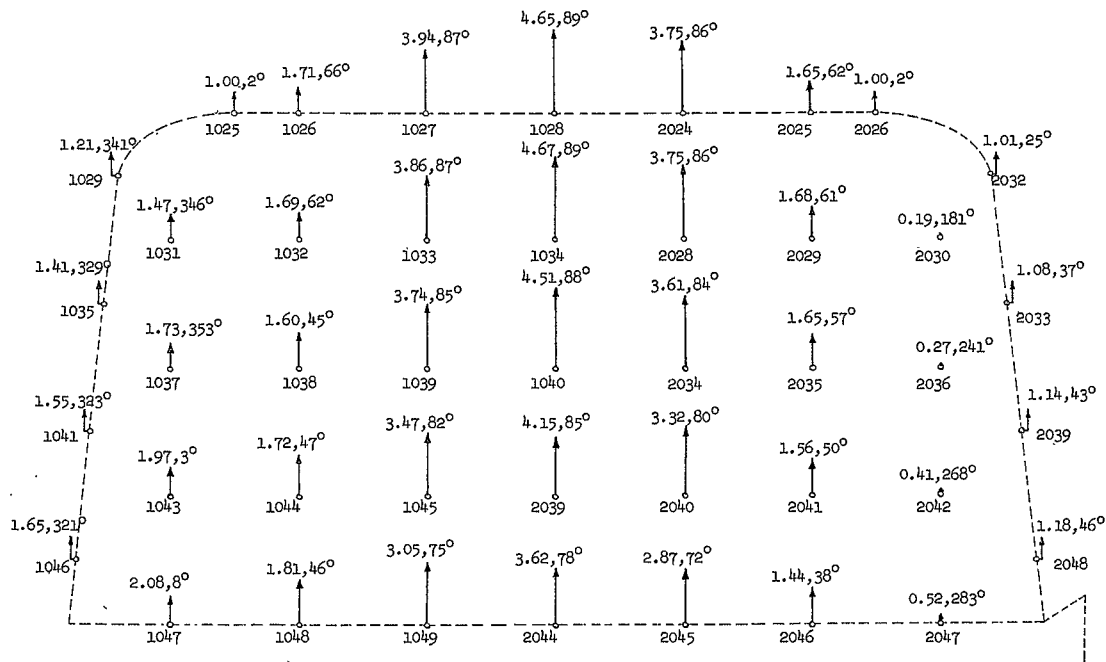


Figure E-22. - Transverse-Axis Mode Shape at 4.5 cps, No Support Spring

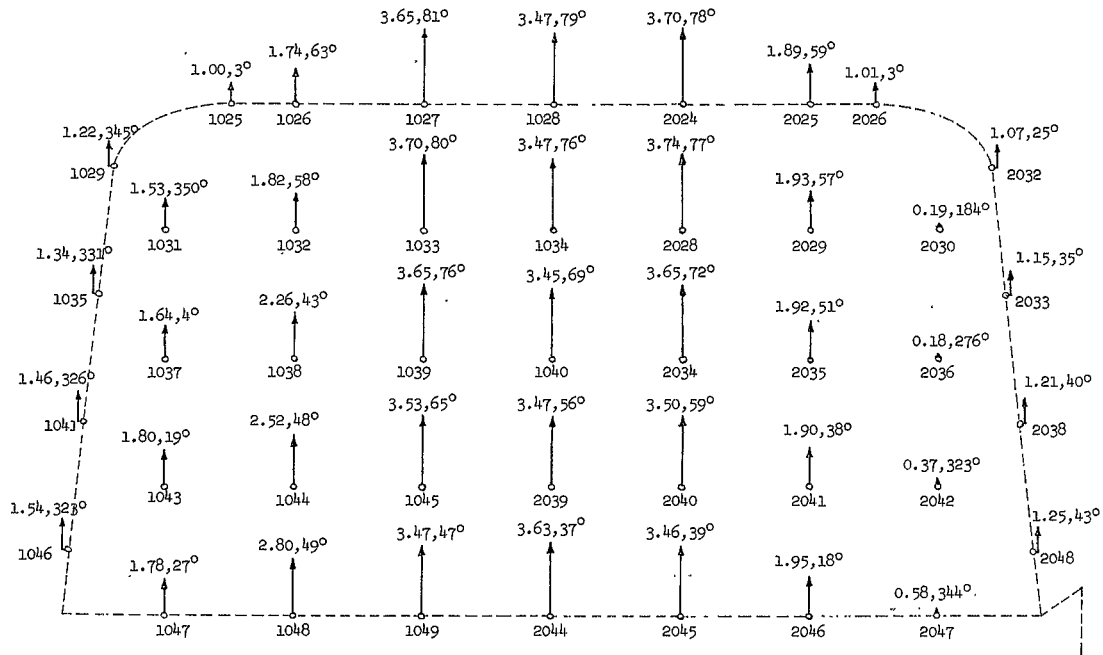


Figure E-23. - Transverse-Axis Mode Shape at 7.0 cps,
12,000,000 lb/in. Support Spring

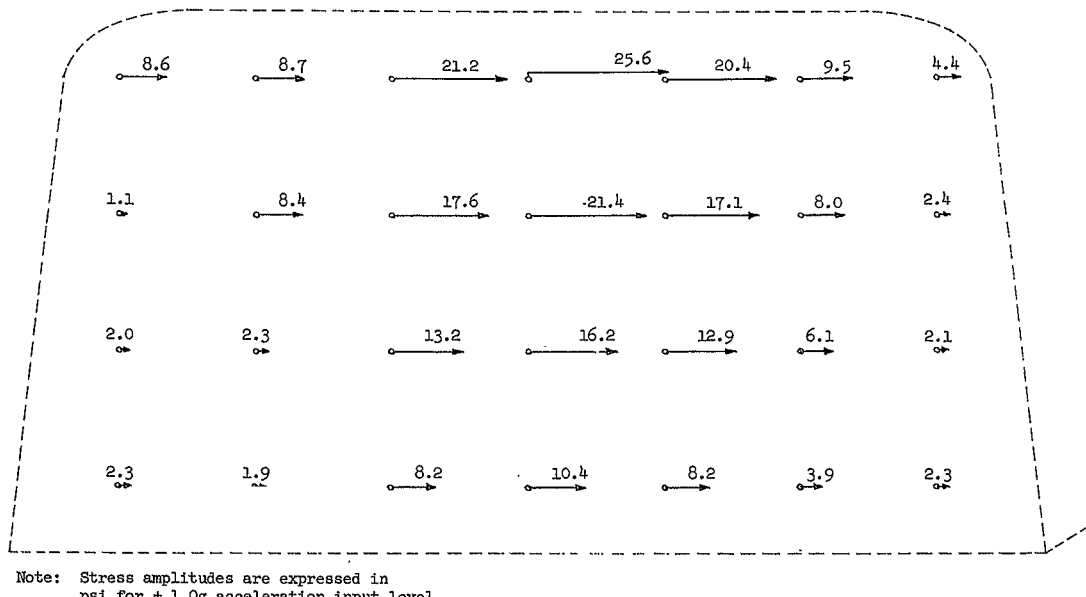


Figure E-24. - Transverse-Axis Dynamic Stress Analysis,
Distribution of Peak Direct Axial Stresses
at 4.5 cps, No Support Spring

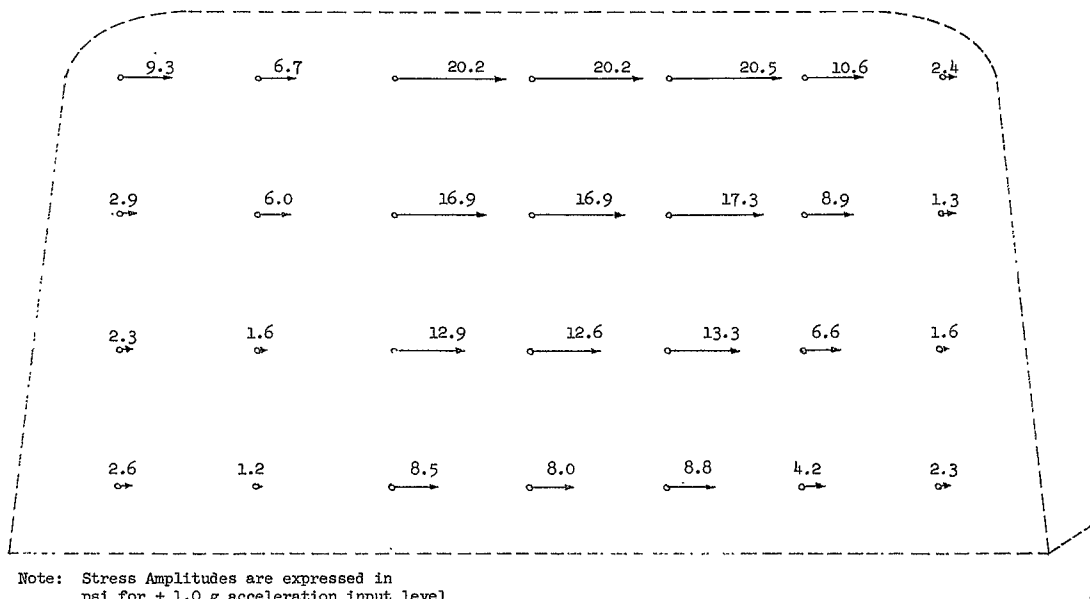


Figure E-26. - Transverse-Axis Dynamic Stress Analysis, Distribution of Peak Direct Axial Stresses at 7.0 cps, 12,000,000 lb/in. Support Spring

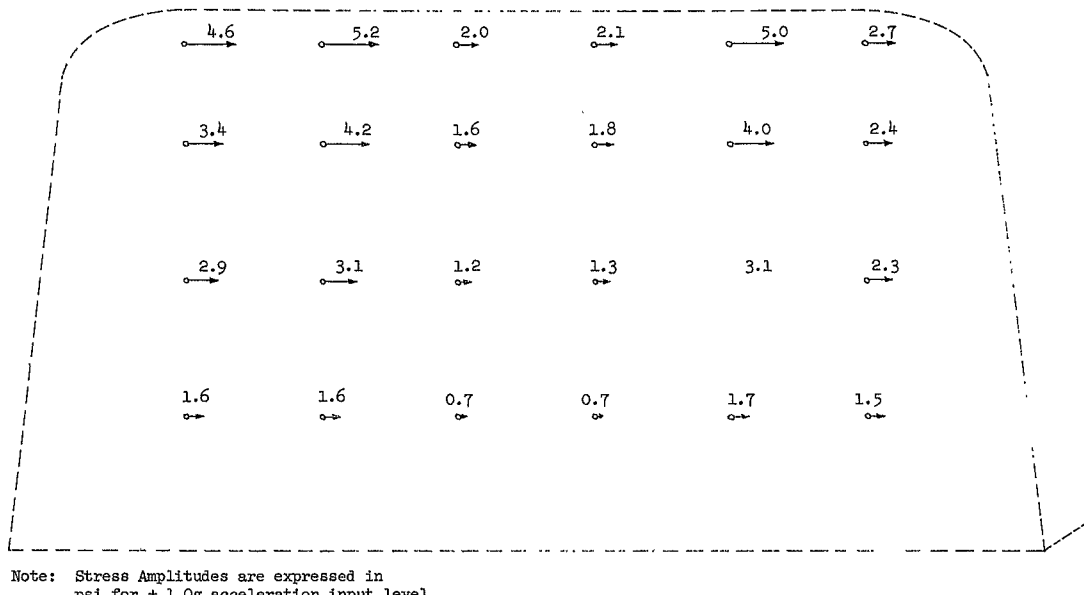


Figure E-25. - Transverse-Axis Dynamic Stress Analysis, Distribution of Peak Shear Stresses at 4.5 cps, No Support Spring

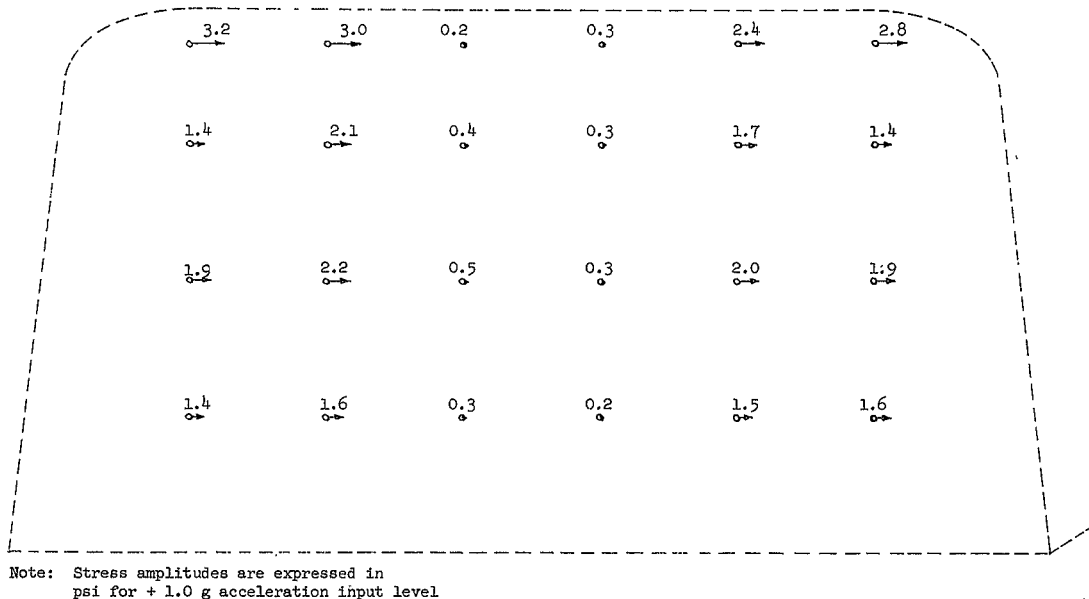


Figure E-27. - Transverse-Axis Dynamic Stress Analysis, Distribution of Peak Shear Stresses at 7.0 cps, 12,000,000 lb/in. Support Spring

GLOSSARY OF ABBREVIATED TERMS

ARD	Auxiliary Repair Dock
C&C	Propellant Cast and Cure Facility
CKAFS	Cape Kennedy Air Force Station
C-T	NASA-KSC Saturn V Crawler-Transporter
DCP	Aerojet/Dade County (Florida) Plant
ETR	Air Force Eastern Test Range
KSC	NASA-Kennedy Space Center
LC	Launch Complex
MILA	NASA-KSC Merritt Island
MSS	KSC Mobile Service Structure
VAFB	Vandenberg Air Force Base, California
WTR	Air Force Western Test Range

LIST OF REFERENCES

1. Solid Motor Logistics Study, Vol. II, Summary Report, Martin Company, Report NASA-CR-63-111, January 1964.
2. Study of Improved Saturn Launch Facilities, Volume III: MLV-SAT-IB-S, Martin Company, Report CR-65-87, January 1966.
3. Craft, G. W., and Starkey, A. W., A Concept for Handling and Launching Large Solid Rockets, Bellcomm, Inc., Report TR-66-330-2, September 1966.
4. Launch Facilities and Operations for Large Solid Motor Study, Douglas Aircraft Co., Report DAC-58078, December 1967.
5. Dawson, R. P., Saturn IB Improvement Study, Volume I, Final Summary Report, Douglas Missile and Space Systems Division, Report SM-51896, March 1966.
6. Saturn V Launch Vehicle with 260-In.-Dia Solid Motors, The Boeing Co., under Contract NAS8-21105, n.d.
7. Development and Production Costs for 260-in.-dia First Stage Vehicle, Aerojet-General Corporation, Report NAS7-513, FR-2, April 1967.
8. Handling Equipment for 260-in.-dia Motors, Task 6 of 260-in.-dia Motor Cost and Technology Studies, Aerojet-General Corporation under Contract NAS7-513, Aerojet 1967.
9. Study of Segmented 260-in.-dia Motors, Task 2 of 260-in.-dia Motor Cost and Technology Studies, Aerojet-General Corporation, Report No. NAS7-513 FR-1, February 1967.
10. Roll-Ramp Actuators - Mark II, Product Brochure PB5M/4-69, Roll-Ramp Corporation, Subsidiary of Philadelphia Gear Corporation, 1969.
11. Carbon, G. R., Ellicott, K.E., and Trudell, R. W., Vibration Environment of the Saturn S-IV-5 Stage During Surface Transportation to the Sacramento Field Station and Air Transportation to the Atlantic Missile Range, Douglas Missile and Space Systems Division, Report SM-44783, 15 Sept. 1965.
12. Explosives Safety Handbook, John F. Kennedy Space Center Safety Office, Document No. GP-469, 1 July 1968.
13. Kingery, C. N., and Pannill, B. F., Peak Overpressure vs Scaled Distance for TNT Surface Blasts (Hemispherical Charges), Ballistic Research Laboratories Memorandum Report No. 1518, April 1964.
14. Abbreviated Master Plan, Vandenberg Air Force Base, Lompoc, California, Department of the Air Force Document, Directorate of Civil Engineering DCS/P&R. Washington, D. C., 31 December 1966.

DISTRIBUTION LIST FOR FINAL REPORT NASA CR-72757

NASA Lewis Research Center 21000 Brookpark Rd Cleveland, Ohio 44135	NASA George C. Marshall Space Flight Center Redstone Arsenal Huntsville, Alabama 35812
Attn: Contracting Officer	Attn: Technical Library (1)
Mail Stop: 500-313	S&E-ASTN-PJ/D. Burrows (1)
Solid Rocket Technology Branch (8)	PM-EP-T.C. M. Mitchell (1)
Mail Stop: 500-205	PM-EP-T/C. T. Ratliff (1)
Technical Library (2)	
Mail Stop: 60-3	
Tech. Report Control Office (1)	Jet Propulsion Laboratory
Mail Stop: 5-5	Calif. Institute of Technology
J. Kennard (1)	4800 Oak Grove Drive
Mail Stop: 3-17	Pasadena, California 91103
Tech. Utilization Office (1)	Attn: Richard Bailey (1)
Mail Stop: 3-19	Technical Library (1)
Patent Counsel (1)	
Mail Stop: 500-311	Scientific & Technical Information Facility
National Aeronautics & Space Admin.	NASA Representative
Washington, D.C., 20546	P.O. Box 33
Attn: RPM/R. Wasel (3)	College Park, Maryland 20740
RPS/Robert W. Ziem (1)	Attn: CRT (6)
ATSS-AL/Technical Library (2)	
BL/J. McCollom (1)	<u>GOVERNMENT INSTALLATIONS</u>
BL/D. Ireland (1)	
NASA Ames Research Center	AF Space Systems Division
Moffett Field, California 94035	Air Force Unit Post Office
Attn: Technical Library (1)	Los Angeles, California 90045
MO/L. R. Alton (1)	Attn: Col. E. Fink (1)
NASA Langley Research Center	AF Research & Technology Division
Langley Station	Bolling AFB, D.C. 20332
Hampton, Virginia 23365	Attn: Dr. Leon Green, Jr. (1)
Attn: Robert L. Swain (1)	AF Rocket Propulsion Laboratory
Technical Library (1)	Edwards AFB, California 93523
NASA Goddard Space Flight Center	Attn: RPM/Mr. C. Cook (2)
Greenbelt, Maryland 20771	AF Materials Laboratory
Attn: Technical Library (1)	Wright Patterson AFB, Ohio 45433
NASA Manned Spacecraft Center	Attn: MANC/D. Schmidt (1)
2101 Webster Seabrook Road	MAAE (1)
Houston, Texas 77058	AF Ballistic Missile Division
Attn: Technical Library (1)	P.O. Box 262
NASA Kennedy Space Center	San Bernadino, California
Florida 32899	Attn: WDSOT (1)
Attn: Technical Library (1)	Structures Division
DE-PSO/N. Salvail (2)	Wright Patterson AFB, Ohio 45433
IS-LOG-21/G. Archdeacon (1)	Attn: FDT/R. F. Hoener (1)

DISTRIBUTION LIST (cont.)

Army Missile Command		Defense Materials Information Center	
Redstone Scientific Information Center		Battelle Memorial Institute	
Redstone Arsenal, Alabama 35809		505 King Avenue	
Attn: Chief, Document Section	(1)	Columbus, Ohio 43201	(1)
Ballistic Research Laboratory		Materials Advisory Board	
Aberdeen Proving Ground,		National Academy of Science	
Maryland 21005		2101 Constitution Ave., N.W.	
Attn: Technical Library	(1)	Washington, D.C. 20418	
		Attn: Capt. A. M. Blamphin	(1)
Picatinny Arsenal		Institute for Defense Analysis	
Dover, New Jersey 07801		1666 Connecticut Ave., N.W.	
Attn: Technical Library	(1)	Washington, D.C.	
		Attn: Technical Library	(1)
Navy Special Projects Office		Advanced Research Projects Agency	
Washington, D.C. 20360		Pentagon, Room 3D154	
Attn: H. Bernstein	(1)	Washington, D.C. 20301	
		Attn: Tech. Information Office	(1)
Naval Air Systems Command			
Washington, D.C. 20360			
Attn: AIR-330/Dr. O. H. Johnson	(1)		
		<u>INDUSTRY CONTRACTORS</u>	
Naval Propellant Plant		Aerojet Solid Propulsion Company	
Indian Head, Maryland 20640		P.O. Box 13400	
Attn: Technical Library	(1)	Sacramento, California 95813	
		Attn: Dr. B. Simmons	(1)
Naval Ordnance Laboratory		L. Westphal	(2)
White Oak		Tech. Information Center	(1)
Silver Spring, Maryland 20910			
Attn: Technical Library	(1)		
		Aerojet-General Corporation	
Naval Ordnance Test Station		P.O. Box 296	
China Lake, California 93557		Azusa, California 91702	
Attn: Technical Library	(1)	Attn: Technical Library	(1)
C. J. Thelen	(1)		
		Aerospace Corporation	
Naval Research Laboratory		2400 East El Segundo Boulevard	
Washington, D.C. 20390		El Segundo, California 90245	
Attn: Technical Library	(1)	Attn: Technical Library	(1)
		Solid Motor Dev. Office	(1)
Chemical Propulsion Information Agency			
Applied Physics Laboratory		Aerospace Corporation	
8621 Georgia Avenue		P.O. Box 95085	
Silver Spring, Maryland 20910	(1)	Los Angeles, California 90045	
		Attn: Technical Library	(1)
Defense Documentation Center			
Cameron Station		Atlantic Research Corporation	
5010 Duke Street		Shirley Highway at Edsall Road	
Alexandria, Virginia 22314	(1)	Alexandria, Virginia 22314	
		Attn: Technical Library	(1)

DISTRIBUTION LIST' (cont)

Battelle Memorial Library 505 King Avenue Columbus, Ohio 43201 Attn: Edward Unger	(1)	Martin Marietta Corporation Baltimore Division Baltimore, Maryland 21203 Attn: Technical Library	(1)
Boeing Company P.O. Box 3999 Seattle, Washington 98124 Attn: Technical Library	(1)	Mathematical Sciences Corporation 278 Renook Way Arcadia, California 91107 Attn: M. Fournery	(1)
Chrysler Corporation Space Division Michoud Operations New Orleans, Louisiana Attn: Technical Library	(1)	Philco Corporation Aeronutronics Division Ford Road Newport Beach, California 92660 Attn: Technical Library	(1)
Chrysler Corporation 8880 Astronaut Blvd. Cape Canaveral, Florida 32920 Attn: CHRY-24 W. E. Dempster	(6)	Rocketdyne Solid Propulsion Operations P.O. Box 548 McGregor, Texas Attn: Technical Library	(1)
Douglas Missiles & Space Systems Huntington Beach, California Attn: T. J. Gordon	(1)	Rohm and Haas Redstone Arsenal Research Division Huntsville, Alabama 35807 Attn: Technical Library	(1)
Grumman Aerospace Corporation Plant No. 25 Bethpage, New York 11714 Attn: M. Dandridge	(1)	Rohr Corporation Space Products Division 8200 Arlington Boulevard Riverside, California	(1)
Hercules, Inc. Allegany Ballistics Laboratory P.O. Box 210 Cumberland, Maryland 21502 Attn: Technical Library	(1)	Thiokol Chemical Corporation Wasatch Division Brigham City, Utah 94302 Attn: Dan Hess Technical Library	(1) (10)
Hercules Company Bacchus Works P.O. Box 98 Magna, Utah 84044 Attn: Technical Library	(1)	Thiokol Chemical Corporation Elkton Division Elkton, Maryland 21921 Attn: Technical Library	(1)
Lockheed Missiles & Space Company P.O. Box 504 Sunnyvale, California Attn: Technical Library	(1)	Thiokol Chemical Corporation Huntsville Division Huntsville, Alabama 35807 Attn: Technical Library	(1)
Lockheed Propulsion Company P.O. Box 111 Redlands, California 93273 Attn: Bud White	(1)		

DISTRIBUTION LIST (cont)

TRW, Inc.
Structures Division
23444 Euclid Avenue
Cleveland, Ohio 44117
Attn: L. Russell (1)

TRW Systems
One Space Park
Redondo Beach, California 90278
Attn: M. Lipow (1)

United Technology Center
P.O. Box 358
Sunnyvale, California 94088
Attn: Technical Library (1)